University of Warsaw
Faculty of Mathematics, Informatics and Mechanics

Piotr Bajger

In search of concise mathematical description of drug-resistant tumour growth

PhD dissertation

Supervisor
prof. dr hab. Urszula Foryś
Institute of Applied Mathematics and Mechanics
Faculty of Mathematics, Informatics, and Mechanics
University of Warsaw

Supervisor
prof. dr hab. inż. Krzysztof Fujarewicz
Institute of Automatic Control
Faculty of Automatic Control, Electronics and Computer Science
Silesian University of Technology

June 2020

Author declaration
I hereby declare that this dissertation is my own work.

24 June 2020
date

Piotr Bajger

Supervisor declaration
This dissertation is ready to be reviewed.

24 June 2020
date

prof. dr hab. Urszula Foryś

24 June 2020
date

dr hab. inż. Krzysztof Fujarewicz, prof. PŚ

Contents

Chapter 1

Introduction

1.1 Motivation

In September 2018 the International Agency for Research on Cancer (IARC) estimated that there would be 18.1 million new cancer cases and 9.6 million cancer deaths in 2018 [20]. Cancer is expected to be the leading or second leading cause of death and factor reducing live expectancy worldwide [11]. While the exact cancer incidence profiles vary between countries, depend on geography, socioeconomic development and other factors, cancer remains to be one of the greatest challenges faced by modern society.

Given the global scale of the issue it is only natural that the problem of cancer has raised interest not only in experimentalists, biologists and clinicians, but also in scientists representing other fields, such as mathematics. Despite the amount of data produced by experimental oncologists, which strongly suggests the use of quantitative methods, virtually no comprehensive mathematical framework has been proposed to analyse this data [24]. Given low clinical trials success rates [13] and the unsettling trends in cancer incidence and deaths [20], a need for cooperation between scientists representing a broad cross-section of fields is being recognised [2, 13, 24]. In particular, mathematics can offer tools to test biological hypotheses, as well expand the reasoning and description of cancer-driving mechanisms behind the usual "linear" intuition [24, 49].

The complexity of the biology and biochemistry of tumour growth makes it virtually impossible to fully understand the entire process without the use of qualitative methods. This is the main motivation for development of mathematical models of tumour growth and their response to therapy. Mathematical modelling aims to utilise the biological data and knowledge to isolate the most

important processes so that the final outcome can be better understood [2, 49]. Mathematical models of solid tumour growth have a long history and offer interesting perspectives [2, 47]. One of the earliest instances in which mathematical models yielded actionable insights is a model by Lasota et al. [41] of erythroid production. This model resulted in recommendations for concrete therapeutic strategies which where then successfully implemented.

One area in which there exists potential for model-driven insights is the problem of acquired drug resistance [22, 47], i.e. a process in which the tumour cells become resistant to the drug (e.g. chemotherapy) throughout the course of the treatment [15, 28]. As acquired drug resistance is usually attributed to mutations, the problem, mathematically speaking, becomes an extension of mathematical ecology framework [49]. In this dissertation a mathematical model of acquired drug resistance is constructed and analysed from the point of view of optimal chemotherapy planning.

1.2 Aims and hypothesis

The aim of this dissertation is to offer insights into the interactions between tumour drug-resistant and drug-sensitive cells and how they are affected by drug administering. This objective is achieved by a construction and analysis of a mathematical model of drug-resistant tumour growth. We hypothesise that by altering the drug delivery schedule we may delay, or even altogether prevent, the onset of drug resistance and extend patient survival.

We will be therefore interested in achieving the following aims:

- **Construct a mathematical model of drug-resistant tumour growth.** When building the model we will focus on interactions between resistant and sensitive cells, i.e. competition and mutations. We will also include the effects of angiogenesis (sprouting of new blood vessels), as it is a crucial process in tumour development [21, 37, 56].

- **Define an optimal control problem specifically aimed at targeting drug resistance.** Traditionally the search of optimal drug scheduling focuses on minimising tumour size [29, 44, 48, 62, 68]. In this dissertation we discuss an extension to that approach by proposing a bespoke objective with an explicit "resistance penalty".

- **Analyse the mathematical model and solve the associated optimal control problem.** By analysing the steady states of the mathematical model we will investigate how the long-term behaviour of the system depends

on the chemotherapy dose. By performing numerical optimisation we will obtain a reasonable candidate for the optimal protocol which can be potentially used to provide feedback for experimental oncologists.

We note that the above aims are all motivated by the following research hypothesis:

By choosing an appropriate chemotherapy scheduling and dosing it is possible to delay the onset of drug resistance and, as a result, maintain the tumour at non-life-threatening size.

Note that this shifts focus from total tumour eradication to tumour *maintenance*. This hypothesis is a result of an emerging trend in chemotherapy planning, i.e. metronomic therapy [1, 31]. Metronomic drug scheduling is characterised by low-dose drug administering with very short drug-free intervals. It stands in opposition to the maximum-tolerated dose therapy (MTD) in which the drug is given in large doses with prolonged drug-free intervals. The results in this dissertation are analysed in relation to metronomic therapy and the research hypothesis above. In particular it should be noted that a successful therapy may not be the one which completely eradicates the tumour (which is often simply not possible due to drug resistance), but the one which delays (or, ideally, prevents) the onset of drug resistance.

1.3 Outline

This dissertation is organised as follows.

In Chapter 2 we provide background on the relevant biological processes. In particular, we will give a high-level overview of the process of tumour growth. We will discuss genetic instability of tumour cells and its implications on therapy and drug resistance. We will then describe the process of angiogenesis. Next, we will move into therapeutic strategies and chemotherapy. Then in Section 2.2 we provide background on relevant topics in mathematical ecology and its applications to tumour modelling. Finally, we will discuss the role of optimal control theory in therapy optimisation.

In Chapters 3 to 5 we construct a relevant mathematical model in a step-by-step manner.

In Chapter 3 we consider a preliminary baseline model of two competing subpopulations representing sensitive and resistant cells. That model, although relaying on a set of potentially oversimplifying assumptions, can be investigated analytically to a large extent. Interestingly we have found that a lot of properties of this model carry over to more complicated models considered in subsequent

Chapters. In Chapter 3 we also define the bespoke objective functional to be used in the optimal control problem and analyse theoretical properties of the optimal control.

In Chapter 4 we extend the baseline model by introducing mutations and generalising the objective functional. We then conduct analysis analogous to that in Chapter 3 to see that the final answer to the optimal control problem does not change to a material degree.

Finally, in Chapter 5 we analyse the full model, i.e. one with generalised competition coefficients (thus allowing for modelling cell fitness) and including the process of angiogenesis. We show that the system may exhibit hysteresis with a switch to a resistant phenotype once a critical chemotherapy dose is exceeded. We then extend the analysis from previous chapters by performing sensitivity analysis of the numerical solution to the optimal control problem with respect to the competition coefficients and mutation rates. We conclude that the solution is very robust and its qualitative shape is preserved for the majority of parameter values.

Chapter 6 consists of concluding remarks and summarises the results in light of the research aims and hypothesis stated in the previous section.

1.4 Publications

In this section we list the relevant publications (and articles which are prepared or submitted to journals) co-authored by the author of this dissertation. The majority of the results described in this dissertation have either been published or are prepared for publication. Chapters 3 to 5 are based on the following works:

- **P. Bajger**, M. Bodzioch, U. Foryś, Singularity of controls in a simple model of acquired chemotherapy resistance. *Discrete and Continuous Dynamical Systems Series B*, 24(5):2039-2052, 2019.

- **P. Bajger**, M. Bodzioch, U. Foryś, Role of Cell Competition in Acquired Chemotherapy Resistance. *Proceedings of the 16th Conference on Computational and Mathematical Methods in Science and Engineering*, 1:132-141, 2016.

- **P. Bajger**, M. Bodzioch, Hahnfeldt's et al. model adapted for heterogeneous tumours, *Proceedings of the XXII National Conference of Applications of Mathematics in Biology and Medicine*, 13-18, 2016.

- **P. Bajger**, M. Bodzioch, U. Foryś, Theoretically optimal chemotherapy protocols: sensitivity to competition coefficients and mutation rates between cancer cells. Submitted to Mathematical Methods in Applied Sciences.

- **P. Bajger**, M. Bodzioch, U. Foryś, Competition between subpopulations: preventing overall growth and domination of resistant subpopulation using optimal control. Submitted to SIAM Journal of Control and Optimization.

Other relevant works co-authored by the author of this thesis on a general topic of tumour growth modelling include:

- **P. Bajger**, M. Bodzioch, Mathematical model of endothelial cell proliferation and maturation, *Mathematica Applicanda* 46(1):3-12, 2018.

- **P. Bajger**, K. Fujarewicz, A. Świerniak, Effects of Pharmacokinetics and DNA Repair on the Structure of Optimal Controls in a Simple Model of Radio-Chemotherapy, *2018 23rd International Conference on Methods & Models in Automation & Robotics (MMAR)*, 2018.

- **P. Bajger**, K. Fujarewicz, A. Świerniak, Optimal Control in a Model of Chemotherapy-induced Radiosensilisation, *Mathematica Applicanda* 47(1):81-91, 2019.

Ackonwledgements

During the writing of this dissertation the author was supported by Polish National Science Centre grant 2016/23/N/ST1/01178. The works above with K. Fujarewicz and A. Świerniak were also supported by the Polish National Science Centre under grant DEC-2016/21/B/ST7/02241.

Chapter 2

Background

2.1 What is cancer?

Cancer is a group of diseases characterised by uncontrolled cell growth and their invasion from a primary site into other (secondary) sites in the body [52]. Although a whole variety of diseases fall into the category of cancer (skin cancer is much different from lung cancer), in the year 2000 Hanahan and Weinberg [32] defined a set of "hallmarks of cancer" which are shared by the majority of cancers. The hallmarks were then revisited by the same authors in 2011 [33] to include two new "emerging hallmarks", as well as two enabling characteristics. These characteristics are summarised in Figure 2.1.

Out of the ten characteristics listed in Figure 2.1 three remain in the centre of focus of this dissertation:

- **Enabling replicative immortality**. Cancer growth is limited only by physical carrying capacity of the environment, i.e. the availability of space and nutrients. In practice this means that cancer cells lack self-regulatory mechanisms to stop them from proliferating. The mathematical models discussed in Chapters 3 to 5 relay on the assumption of unconstrained growth all the way up to the carrying capacity.

- **Genome instability & mutation**. Cancer cells are usually characterised by faulty DNA repair pathways [52] which makes them particularly hard to kill. What is more, high proliferation rate coupled with high mutation rates render tumour cells highly adaptive to the environment. This is par-

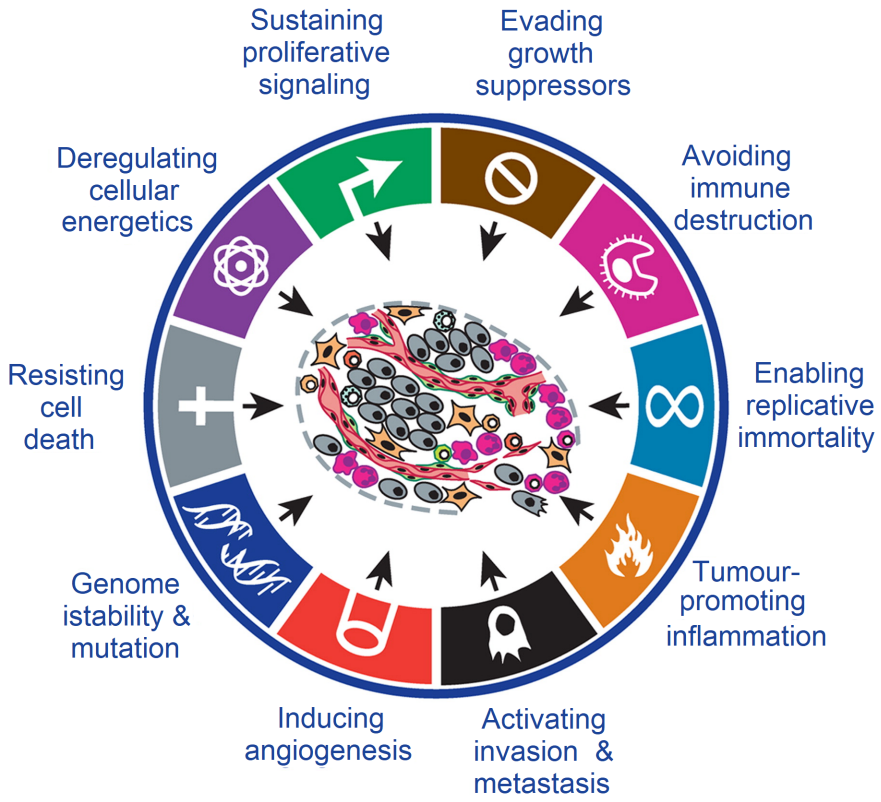

Figure 2.1: Hallmarks of cancer, including two enabling characteristics (genome instability and tumour-promoting inflammation) and two emerging hallmarks (deregulated cellular energetics and avoiding immune destruction). Reprinted and modified from [33].

ticularly important in the presence of a strong selective force imposed by the chemotherapeutic agent as it may (and often does) give rise to drug resistance [22, 28] which is the main focus of this dissertation.

- **Inducing angiogenesis**, i.e. the recruitment of new blood vessels by hypoxic (oxygen-deprived) cancer cells [21]. In Chapter 5 we will investigate the potential of limiting cancer growth by targeting its delivery system: blood vessels [37].

With so many different diseases falling under the "cancer" category, there exist a variety of different treatments. In this dissertation we focus on one particular form of treatment: chemotherapy.

2.1.1 Chemotherapy

First uses of pharmacological agents to treat cancer, which can be viewed as a birth of modern chemotherapy, date back to 1943 when Goodman et al. [27] discovered that mustard nitrogen could be used in treatment of human lymphomas [22]. Although the achieved remissions were brief, the work by Goodman ignited a discussion within the community on the possibility of curing cancer using drugs [17]. A research on other agents soon followed [19], but even in the 1960s whether cancer drugs did more harm than good was a subject of debate [17].

The fact that a single cancer cell is enough to kill a mouse had been already known since 1937 [23]. This realisation motivated a "total eradication" principle which says that in order to prevent remission, all cancer cells need to be killed. This not only prompted a change in chemotherapy dosing strategies, but also resulted in a "cell kill" (or "log-kill") hypothesis which states that the given dose of drug kills a constant fraction of tumour cells, rather than a constant number [61]. This hypothesis remains fundamental in mathematical modelling of tumour growth to this date, although certain alternatives have since been proposed [59].

The principle of total tumour eradication is closely related to the Maximum Tolerated Dose (MTD) paradigm in which the chemotherapy is administered in highest possible doses of tolerable toxicity to host's healthy cells with prolonged drug-free periods with an aim to maximise cell kill [38]. Establishing the MTD for newly discovered agents remains a primary goal of first phase clinical trials [70].

Chemotherapy remains one of the major treatment strategies with a high success rates for particular types of cancer, e.g. testicular, Hodgkin disease and high-grade lymphomas, but for the majority of patients with metastatic solid tumours, the cure remains impossible [57]. In this dissertation we focus on those cancers whose intrinsic properties (e.g. resistance) render them ineradicable regardless of the actual drug being used [48, 57]. The ultimate goal is therefore not to completely eradicate the tumour (which may not be possible), but to extend survival time by finding means to *manage* the tumour by using appropriate chemotherapy dosing.

Acquired drug resistance

Acquired drug resistance is a well-known phenomenon in which cancer develops resistance to the drug (e.g. cytotoxic chemotherapy) throughout the course of the treatment. There are many different mechanisms by which tumours can acquire

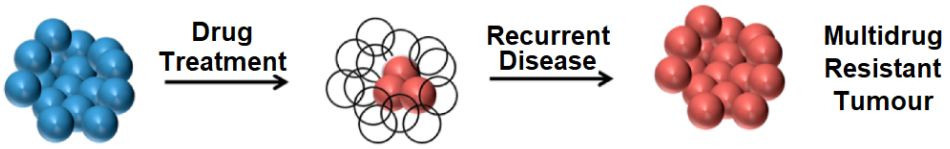

Figure 2.2: Treatment-induced drug resistance. Sensitive (blue) cells are killed by the treatment which leaves an abundance of resources for the resistant (red) cells to repopulate tumour site. Reproduced and modified from [72].

resistance. One of the most studied mechanisms is increased drug efflux [10]. Most importantly, unlike other possible mechanisms such as drug inactivation or drug target alteration, increased drug efflux is not drug-specific and gives rise to multidrug resistance [28, 36].

Resistance to chemotherapy remains a major obstacle in chemotherapy planning [22]. The main mechanisms in which cancer cells achieve resistance is through genetic or epigenetic mutations [28]. For example increased drug efflux is a result of amplification or overexpression of membrane transporters from the p-glycoprotein family (e.g. MDR1, MRP or LRP) [10, 16, 22].

Acquired drug resistance is closely related to the MTD paradigm. The cytotoxic agent imposes a strong selective force on the tumour cell population which results in killing off the sensitive population, while leaving the cells which gained resistance through random mutations intact. Those resistant cells then have an abundance of space and resources to grow, resulting in a relapse [72], a process illustrated in Figure 2.2. This observation resulted in an alternative approach to chemotherapy dosing: the metronomic therapy.

Metronomic therapy

The concept of metronomic therapy stands in contrast to the previously discussed standard Maximum Tolerated Dose approach. While the latter aims to maximise cell kill in hope to fully eradicate the tumour, the goal of metronomic therapy is quite different. Metronomic therapy is characterised by an application of low, less toxic doses, but at much more frequent intervals. This shifts the therapeutic paradigm from maximising cell kill to recognition that cancer is a chronic disease and should be treated as such [38, 58].

Metronomic therapy offers a number of benefits, among which perhaps the most significant is its potential in preventing drug resistance. It is hypothesised that by maintaining a certain level of drug sensitive population of tumour cells will prevent the resistant cell population from overcoming the tumour site [38]. This would require careful dosing and a deep understanding of the interplay be-

tween the resistant and sensitive subpopulations to which mathematical modelling can contribute.

Other benefits of metronomic chemotherapy include anti-angiogenic effects (which we will address partially in Chapter 5) and enhancing immune system response (which is outside the scope of this dissertation) [38].

2.2 Mathematical models

Mathematical models considered in this dissertation are strongly rooted in mathematical ecology. We will consider two populations of cancer cells – sensitive and resistant – occupying the same site in the body, both requiring oxygen and nutrients. The ecological framework is therefore a natural starting point for tumour growth modelling.

2.2.1 Single population

Before we proceed to mathematical models of interacting populations, let us first discuss briefly the possible approaches to modelling of a single population. The most basic continuous model of population growth is due to Malthus and dates back to 1798 [46]:

$$\frac{dN}{dt} = \lambda N,$$

where N is the population size and λ is the net factor of births, deaths and migration. This model results in exponential growth and, for obvious reasons, its predictive potential is limited, as no population can possibly grow in a completely unbounded manner. Although the above model has been successfully used as a building block in many models of tumour growth [43, 69] and it may in fact very well approximate tumour growth in its initial stage, in this dissertation we focus on models in which the population does not grow boundlessly.

To address the issue of unbounded growth, Verhulst [73] proposed a nonlinear model which includes a self-limiting quadratic term. The model, often referred to as "logistic model" reads as follows:

$$\frac{dN}{dt} = \lambda N\left(1 - \frac{N}{K}\right),$$

where λ is again the growth rate and K is the so-called carrying capacity. Carrying capacity measures the population size which can be supported by a given environment in terms of resources (e.g. space and food). This model can be easily seen to have a globally (in $\mathbb{R}^+$) stable steady state $N = K$. This model has

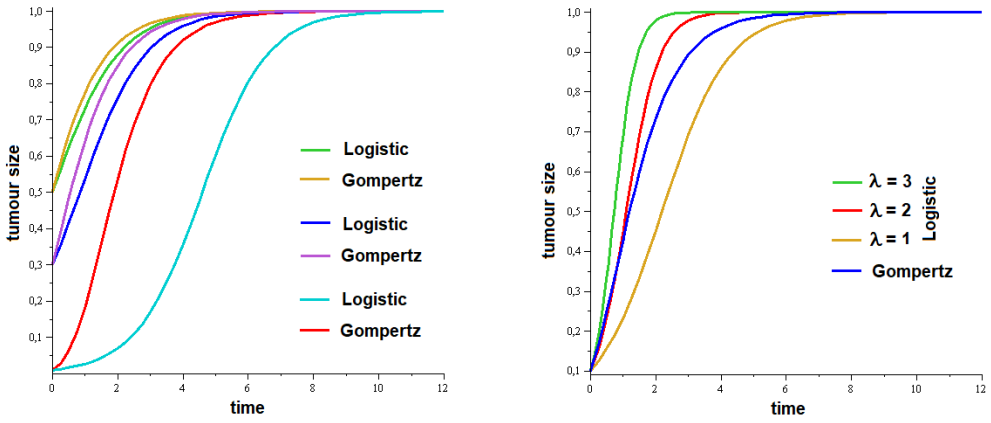

Figure 2.3: Comparison of logistic and Gompertz population growth models. The growth rate is set to $\lambda = 1$ for all curves in the left-hand side panel and for the Gompertz curve in the right-hand side panel

a whole class of generalisations [71], but we will limit our attention to its original form above.

Another possibility, with similar properties to the logistic equation, is the Gompertz model [26]:

$$\frac{dN}{dt} = -\lambda N \log \frac{N}{K}.$$

Gompertz model has been historically used to model the growth of tumours as good fits to experimental and clinical data were obtained, initially by Laird [39, 40], and subsequently by other authors [60, 64].

The logistic and Gompertz equations share a lot of properties. In particular, they both have (for positive λ) a single, globally (in $\mathbb{R}^+$) asymptotically stable positive steady state at $N = K$. Figure 2.3 illustrates the behaviour of the solutions to those models for different values of the parameter λ and initial conditions. Note that the dependent variable was rescaled so that $K = 1$. The Gompertz curve is characterised by a faster initial growth which is often a better fit to experimental data. This effect, however, becomes less significant as the tumour becomes larger (left panel) and can be partially compensated by increasing λ in the logistic equation (right panel).

A drawback of the Gompertz model is that it is purely phenomenological with no biological justification and is more complicated mathematically than the logistic equation. In this work we will use the logistic equation due to its more desirable mathematical properties (e.g. being well-defined at 0 with no additional justification) and simplicity. This choice is made bearing in mind all the qualitative similarities between the two approaches, although we note that

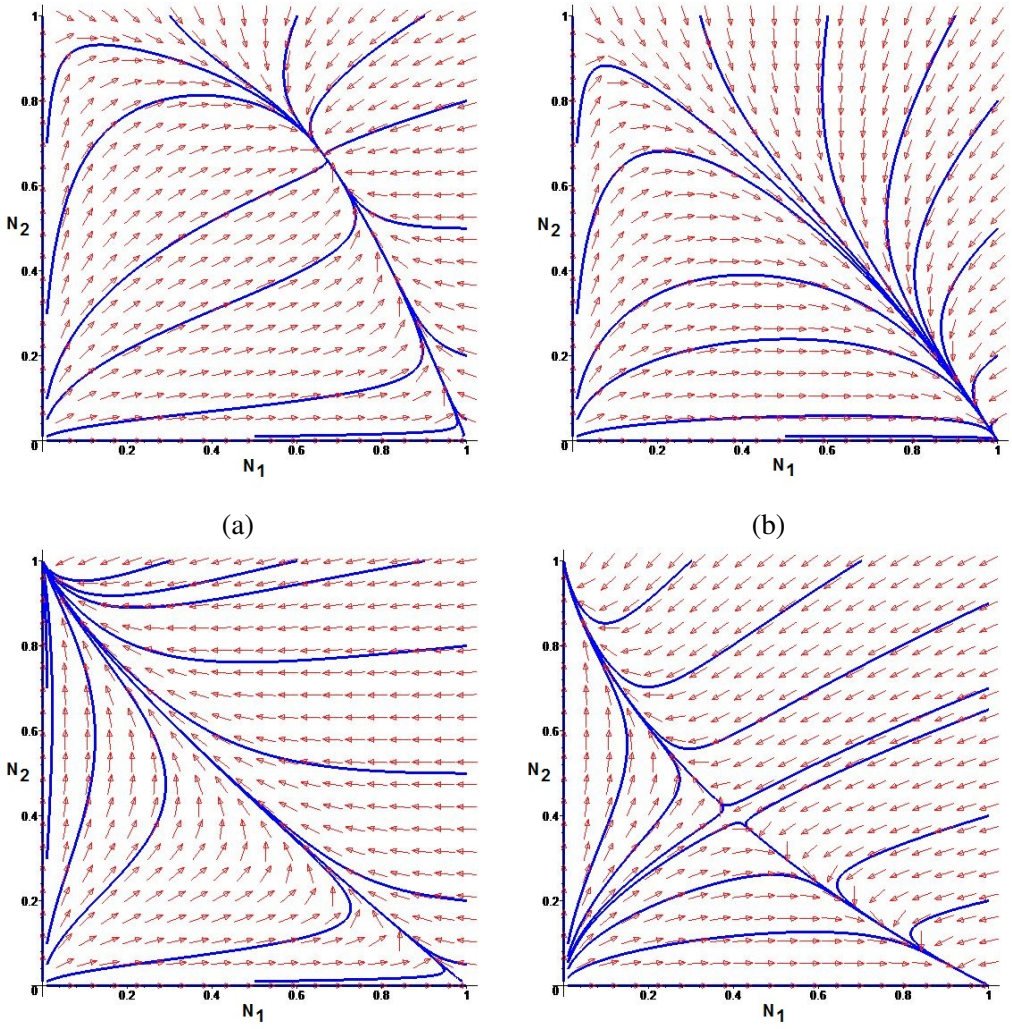

Figure 2.4: Phase space for System (2.1) with $K_1 = K_2 = 1$, $\lambda_1 = 0.192$, $\lambda_2 = 0.096$ and four different pairs of competition coefficients $(\alpha_{12}, \alpha_{21})$: (a) $(0.5, 0.5)$, (b) $(0.5, 1.5)$, (c) $(1.5, 0.5)$, (d) $(1.5, 1.5)$.

each tumour is different and an actual choice should be ideally done on a case-by-case basis.

2.2.2 Interacting populations

So far we have only considered a single population. In this dissertation we are particularly interested in a system of two populations competing for the same resources. For two arbitrary populations mathematical ecology has been describing

such a situation in the following way [49]:

$$\begin{aligned} \frac{dN_1}{dt} &= \lambda_1 N_1 \left(1 - \frac{N_1 + \alpha_{12} N_2}{K_1}\right), \\ \frac{dN_2}{dt} &= \lambda_2 N_2 \left(1 - \frac{N_2 + \alpha_{21} N_1}{K_2}\right), \end{aligned} \tag{2.1}$$

where N_1 and N_2 denote the sizes of the two populations. Of course the logistic growth function may be replaced by other growth functions with similar properties (e.g. Gompertzian). To interpret the system above we can make the following observation: in the absence of one population (say $N_j \equiv 0$), the other population follows a logistic growth model with a growth rate λ_i and carrying capacity K_i (where $i, j \in \{1, 2\}$, $i \neq j$). The coefficients α_{12} and α_{21} are the competition coefficients which quantify the competitive effect of one population on the other. Intuitively, one population occupies a portion of the carrying capacity of the other species to a degree measured by the competition coefficient.

The dynamics of the model above depends on the competition coefficients α_{12} and α_{21}, as shown in Figure 2.4. Note that a coexistence of both populations is only possible if both coefficients are smaller than 1.

The model defined above will be an entry point for more complicated models of tumour growth described later. In particular, we will modify this system to include the effects of chemotherapy, mutations and varying carrying capacity which are not present in this basic ecological model.

2.2.3 Optimal control

Another aspect of mathematical framework prominently featured in models of tumour growth is optimal control theory [42, 65, 67]. As the problem at hand often becomes that of choosing an appropriate drug dosing schedule, it fits very well within the optimal control framework.

In general, optimal control theory deals with finding a (possibly multidimensional) control, i.e. a measurable function $u : [0, T] \to U$ such that given objective function $J = J(u(\cdot))$ is minimised (or maximised) subject to dynamics generally given by:

$$\frac{dN}{dt} = f(N, u),$$

where $f : \mathbb{R}^n \times U \to \mathbb{R}^n$ is a continuously differentiable function.

In case of tumour modelling, u typically represents a therapeutic strategy (e.g. dose of drug or irradiation), N contains, among others, tumour cell population size, and f is the dynamics of tumour growth (and possibly its interactions

with microenvironment). The objective function J may then take various forms, but the general idea is, in line with the "log-kill" hypothesis, to maximise cell kill. The objective J may therefore become the tumour size at the end of the treatment [7, 69], or possibly include a term representing the mean tumour size over the course of the treatment or/and a drug dose penalty to minimise the cytotoxic effects of the drug on non-malignant cells [42, 43].

In this dissertation one of the main objects of study is the objective function. In line with the metronomic therapy approach, we propose a new objective which includes an explicit penalty for resistance [5].

2.2.4 Numerical Procedures

To find a candidate for the optimal control in problems considered throughout this dissertation we often refer to numerical methods. For problems in Chapters 3 and 4 a gradient-based method was developed by us based on the work by Śmieja et al. [63] and described in more details in Appendix A. For Chapter 5 we used a Python-based open-source optimisation modelling language Pyomo (www.pyomo.org) [34, 35] with its differential algebraic equation extension Pyomo.DAE [50].

The numerical procedures used in this dissertation are available on the author's public GitHub page: www.github.com/piotrbajger.

Chapter 3

Base Model

The optimal control problems are rarely analytically traceable and attempts to solve them fully analytically quickly become complicated, especially as the number of equations grows. We have therefore adopted a bottom up approach of constructing a mathematical model where we start with the simplest possible one and attempt to push the theoretical analysis to its limits. This is done in the hope that the results will carry over to more complicated models. In more complex models we seek confirmation of those results by resorting to numerical methods.

As a consequence, in this chapter we discuss the simplest possible mathematical model describing the underlying biological phenomenon. This model by no means attempts to capture all biological features of the problem and should be thought of as a "baseline" model or a foundation upon which we will build in the Chapters to follow.

3.1 Formulation

The main building blocks for our mathematical model are the population models discussed in Section 2.2. We assume that the malignant cell population is subdivided into two compartments which differ in their resistance to therapy. Such an approach has been used by multiple authors in the past [44, 48] and, despite being a simplification, it still may offer valuable insights into the actual biological phenomena.

Recall that a growth of a single population may be described by the logistic

equation [49, 73]:

$$\dot{N} = \lambda N\left(1 - \frac{N}{K}\right),$$

where $N(t)$ is the population size at time t, λ is the proliferation rate and K is the carrying capacity. The carrying capacity is a quantity which effectively represents the maximum size of a population (in this case the population of tumour cells) may achieve due to limitations of space and nutrients (oxygen, glucose, etc.). We will in general restrict our attention to a biologically realistic set $[0, K]$ (which is invariant under the system above), noting however that in general mathematical ecology the model remains valid also for $N > K$ [49]. In our case N denotes the volume of the tumour. Note that we could use raw cell count as the measure of the size of the tumour. We adapt an assumption of constant density of malignant cells per unit volume [48] so that those two quantities are proportional. In the remaining of this thesis we will also use the term "tumour size" to mean tumour volume.

We will consider two classes of tumour cells, sensitive and resistant, which compete for the same resources and occupy the same location. To model this coexistence in the baseline model we adapted the well-known competition model from mathematical ecology [49]:

$$\begin{aligned} \dot{N}_1 &= \lambda_1 N_1\left(1 - \frac{N_1 + N_2}{K}\right), & N_1(0) &= N_1^0, \\ \dot{N}_2 &= \lambda_2 N_2\left(1 - \frac{N_1 + N_2}{K}\right), & N_2(0) &= N_2^0, \end{aligned} \tag{3.1}$$

where N_1 and N_2 denote the sizes of sensitive and resistant cancer cell subpopulations respectively with N_1^0, N_2^0 both non-negative. Note that the proliferation rates λ_1, λ_2 may be different. It is typically assumed that the tumour consists of rapidly-proliferating sensitive cells and slowly-proliferating resistant cells [44]. In terms of the mathematical model above, this translates to the following condition: $\lambda_1 > \lambda_2$.

System (3.1) does not include the effects of chemotherapy. As the tumour cells are assumed to differ only in their level of resistance and are otherwise identical, we assume that the carrying capacities for both cell types are equal. To model the effects of chemotherapy, we will use the commonly adapted log-kill [65] hypothesis which states that the number of tumour cells killed by chemotherapy is proportional to both the number of tumour cells and to the drug concentration. The final model we will consider in this section takes the following

form:

$$\begin{aligned} \dot{N}_1 &= \lambda_1 N_1 \left(1 - \frac{N_1 + N_2}{K}\right) - \beta_1 N_1 u(t), & N_1(0) &= N_1^0, \\ \dot{N}_2 &= \lambda_2 N_2 \left(1 - \frac{N_1 + N_2}{K}\right), & N_2(0) &= N_2^0, \end{aligned} \tag{3.2}$$

where $u(t) \in [0, 1]$ is the concentration of the chemotherapeutic drug in blood at time t expressed as the fraction of Maximum Tolerated Dose (MTD) and β_1 is the parameter which controls how sensitive the cells are to the drug. The drug is assumed to have no effect on the resistant subpopulation.

Before we proceed to the analysis of the above model, we will perform a non-dimensionalisation, i.e. a rescaling of model parameters in order to reduce their number. The non-dimensionalised model becomes:

$$\begin{aligned} \frac{dn_1}{dt^*} &= \lambda_1^* n_1 \left(1 - n_1 - n_2\right) - n_1 u^*(t^*), & n_1(0) &= n_1^0, \\ \frac{dn_2}{dt^*} &= \lambda_2^* n_2 \left(1 - n_1 - n_2\right), & n_2(0) &= n_2^0, \end{aligned} \tag{3.3}$$

where:

$$t^* = \beta_1 t, \quad n_i(t^*) = \frac{N_i(t)}{K}, \quad n_i^0 = \frac{N_i^0}{K}, \quad \lambda_i^* = \frac{\lambda_i}{\beta_1}, \quad u^*(t^*) = u(t),$$

for $i = 1, 2$. We will henceforth drop the asterisks for notational convenience.

3.2 Theoretical Properties

In the following section we will recall the theoretical properties of System (3.3) for a constant chemotherapy dose, i.e. with $u(t) \equiv u \in [0, 1]$.

Given that the dependent variables describe population sizes, our biologically relevant domain of interest consists of the first quadrant, i.e.:

$$\mathbb{R}^2_+ = \{(n_1, n_2) : n_1 \geq 0 \text{ and } n_2 \geq 0\}.$$

We note first that the right hand side of System (3.3) is of class $\mathbf{C}^\infty$ in $\mathbb{R}^2_+$, hence the Picard-Lindelöf theorem [45] yields local uniqueness and existence of solutions with any given non-negative initial condition.

We can also show that:

Proposition 1. *The domain $\mathbb{R}^2_+$ is invariant under System (3.3).*

Proof. It is enough to note that the lines $n_1 = 0$ and $n_2 = 0$ are invariant under System (3.3). As a trajectory starting inside $\mathbb{R}^2_+$ can only leave $\mathbb{R}^2_+$ through one of those lines, we conclude that $\mathbb{R}^2_+$ is indeed invariant under System (3.3). □

Proposition 2. *A solution to System* (3.3) *with an initial condition* $(n_1^0, n_2^0) \in \mathbb{R}^2_+$ *exists and satisfies* $n_1(t) + n_2(t) \leq \max(n_1^0 + n_2^0, 1)$ *for all* $t \geq 0$.

Proof. We already noted that there is a unique solution passing through (n_1^0, n_2^0). If now the initial condition is such that $n_1^0 + n_2^0 > 1$, then we have $\dot{n}_1 + \dot{n}_2 < 0$ when $n_1 + n_2 = n_1^0 + n_2^0$, so $n_1 + n_2$ can never exceed the $n_1^0 + n_2^0$ bound.

For solutions with initial condition $n_1^0 + n_2^0 < 1$ it is enough to note that if $n_1 + n_2 = 1$, then $\dot{n}_1 + \dot{n}_2 = -un_1 < 0$ for $n_1 > 0$. Therefore no trajectory can leave the triangle

$$n_1 \geq 0 \qquad \text{and} \qquad n_2 \geq 0 \qquad \text{and} \qquad n_1 + n_2 \leq 1.$$

Therefore at all times we must have:

$$n_1(t) + n_2(t) \leq \max(n_1^0 + n_2^0, 1)$$

which, together with non-negativity of n_1 and n_2 yields global existence and boundedness of solutions. □

A simple application of Bendixson-Dulac [8] theorem shows that:

Proposition 3. *System* (3.3) *has no periodic orbits in the interior* $\mathbb{R}^2_+$.

Proof. Let $\mathbf{f} = (f_1, f_2)^T : \mathbb{R}^2_+ \to \mathbb{R}^2$ denote the vector field on the right hand side of System (3.2) and let $\phi(n_1, n_2) = \frac{1}{n_1 n_2}$ in the interior of $\mathbb{R}^2_+$. Then

$$\frac{\partial}{\partial n_1}(\phi f_1) + \frac{\partial}{\partial n_2}(\phi f_2) = -\frac{\lambda_1}{n_2} - \frac{\lambda_2}{n_1} < 0$$

as $n_1, n_2 > 0$ in the interior of $\mathbb{R}^2_+$. The Bendixson-Dulac theorem therefore applies. □

We note so far we have considered the domain to be $\mathbb{R}^2_+$. From a biological perspective, however, any situation where the tumour is above its carrying capacity is irrelevant. For the remaining part of this chapter we will restrict our attention to a biologically relevant region defined by:

$$\Omega = \{(n_1, n_2) : n_1,\ n_2 \geq 0 \ \text{ and } \ n_1 + n_2 \leq 1\},$$

as shown in Figure 3.1.

We immediately note that Ω is invariant under System 3.3, as seen in the proof of Proposition 2.

Equipped with the above results we may now proceed to the analysis of steady states.

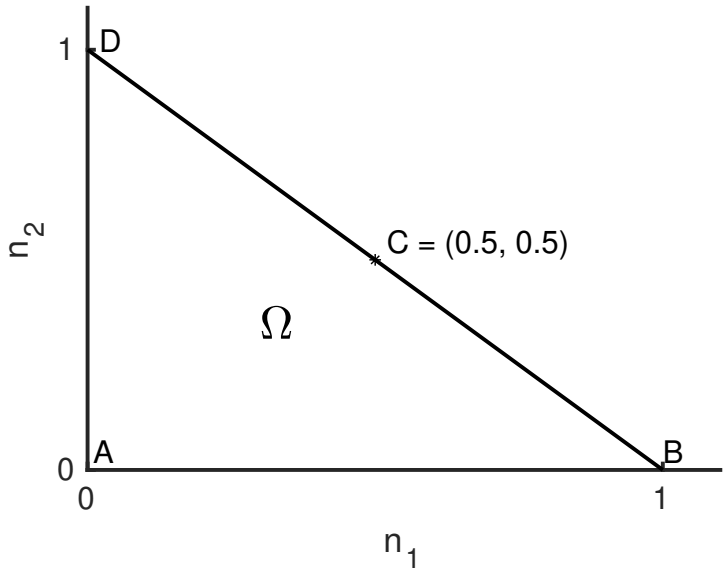

Figure 3.1: Biologically relevant domain, invariant under System (3.3).

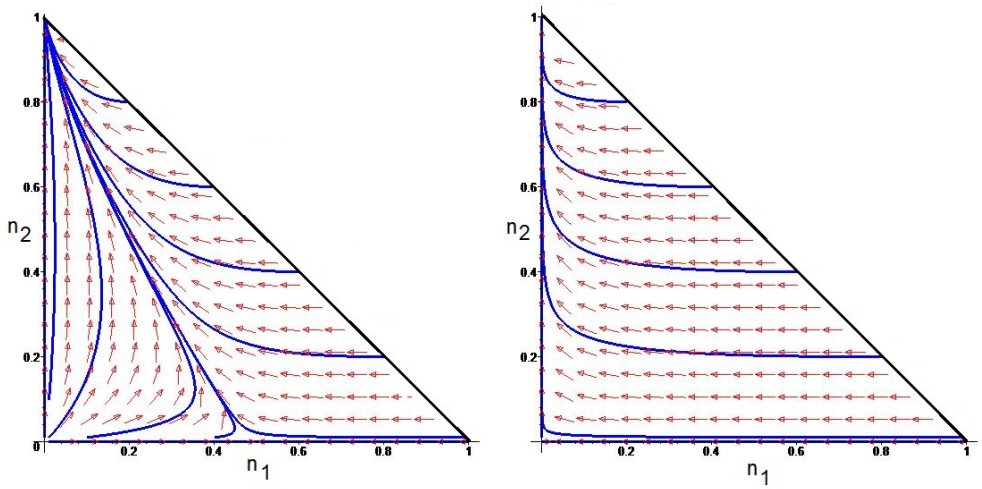

(a) (b)

Figure 3.2: Phase space with sample trajectories with (a) $u = 0.1$, and (b) $u = 0.5$.

3.2.1 Steady States

In order to gain understanding about the long-term behaviour of the solutions to System (3.3) for a constant chemotherapy dose $u(t) \equiv u \in (0, 1]$ we analyse the steady state of that system. We are in particular interested in the bifurcations with respect to the chemotherapy dose u as this is the parameter which we are in

theory able to control.

To find the steady states we equate the right hand side of System (3.3) to 0. From the first equation we obtain that either $n_1 = 0$ or $\lambda_1(1 - n_1 - n_2) - u = 0$ at a steady state. Similarly, from the second equation, either $n_2 = 0$ or $1-n_1-n_2 = 0$ at a steady state. Therefore, the system has at most three steady states:

$$S_1^* = (0, 0), \qquad S_2^* = (0, 1), \qquad S_3^* = \left(1 - \frac{u}{\lambda_1}, 0\right),$$

where S_3^* exists provided $u < \lambda_1$.

The Jacobian of the system is:

$$J(n_1, n_2) = \begin{pmatrix} \lambda_1(1 - 2n_1 - n_2) - u & -\lambda_1 n_1 \\ -\lambda_2 n_2 & \lambda_2(1 - n_1 - 2n_2) \end{pmatrix}.$$

At S_1^* we have:

$$J(S_1^*) = \begin{pmatrix} \lambda_1 - u & 0 \\ 0 & \lambda_2 \end{pmatrix}.$$

It can be easily seen that S_1^* is a saddle point if $u < \lambda_1$ and an unstable node if $u > \lambda_1$.

Similarly, at the steady state S_2^* we have:

$$J(S_2^*) = \begin{pmatrix} -u & 0 \\ -\lambda_2 & -\lambda_2 \end{pmatrix}$$

which has two negative eigenvalues. The steady state S_2^* is therefore a stable node.

At S_3^* we have

$$J(S_3^*) = \begin{pmatrix} -\lambda_1 + u & -\lambda_1 + u \\ 0 & \frac{\lambda_2}{\lambda_1} u \end{pmatrix}$$

which is an unstable node if $u < \lambda_1$ and a saddle point if $u > \lambda_1$.

Given that only S_2^* is stable we can, using Propositions 2 and Proposition 3, deduce that:

Proposition 4. *The steady state $S_2^* = (0, 1)$ of System (3.3) is globally asymptotically stable in the interior of Ω.*

Proof. By Proposition 2 the trajectories are bounded and by Proposition 3 there can be no periodic solutions. The Poincaré-Bendixson Theorem [8] therefore states that each trajectory has to converge to a fixed point. Note that the stable manifolds corresponding to cases in which S_1^* or S_3^* are saddles are the $n_1 = 0$ and $n_2 = 0$ rays which do not lie in the interior of Ω. As S_2^* is the only stable steady state, it has to be globally asymptotically stable. □

Parameter	Value	Unit	Role
T	30	day	therapy duration
λ_1	0.192	1/day	proliferation rate of sensitive cells
λ_2	0.096	1/day	proliferation rate of resistant cells
K	17000	mm^3	carrying capacity
β_1	0.45	1/day	chemotherapy sensitivity parameter
$N_1(0)$	280	mm^3	initial volume of tumour sensitive cells
$N_2(0)$	20	mm^3	initial volume of tumour resistant cells
η	3	–	weight for overall tumour burden in the objective functional
ω	60	–	weight for the terminal tumour volume in the objective functional
ξ	1	–	weight for the resistance penalty in the objective functional
ε	0.01	–	smoothing factor for the resistance penalty G

Table 3.1: Nominal values of the parameters used in the simulations. Note that the parameters for the objective functional are given for the nondimensionalised version.

Phase space of System (3.3) with sample trajectories is shown in Figure 3.2. Dimensional parameter values used in simulations are shown in Table 3.1.

3.3 Optimal control

3.3.1 Existence of Optimal Control – General Case

In this and the following two chapters of this thesis we consider problems of optimal control. Before we define the details of these problems, let us first verify that they all have an optimal solution. In order to do that we will apply a suitable version of Filippov Existence Theorem ([12, 14]). In the next few paragraphs we define our general set-up.

Let $T > 0$ be fixed and let $\Gamma \subset \mathbb{R}^n$ be an open set. Let $U = [0, 1]$. Let $L : \Gamma \times U \to \mathbb{R}$, $M : \Gamma \to \mathbb{R}$, and $\mathbf{F} : \Gamma \times U \to \mathbb{R}^n$ be continuous functions. For $\mathbf{x} \in \Gamma$ let

$$Q(\mathbf{x}) = \{(\bar{y}, \mathbf{y}) : \bar{y} \geq L(\mathbf{x}, v), \mathbf{y} = \mathbf{F}(\mathbf{x}, v) \text{ for some } v \in U\}.$$

We consider the problem of minimising the objective functional

$$J(u(\cdot)) = M(\mathbf{x}(T)) + \int_0^T L(\mathbf{x}(t), u(t))\, dt, \tag{3.4}$$

among all measurable functions $u : [0, T] \to U$ such that $\mathbf{x}$ and u satisfy:

$$\begin{aligned} \dot{\mathbf{x}}(t) &= \mathbf{F}(\mathbf{x}(t), u(t)), \\ \mathbf{x}(0) &= \mathbf{x}_0 \in \Gamma \end{aligned} \tag{3.5}$$

for almost all $t \in [0, T]$.

Any measurable function $u : [0, T] \to U$ will be called an "admissible control". By an "admissible trajectory" we will understand a function $\mathbf{x} : [0, T] \to \Gamma$ which is a solution of (3.5) for some admissible control u. Such a pair $(\mathbf{x}, u)$ will be called an "admissible pair". In order to prove that an optimal solution to the above problem exists, we will need the following Lemma (Corollary 3.3.2 in [12]):

Lemma 1. *Suppose the function $\mathbf{F} : \Gamma \times U \to \mathbb{R}^n$ is continuous in all variables and continuously differentiable with respect to $\mathbf{x}$. Let $\mathbf{x}^k$ be a sequence of trajectories converging to a function $\mathbf{y}$ uniformly on $[0, T]$. If $\mathbf{y}(t) \in \Gamma$ for each $t \in [0, T]$ and for each $\mathbf{x} \in \Gamma$ the set $V(\mathbf{x}) = \{\mathbf{F}(\mathbf{x}, v) : \text{for some } v \in [0, 1]\}$ is convex, then $\mathbf{y}$ is also a trajectory of System (3.5).*

The version of the Filippov Existence Theorem [12, 14] adapted for this problem is stated below. We will follow the proof method used in [12].

Theorem 1. *Let $A \subseteq \Gamma$ be compact and suppose that all trajectories of (3.5) are confined to lie in A. Suppose that M is continuous on A and that L, $\mathbf{F}$ are continuously differentiable on $A \times U$. Assume that for all $\mathbf{x} \in \Gamma$ the sets $Q(\mathbf{x})$ are convex. Then the problem (3.4)-(3.5) has an optimal solution.*

Proof. 1. Because A is assumed compact all trajectories $\mathbf{x}$ are uniformly bounded on $[0, T]$. Since L is continuous and U is compact, there exists a constant $\bar{L}$ such that

$$|L(\mathbf{x}(t), v)| < \bar{L}$$

for all $t \in [0, T]$, $v \in U$ and trajectory $\mathbf{x}$.

2. Consider an auxiliary optimisation problem on $\mathbb{R}^{n+1}$: minimise

$$\hat{J}(u_0(\cdot), u(\cdot)) = x_0(T) + M(\mathbf{x}(T))$$

among all measurable functions $u_0, u : [0, T] \to [0, 1]$ subject to dynamics

$$\begin{aligned} \dot{x}_0 &= F_0(\mathbf{x}, u_0, u) := \bar{L}u_0(t) + (1 - u_0(t))L(\mathbf{x}(t), u(t)), \\ \dot{\mathbf{x}} &= \mathbf{F}(\mathbf{x}, u) \end{aligned}$$

with $(x_0(0), \mathbf{x}(0)) = (0, \mathbf{x}_0)$. Let $\mathbf{u} = (u_0, u)$ and $\mathbf{z} = (x_0, \mathbf{x})$.

3. Notice that the trajectories of the above system are uniformly bounded. Each $\mathbf{x}$ is confined to lie in a compact set A and we have

$$\dot{x}_0 \leq \bar{L}$$

which implies $\dot{x}_0(t) \leq \bar{L}T$ for all $t \in [0, T]$. Hence there exists a constant C such that

$$|\mathbf{z}(t)| \leq C \qquad \text{for all } t \in [0, T].$$

4. Consider a sequence of controls $\mathbf{u}^k$ such that

$$\lim_{k\to\infty} \hat{J}(\mathbf{u}^k(\cdot)) = \inf_{\mathbf{u}} \hat{J}(\mathbf{u}(\cdot)).$$

Such a sequence exists as the set $\{J(\mathbf{u}) : \mathbf{u} \text{ an admissible control}\} \subset \mathbb{R}$ exists and is bounded from below (e.g. by 0). Let $\mathbf{z}^k$ be a sequence of corresponding trajectories. The sequence $\mathbf{z}^k$ is uniformly bounded as noted above. Furthermore the function $(F_0, \mathbf{F})$ is bounded on the compact set A by continuity. Therefore the sequence $\mathbf{z}^k$ is uniformly Lipschitz continuous. Using Ascoli's Compactness Theorem there exists a subsequence $\mathbf{z}^{k_m}$ and a function $\mathbf{z}^* = (x_0^*, \mathbf{x}^*)$ such that $\mathbf{z}^{k_m} \to \mathbf{z}^*$ uniformly on $[0, T]$.

5. Because A is compact and Γ open, there exist sets Γ' and A' such that Γ' is open, A' is compact and $A \subset \Gamma' \subset A' \subset \Gamma$. Notice that since A is closed, $\mathbf{z}^*(t) \in [0, \bar{L}T] \times A \subset \mathbb{R} \times \Gamma'$ for each $t \in [0, T]$. Furthermore, analogously as in 1., L is absolutely bounded on $A' \times U$ and hence on $\Gamma' \times U$ by some constant $\bar{L}'$.

Furthermore for any $(x_0, \mathbf{x}) \in \mathbb{R} \times \Gamma'$ the set:

$$\begin{aligned} V(x_0, \mathbf{x}) &= \{(F_0(\mathbf{x}, v_0, v), \mathbf{F}(\mathbf{x}, v)) : \text{ for some } (v_0, v) \in [0, 1] \times U\} \\ &= \left\{(y_0, \mathbf{y}) : L(\mathbf{x}, v) \leq y_0 \leq \bar{L}, \mathbf{y} = \mathbf{F}(\mathbf{x}, v) \text{ for some } v \in [0, 1]\right\} \\ &= Q(\mathbf{x}) \cap \left((-\infty, \bar{L}'] \times \mathbb{R}^n)\right) \end{aligned}$$

is convex, being an intersection of two convex sets ($Q(\mathbf{x})$ is convex by assumption). By Lemma 1 (applied to $(F_0, \mathbf{F})$ on set $\mathbb{R} \times \Gamma'$) the function $\mathbf{z}^*$ is a trajectory of the auxiliary system and there exists a corresponding control (u_0^*, u^*).

6. We then have:

$$\inf_{\mathbf{u}} \hat{J}(\mathbf{u}(\cdot)) = x_0^*(T) + M(\mathbf{x}^*(T)).$$

Notice however that since for each time $t \in [0, T]$ we have $L(\mathbf{x}^*(t), u^*(t)) < \bar{L}$ it has to be that $u_0 \equiv 0$ almost everywhere as otherwise a control $(0, u^*)$

would achieve a lower value of $\hat{J}$ (since $x_0(T)$ would decrease). Therefore the control u^* is an optimal solution to the original problem (3.4)-(3.5).

□

We will refer to Theorem 1 in this and subsequent chapters of this thesis to verify that an optimal control exists in each of the considered problems.

3.3.2 Objective

The long term behaviour of the solutions shows that, under the dynamics given by System (3.3), the tumour is incurable using chemotherapy due to drug resistance. Indeed, no matter what chemotherapy dosage we choose, we cannot stop the tumour from eventually becoming resistant and growing up to its carrying capacity.

As this situation is not uncommon in clinical practice [57], the main aim of this study is to explore ways to prevent or delay the onset of drug resistance. We reiterate here some of the points made in Section 2.1.1 – our therapeutic goal is not to completely eradicate tumour (which may not be possible), but to delay or altogether contain its growth. As it is hypothesised that low dose/metronomic (as opposed to Maximum Tolerated Dose) therapy would actually be prove to be more efficient in case of tumours which develop drug resistance [31, 51, 58], we aim to construct a suitable objective functional for the optimal control problem which focuses on tumour *maintenance*, rather than eradication (which, as we have seen, may not be possible).

A typical objective functional for a homogeneous tumour may look as follows:

$$J(u(\cdot)) = \omega n(T) + \int_0^T \Big(\eta n(t) + \theta u(t)\Big)dt,$$

where n denotes the tumour size [42]. The motivation for such a functional is as follows: ultimately, the goal is to minimise the tumour size at the end of the treatment, hence the $n(T)$ term. On the other hand one needs to control the tumour size during the course of the treatment as the tumour cannot be allowed to grow uncontrollably, hence the $n(t)$ term in the integrand in the above expression. Finally, the $\theta u(t)$ term under the integral is responsible for penalising the toxicity of the drug.

The functional above can be adapted to nonhomogeneous tumours. The typical objective functional used in models of drug resistance typically consists of a penalty (both terminal and Lagrangian) for a weighted sum across the subpopulations with the more resistant subpopulations receiving higher weightings [44].

In case of two resistance levels it can be represented as follows:

$$J(u(\cdot)) = \omega_1 n_1(T) + \omega_2 n_2(T) + \int_0^T \Big(\eta_1 n_1(t) + \eta_2 n_2(t) + \theta u(t)\Big)dt,$$

with $\omega_1 \leq \omega_2$ and $\eta_1 \leq \eta_2$. Even though an objective formulated as above may penalise drug resistance by a suitable choice of weights, it still is mostly concerned with maximising cell kill. In order to address this issue, we propose to include an explicit penalty for resistance in the Lagrangian part of the functional. This is achieved by a general non-linear penalty $G : \mathbb{R} \to [0, 1]$ by re-defining J in the following way:

$$\begin{aligned} J(u(\cdot)) &= M\left(n_1(T) + n_2(T)\right) + \int_0^T L\left(n_1(t), n_2(t), u(t)\right) dt \\ &= \omega\left(n_1(T) + n_2(T)\right) + \int_0^T \left(\eta\left(n_1(t) + n_2(t)\right) + \xi G\left(\frac{n_2(t) - n_1(t)}{\varepsilon}\right)\right) dt, \end{aligned} \tag{3.6}$$

where ξ, ε are positive and G is chosen so that $G(x) \approx 1$ when x is large and positive, while $G(x) \approx 0$ when x is large and negative. Note that we assumed equal weightings for both cell types. This is done partially for simplicity and partially because resistance is penalised through the function G. This assumption will be relaxed in subsequent chapters. We also assumed no penalty for chemotherapy toxicity (i.e. $\theta = 0$). This is because we have found that the resistance penalty G limits the amount of drug used in a very natural way.

Now, more formally, we require the function G of class $\mathbf{C}^2$ to have the following properties:

1. $G(x) \to 0$ as $x \to -\infty$,
2. $G(x) \to 1$ as $x \to +\infty$,
3. $G'(x) > 0$ for all x,
4. $xG''(x) < 0$ for $x \neq 0$,
5. $G(0) = 1/2$ and $G'(0) = 1/2$.

The last property is the normalisation of the penalty function G.

Function G may be thought of as a "smoothed out" Heaviside function. The positive parameter ε controls the steepness of the slope of G. In practice, ε allows us to control how close the resistant subpopulation has to become to the sensitive subpopulation for the penalty become relevant. The lower the ε, the narrower gap

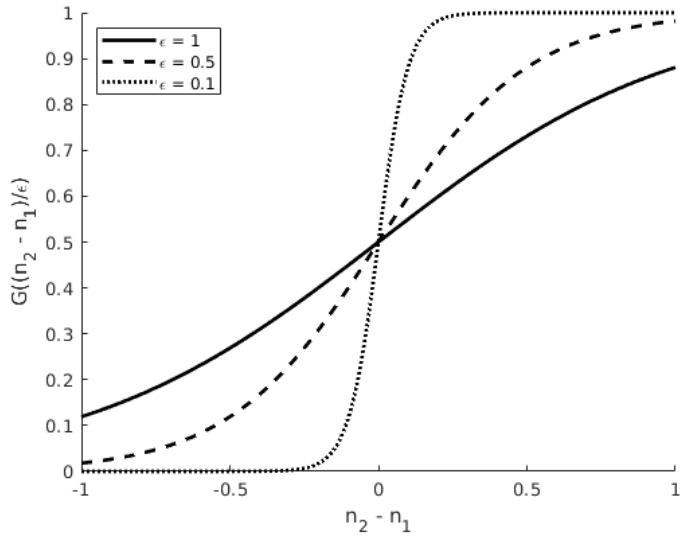

Figure 3.3: Typical choice for a resistance penalty: $G(z) = \frac{1}{2}(1 + \tanh(z))$.

between the subpopulations is allowed, with the limiting case being $\varepsilon \to 0$ when no penalty is applied until $n_2 > n_1$. A typical function G is shown in Figure 3.3.

In this section we furthermore assume that the weights attached to both subpopulations are the same, e.g. we define $\eta := \eta_1 = \eta_2$ and $\omega := \omega_1 = \omega_2$. This is so that the weights control solely the overall size of the tumour, while the resistance is penalised only by the nonlinear term.

The problem we will consider in the remaining of this section is therefore to find, for a fixed therapy time T, a measurable function $u : [0, T] \to [0, 1]$ such that J given by (3.6) is minimised subject to dynamics given by (3.3). We first re-formulate the problem so that it fits into the framework described in Section 3.3.1.

3.3.3 Existence of Optimal Control – Base Model

As mentioned earlier in this chapter, we will refer to Theorem 1 to show that the optimal control problem does have an optimal solution.

Using the notation from Section 3.3.1, we take $\Gamma = \mathbb{R}^2$ and A to be the set Ω. As we have shown it to be invariant under System (3.3), this choice satisfies the assumption of Theorem 1. Furthermore, the right-hand side of (3.3), i.e. function

$$\mathbf{F}(n_1, n_2, u) = \begin{pmatrix} F_1(n_1, n_2, u) \\ F_2(n_1, n_2) \end{pmatrix} = \begin{pmatrix} \lambda_1 n_1(1 - n_1 - n_2) - n_1 u(t) \\ \lambda_2 n_2(1 - n_2 - n_1) \end{pmatrix}$$

is continuously differentiable with respect to all variables in $A \times U$, while the functions L and M appearing in the objective functional J (3.6) are continuously differentiable on A and $A \times U$ respectively. Finally, noting that L does not depend on the control u and $\mathbf{F}$ is linear in u, the sets

$$\begin{aligned} Q(n_1, n_2) &= \{(\bar{y}, \mathbf{y}) : \bar{y} \geq L(n_1, n_2, v), \mathbf{y} = \mathbf{F}(n_1, n_2, v) \text{ for some } v \in [0, 1]\}, \\ &= [L(n_1, n_2, 0), \infty) \times [F_1(n_1, n_2, 1), F_1(n_1, n_2, 0)] \times \{F_2(n_1, n_2)\} \end{aligned}$$

are convex for all $(n_1, n_2) \in \Gamma$. The assumptions of Theorem 1 are therefore satisfied and an optimal control exists.

3.3.4 Pontryagin Minimum Principle

Let us introduce the following notation:

$$\mathbf{n} = \begin{pmatrix} n_1 \\ n_2 \end{pmatrix}, \quad \mathbf{f}(\mathbf{n}) = \begin{pmatrix} \lambda_1 n_1 (1 - n_1 - n_2) \\ \lambda_2 n_2 (1 - n_2 - n_1) \end{pmatrix}, \quad \mathbf{g}(\mathbf{n}) = \begin{pmatrix} -n_1 \\ 0 \end{pmatrix} \quad \text{and} \quad \mathbf{p} = \begin{pmatrix} p_1 \\ p_2 \end{pmatrix},$$

where p_1 and p_2 are the adjoint variables.

In order to examine theoretical properties of the optimal control, we will use Pontryagin Minimum Principle [55].

The version of Pontryagin Minimum Principle which is suitable for our problem is the following Theorem:

Theorem 2. *Let u^* be an optimal control and $\mathbf{n}^*$ denote the corresponding trajectory, then there exists a co-state vector $\mathbf{p} : [0, T] \to (\mathbb{R}^*)^2$ which satisfies the adjoint equation*

$$\dot{\mathbf{p}} = -\frac{\partial H}{\partial \mathbf{n}}, \tag{3.7}$$

with terminal condition $\mathbf{p}(T) = (\omega, \omega)$ such that the Hamiltonian H defined by

$$H(\mathbf{p}, \mathbf{n}, u) = \mathbf{p}^T (\mathbf{f}(\mathbf{n}) + \mathbf{g}(\mathbf{n})u) + L(\mathbf{n}, u) \tag{3.8}$$

is minimised a.e. on $[0, T]$ by u^* along the optimal trajectory with a constant minimum value c, i.e.

$$H(\mathbf{p}(t), \mathbf{n}^*(t), u^*(t)) = \min_{0 \leq v \leq 1} H(\mathbf{p}(t), \mathbf{n}^*(t), v) \equiv c.$$

Following standard terminology used in optimal control theory, a pair $(\mathbf{n}, u)$ consisting of a trajectory and a corresponding control for which there exist a co-state vector $\mathbf{p}$ satisfying the above conditions will be called extremal pair. A triple $(\mathbf{n}, u, \mathbf{p})$ will be called an extremal lift.

We note immediately that in our case

$$\begin{aligned} H(\mathbf{p}, \mathbf{n}, u) = p_1(\lambda_1 n_1(1 - n_1 - n_2) - n_1 u) \\ + p_2\lambda_2 n_2(1 - n_2 - n_1) \\ + \eta(n_1 + n_2) + \xi G(\tfrac{n_2 - n_1}{\varepsilon}), \end{aligned}$$

so the Hamiltonian is linear in the control which motivates the definition of a switching function [42]:

$$\varphi(t) = \frac{\partial H}{\partial u} = -p_1 n_1. \tag{3.9}$$

We see that if $u^*(t)$ is an optimal control, then

$$u^*(t) = \begin{cases} 0 & \text{if } \varphi(t) > 0, \\ 1 & \text{if } \varphi(t) < 0. \end{cases}$$

If $\varphi(t) = 0$ for some t, but φ is non-zero in some neighbourhood of t, then typically the control switches from 0 to 1 or vice-versa. If, however, φ vanishes identically over an interval, then the control is singular and may admit intermediate values between 0 and 1. We note that singular controls are of particular interest in our context as they may give rise to intermediate dosage and, consequently, lead to a conclusion that metronomic therapy may in fact be optimal. Much of this section is therefore devoted towards examining the possibility of existence of singular controls.

3.3.5 Singular control

In this section we will explore the possibility of existence of locally optimal singular controls, i.e. those satisfying the Pontryagin Minimum Principle. Singular controls are characterised by the switching function φ vanishing over an interval. In order to find them we therefore equate φ and all its derivatives to 0:

$$\varphi = \dot{\varphi} = \ddot{\varphi} = \cdots \equiv 0.$$

As the System (3.2) is control-affine we will adapt a method summarised by Ledzewicz and Schättler in [42] which simplifies the computations using Lie brackets.

For differentiable functions $\mathbf{F}, \mathbf{G} : \mathbb{R}^n \to \mathbb{R}^n$ the Lie bracket is defined as

$$[\mathbf{F}, \mathbf{G}] := \frac{\partial \mathbf{G}}{\partial \mathbf{x}}\mathbf{F} - \frac{\partial \mathbf{F}}{\partial \mathbf{x}}\mathbf{G}.$$

Using Lie brackets we can express the formulae for the derivatives of φ as follows [42, 44]:

$$\begin{aligned}
\dot{\varphi} &= \mathbf{p}^{\mathrm{T}}[\mathbf{f},\mathbf{g}] - \frac{\partial L}{\partial \mathbf{n}}^{\mathrm{T}}\mathbf{g},\\
\ddot{\varphi} &= \mathbf{p}^{\mathrm{T}}[\mathbf{f},[\mathbf{f},\mathbf{g}]] - \frac{\partial L}{\partial \mathbf{n}}^{\mathrm{T}}\left([\mathbf{f},\mathbf{g}] + \frac{\partial \mathbf{g}}{\partial \mathbf{n}}\mathbf{f}\right) - \mathbf{f}^{\mathrm{T}}\frac{\partial^2 L}{\partial \mathbf{n}^2}\mathbf{g}\\
&\quad + \left(\mathbf{p}^{\mathrm{T}}[\mathbf{g},[\mathbf{f},\mathbf{g}]] - \frac{\partial L}{\partial \mathbf{n}}^{\mathrm{T}}\frac{\partial \mathbf{g}}{\partial \mathbf{n}}\mathbf{g} - \mathbf{g}^{\mathrm{T}}\frac{\partial^2 L}{\partial \mathbf{n}^2}\mathbf{g}\right)u.
\end{aligned} \tag{3.10}$$

Note that in our case the above expressions can be simplified using the proposition below:

Proposition 5. *The following relationships hold:*

$$\begin{aligned}
&(A) \quad [\mathbf{f},\mathbf{g}] = \begin{pmatrix} -\lambda_1 n_1^2 \\ -\lambda_2 n_1 n_2 \end{pmatrix},\\
&(B) \quad [\mathbf{g},[\mathbf{f},\mathbf{g}]] = -[\mathbf{f},\mathbf{g}],\\
&(C) \quad [\mathbf{f},[\mathbf{f},\mathbf{g}]] = (\lambda_1 - \lambda_1 n_2 + \lambda_2 n_2)[\mathbf{f},\mathbf{g}].
\end{aligned} \tag{3.11}$$

Proof. By direct calculation we obtain

$$\frac{\partial \mathbf{g}}{\partial \mathbf{n}} = \begin{pmatrix} -1 & 0 \\ 0 & 0 \end{pmatrix} \quad \Longrightarrow \quad \frac{\partial \mathbf{g}}{\partial \mathbf{n}}\mathbf{f} = \begin{pmatrix} -\lambda_1 n_1(1-n_1-n_2) \\ 0 \end{pmatrix},$$

and

$$\frac{\partial \mathbf{f}}{\partial \mathbf{n}} = \begin{pmatrix} \lambda_1(1-2n_1-n_2) & -\lambda_1 n_1 \\ -\lambda_2 n_2 & \lambda_2(1-n_1-2n_2) \end{pmatrix} \Longrightarrow \frac{\partial \mathbf{g}}{\partial \mathbf{n}}\mathbf{f} = \begin{pmatrix} -\lambda_1 n_1(1-2n_1-n_2) \\ \lambda_2 n_1 n_2 \end{pmatrix},$$

yielding (A).

Next, we have

$$\frac{\partial [\mathbf{f},\mathbf{g}]}{\partial \mathbf{n}} = \begin{pmatrix} -2\lambda_1 n_1 & 0 \\ -\lambda_2 n_2 & -\lambda_2 n_1 \end{pmatrix} \quad \Longrightarrow \quad \frac{\partial [\mathbf{f},\mathbf{g}]}{\partial \mathbf{n}}\mathbf{g} = \begin{pmatrix} 2\lambda_1 n_1^2 \\ \lambda_2 n_1 n_2 \end{pmatrix},$$

and

$$\frac{\partial \mathbf{g}}{\partial \mathbf{n}}[\mathbf{f},\mathbf{g}] = \begin{pmatrix} -1 & 0 \\ 0 & 0 \end{pmatrix}\begin{pmatrix} -\lambda_1 n_1^2 \\ -\lambda_2 n_1 n_2 \end{pmatrix} = \begin{pmatrix} \lambda_1 n_1^2 \\ 0 \end{pmatrix},$$

yielding (B).

Finally,

$$\begin{aligned}
\frac{\partial [\mathbf{f},\mathbf{g}]}{\partial \mathbf{n}}\mathbf{f} &= \begin{pmatrix} -2\lambda_1 n_1 & 0 \\ -\lambda_2 n_2 & -\lambda_2 n_1 \end{pmatrix}\begin{pmatrix} \lambda_1 n_1(1-n_1-n_2) \\ \lambda_2 n_2(1-n_2-n_1) \end{pmatrix}\\
&= \begin{pmatrix} -2\lambda_1^2 n_1^2(1-n_1-n_2) \\ -\lambda_2(\lambda_1+\lambda_2) n_1 n_2(1-n_2-n_1) \end{pmatrix},
\end{aligned}$$

and

$$\frac{\partial \mathbf{f}}{\partial \mathbf{n}}[\mathbf{f},\mathbf{g}] = \begin{pmatrix} \lambda_1(1-2n_1-n_2) & -\lambda_1 n_1 \\ -\lambda_2 n_2 & \lambda_2(1-n_1-2n_2) \end{pmatrix} \begin{pmatrix} -\lambda_1 n_1^2 \\ -\lambda_2 n_1 n_2 \end{pmatrix}$$
$$= \begin{pmatrix} \lambda_1 n_1^2(\lambda_2 n_2 - \lambda_1(1-2n_1-n_2)) \\ \lambda_2 n_1 n_2(\lambda_1 n_1 - \lambda_2(1-n_1-2n_2)) \end{pmatrix},$$

yielding (C). □

We also note that Theorem 2 give only first order conditions for optimality. If the switching function vanishes over an interval, we do not know *a priori* if the resulting singular control is minimising, or maximising. In order to verify that it is indeed minimising, we refer to the strengthened Legendre-Clebsch condition [42]:

Theorem 3. *Let there be a singular lift consisting of a controlled trajectory* $(\mathbf{n}^*, u^*)$ *and the corresponding adjoint vector* $\mathbf{p} : [0,T] \to \left(\mathbb{R}^2\right)^*$. *If the controlled trajectory is optimal and the singular control* u^* *is of order* 1 *over an open interval* $I \subset [0,T]$, *then*

$$-\frac{\partial}{\partial u}\frac{d^2}{dt^2}\varphi\left(\mathbf{p}(t), \mathbf{n}^*(t), u^*(t)\right) \geq 0 \text{ for all } t \in I.$$

With the above observations we may now proceed to the computation of singular arc and the corresponding control:

Proposition 6. *If a control u is singular on some interval I, it is of order 1. The strengthened Legendre-Clebsch condition is satisfied if and only if* $n_1 > n_2$. *If this is the case, then the singular control, as a feedback function of the state variables, is given by*

$$u_{sing}(n_1,n_2) = \frac{\lambda_1 n_1 - \lambda_2 n_2}{n_1}(1-n_1-n_2) + 2\varepsilon\lambda_2 \frac{n_2}{n_1}\frac{G'(\frac{n_2-n_1}{\varepsilon})}{G''(\frac{n_2-n_1}{\varepsilon})}. \tag{3.12}$$

The corresponding locally minimising singular trajectory lies in the curve defined by $F_{arc}(n_1,n_2;c) = 0$, *where:*

$$F_{arc}(n_1,n_2;c) = \varepsilon\eta + \varepsilon\xi G\left(\frac{n_2-n_1}{\varepsilon}\right) - \xi(1-n_2-n_1)G'\left(\frac{n_2-n_1}{\varepsilon}\right) - \varepsilon c, \tag{3.13}$$

where c is the value of the Hamiltonian along the extremal trajectory.

Proof. If a control is singular on an interval $I \subset [0,T]$, then $0 = \varphi = \dot{\varphi} = \ddot{\varphi} = ...$ identically on I. Furthermore, by the Pontryagin Minimum Principle, it must be

that $H \equiv c = \text{const}$. In particular, the following three relations must hold for all t in I:

$$c = H = \mathbf{p}^{\mathrm{T}}\mathbf{f} + \mathbf{p}^{\mathrm{T}}\mathbf{g}u + L, \tag{3.14}$$

$$0 = \varphi = \frac{\partial L}{\partial u} + \mathbf{p}^{\mathrm{T}}\mathbf{g}, \tag{3.15}$$

$$0 = \dot{\varphi} = \mathbf{p}^{\mathrm{T}}[\mathbf{f}, \mathbf{g}] - \frac{\partial L}{\partial \mathbf{n}}^{\mathrm{T}} \mathbf{g}. \tag{3.16}$$

As L does not depend on u in the case we consider, from (3.15) we obtain

$$\mathbf{p}^{\mathrm{T}}\mathbf{g} = 0,$$

and substituting it into (3.14) yields

$$\mathbf{p}^{\mathrm{T}}\mathbf{f} = c - \eta(n_1 + n_2) - \xi G(\tfrac{n_2 - n_1}{\varepsilon}),$$

while from (3.16) we calculate

$$\mathbf{p}^{\mathrm{T}}[\mathbf{f}, \mathbf{g}] = -n_1 \left(\eta - \frac{\xi}{\varepsilon} G'(\tfrac{n_2 - n_1}{\varepsilon})\right). \tag{3.17}$$

Substituting for $\mathbf{f}, \mathbf{g}$ and the Lie bracket $[\mathbf{f}, \mathbf{g}]$ yields

$$\begin{aligned} p_1\lambda_1 n_1(1 - n_1 - n_2) + p_2\lambda_2 n_2(1 - n_1 - n_2) &= c - \eta(n_1 + n_2) - \xi G(\tfrac{n_2 - n_1}{\varepsilon}), \\ -p_1 n_1 &= 0, \\ -p_1\lambda_1 n_1^2 - p_2\lambda_2 n_1 n_2 &= -n_1 \left(\eta - \frac{\xi}{\varepsilon} G'(\tfrac{n_2 - n_1}{\varepsilon})\right). \end{aligned}$$

The last two equations allow for computing the co-state variables as functions of the state variables:

$$p_1 = 0, \qquad p_2 = \frac{\eta - \frac{\xi}{\varepsilon} G'(\frac{n_2 - n_1}{\varepsilon})}{\lambda_2 n_2}.$$

Substituting these relations into the first equation gives the required equation for the singular arc:

$$\varepsilon c = \varepsilon\eta + \varepsilon\xi G\left(\frac{n_2 - n_1}{\varepsilon}\right) - \xi(1 - n_2 - n_1) G'\left(\frac{n_2 - n_1}{\varepsilon}\right).$$

It remains to be shown that the equation above, or, equivalently $F_{arc}(n_1, n_2; c) = 0$ does indeed define a family of curves in the (n_1, n_2)-space parametrised by c. If c is such that a pair (n_1, n_2) satisfying $F_{arc}(n_1, n_2; c) = 0$ exists, then by the implicit

function theorem it is enough to show that the gradient of F_{arc} does not vanish at any point in Ω. We have:

$$\nabla F_{arc}(n_1, n_2; c) = \begin{pmatrix} \frac{\xi}{\varepsilon}(1 - n_1 - n_2)G''\left(\frac{\bar{n}_2 - \bar{n}_1}{\varepsilon}\right) \\ 2\xi G'\left(\frac{n_2 - n_1}{\varepsilon}\right) - \xi(1 - n_2 - n_1)G''\left(\frac{n_2 - n_1}{\varepsilon}\right) \end{pmatrix}.$$

For the first coordinate to vanish it has to be either that $n_1 + n_2 = 1$, or $n_1 = n_2$. In either case the second coordinate is equal to $2\xi G'\left(\frac{n_2 - n_1}{\varepsilon}\right) > 0$. Hence both coordinates cannot vanish simultaneously and the implicit function theorem applies.

To verify whether the Legendre-Clebsch condition is satisfied along the above arc, we need to determine the coefficient next to the control u in the expression for $\ddot{\varphi}$. Using Equation (3.10) we have:

$$\begin{aligned} \frac{\partial}{\partial u}\frac{\partial^2}{\partial t^2}\varphi &= \mathbf{p}^{\mathrm{T}}[\mathbf{g}, [\mathbf{f}, \mathbf{g}]] - \frac{\partial L}{\partial \mathbf{n}}^{\mathrm{T}} \frac{\partial \mathbf{g}}{\partial \mathbf{n}}\mathbf{g} - \mathbf{g}^{\mathrm{T}}\frac{\partial^2 L}{\partial \mathbf{n}^2}\mathbf{g} \\ &= -\frac{\partial L}{\partial \mathbf{n}}^{\mathrm{T}} \mathbf{g} - \frac{\partial L}{\partial \mathbf{n}}^{\mathrm{T}} \frac{\partial \mathbf{g}}{\partial \mathbf{n}}\mathbf{g} - \mathbf{g}^{\mathrm{T}}\frac{\partial^2 L}{\partial \mathbf{n}^2}\mathbf{g} \\ &= -\frac{n_1^2}{\varepsilon^2}\xi G''(\tfrac{n_2 - n_1}{\varepsilon}), \end{aligned}$$

where the second equality follows from Equations (3.11) (Prop. 5) and (3.16), while the second one follows from the relation $\frac{\partial \mathbf{g}}{\partial \mathbf{n}}\mathbf{g} = -\mathbf{g}$.

Using our assumptions about G, we see that the Legendre-Clebsch condition $(-1)^1 \frac{\partial}{\partial u}\frac{\partial^2}{\partial t^2}\varphi > 0$ is satisfied if and only if $n_1 > n_2$.

The singular control u_{sing} may be computed as a feedback function of the state variables by equating $\ddot{\varphi}$ to 0. Firstly, we note that using Equations (3.11) and (3.16) we have

$$\begin{aligned} \mathbf{p}^{\mathrm{T}}[\mathbf{f}, [\mathbf{f}, \mathbf{g}]] &= (\lambda_1 - \lambda_1 n_2 + \lambda_2 n_2)\mathbf{p}^{\mathrm{T}}[\mathbf{f}, \mathbf{g}], \\ &= -n_1(\lambda_1 - \lambda_1 n_2 + \lambda_2 n_2)\left(\eta - \frac{\xi}{\varepsilon}G'(\tfrac{n_2 - n_1}{\varepsilon})\right), \end{aligned} \tag{3.18}$$

so that from Equation (3.10) we get:

$$\begin{aligned} 0 = \ddot{\varphi} = &-n_1(\lambda_1 - \lambda_1 n_2 + \lambda_2 n_2)\left(\eta - \frac{\xi}{\varepsilon}G'(\tfrac{n_2 - n_1}{\varepsilon})\right) \\ &+ n_1(\lambda_1 - \lambda_1 n_2)\left(\eta - \frac{\xi}{\varepsilon}G'(\tfrac{n_2 - n_1}{\varepsilon})\right) + \lambda_2 n_1 n_2\left(\eta + \frac{\xi}{\varepsilon}G'(\tfrac{n_2 - n_1}{\varepsilon})\right) \\ &+ n_1\frac{\xi}{\varepsilon^2}G''(\tfrac{n_2 - n_1}{\varepsilon})(\lambda_1 n_1 - \lambda_2 n_2)(1 - n_1 - n_2) - n_1^2\frac{\xi}{\varepsilon^2}G''(\tfrac{n_2 - n_1}{\varepsilon})u_{\text{sing}} \\ = &\, 2\frac{\xi}{\varepsilon}\lambda_2 n_1 n_2 G'(\tfrac{n_2 - n_1}{\varepsilon}) + n_1\frac{\xi}{\varepsilon^2}G''(\tfrac{n_2 - n_1}{\varepsilon})(\lambda_1 n_1 - \lambda_2 n_2)(1 - n_1 - n_2) \\ &- n_1^2\frac{\xi}{\varepsilon^2}G''(\tfrac{n_2 - n_1}{\varepsilon})u_{\text{sing}}. \end{aligned}$$

Hence we obtain the singular control:

$$u_{\text{sing}} = \frac{\lambda_1 n_1 - \lambda_2 n_2}{n_1}(1 - n_1 - n_2) + 2\varepsilon\lambda_2 \frac{n_2}{n_1} \frac{G'(\frac{n_2-n_1}{\varepsilon})}{G''(\frac{n_2-n_1}{\varepsilon})}.$$

□

We have established there where is a region in Ω in which the Legendre-Clebsch condition is satisfied. However, it remains to be investigated if the singular arc may have a non-empty intersection with Ω. The following proposition gives the necessary conditions for that to happen:

Proposition 7. *The curve defined by $F_{arc}(n_1, n_2; c) = 0$ in Equation (3.13) may have a non-empty intersection with the interior of Ω only if $c \in \left(\eta - \frac{\xi}{2\varepsilon}, \eta + \xi\right)$.*

Proof. Note that in Ω we have $1 - n_1 - n_2 > 0$. If $c < \eta - \frac{\xi}{2\varepsilon}$, then

$$F_{\text{arc}}(n_1, n_2; c) > \tfrac{\xi}{2} - \xi(1 - n_1 - n_2)G'(\tfrac{n_2-n_1}{\varepsilon}) > \xi\left(\tfrac{1}{2} - G'(\tfrac{n_2-n_1}{\varepsilon})\right) > 0.$$

If $c > \eta + \xi$, then

$$F_{\text{arc}}(n_1, n_2; c) < \varepsilon\xi\left(G(\tfrac{n_2-n_1}{\varepsilon}) - 1\right) - \xi(1 - n_1 - n_2)G'(\tfrac{n_2-n_1}{\varepsilon}) < 0.$$

□

Equation $F_{\text{arc}}(n_1, n_2; c) = 0$ defines a whole family of singular arcs. We will now investigate geometric properties of this family of curves to see how singular arcs may intersect the domain Ω. We will be in particular interested in the portion of the singular arc which lies in the region where $n_1 > n_2$, i.e. where the Legendre-Clebsch condition is satisfied. Let us therefore consider the following propositions:

Proposition 8. *1. A tangent to the singular arc $F_{arc}(n_1, n_2; c) = 0$ at a point $(\bar{n}_1, \bar{n}_2)$ is parallel to the n_1-axis if and only if $\bar{n}_1 = \bar{n}_2$ or $1 - \bar{n}_1 - \bar{n}_2 = 0$.*

2. No admissible trajectory may reach the $n_1 = n_2$ line of Ω along the singular arc.

Proof. 1. Let $(\bar{n}_1, \bar{n}_2)$ be a point at which the tangent is parallel to the n_1-axis. At such point the n_1 coordinate of the normal to singular arc is 0, that is

$$\begin{aligned} 0 &= \frac{\partial}{\partial n_1}\left(\varepsilon\eta + \varepsilon\xi G\left(\frac{n_2 - n_1}{\varepsilon}\right) - \xi(1 - n_2 - n_1)G'\left(\frac{n_2 - n_1}{\varepsilon}\right)\right)\Big|_{\substack{n_1=\bar{n}_1 \\ n_2=\bar{n}_2}} \\ &= \frac{\xi}{\varepsilon}(1 - \bar{n}_1 - \bar{n}_2)G''\left(\frac{\bar{n}_2 - \bar{n}_1}{\varepsilon}\right). \end{aligned}$$

Hence the point $(\bar{n}_1, \bar{n}_2)$ must lie on either of the lines: $n_1 = n_2$ or $n_1 + n_2 = 1$ (and any point lying on those lines satisfies the above condition).

2. It is enough to notice that $u_{\text{sing}} \to \infty$ as $|n_1 - n_2| \to 0$. Clearly, we have $G'(0) = 1/2$ and $G''(0) = 0$, as G'' changes its sign at 0. Hence there exists $\delta > 0$ such that if $|n_1 - n_2| < \delta$, then $u_{\text{sing}} > 1$ and the trajectory along the singular arc becomes inadmissible before it reaches the $n_1 = n_2$ line.

□

Proposition 9. *Let $c \in \mathbb{R}$ be fixed. Let $A = (0,0)$, $B = (1,0)$, $C = (1/2, 1/2)$, $D = (0,1)$.*

1. *Singular arc defined by $F_{arc}(n_1, n_2; c) = 0$ may intersect each of the line segments AC and BD at most once.*
2. *Singular arc defined by $F_{arc}(n_1, n_2; c) = 0$ may intersect line segment AB at most once.*
3. *Singular arc defined by $F_{arc}(n_1, n_2; c) = 0$ may intersect line segment AD at most once.*

Proof. 1. Consider line segment AC first. At the point of intersection it must be that $n_1 = n_2 = n \in \mathbb{R}$ and

$$0 = F_{\text{arc}}(n, n; c) = \varepsilon(\eta - c) + \varepsilon\xi G(0) - \xi(1 - 2n)G'(0).$$

Recall that $G(0) = G'(0) = 1/2$, so that the only solution is

$$n = \frac{1}{2} - \varepsilon\left(\frac{1}{2} + \frac{\eta - c}{\xi}\right)$$

and there may only be one intersection point.

For the line segment BD it must be that $n_1 + n_2 = 1$ and

$$\begin{aligned} 0 &= F_{\text{arc}}(n_1, n_2; c), \\ &= \varepsilon(\eta - c) + \varepsilon\xi G\left(\frac{n_2 - n_1}{\varepsilon}\right), \end{aligned}$$

so that

$$G\left(\frac{n_2 - n_1}{\varepsilon}\right) = \frac{c - \eta}{\xi}.$$

There are now two possible cases: either c is such that the right hand side of the above equation is outside the range of G and there is no intersection point, or c is such that G may be inverted and n_1 and n_2 may be determined uniquely. Hence there may be at most one intersection point.

2. Suppose for a contradiction that the singular arc intersects the line segment AB at least twice. Let $n_1^{(1)}$ and $n_1^{(2)}$ be the n_1 coordinates of these intersection points with $n_1^{(1)} < n_1^{(2)}$. Then there exists a point $\left(n_1^{(0)}, n_2^{(0)}\right)$ with $n_1^{(0)} \in \left(n_1^{(1)}, n_1^{(2)}\right)$ such that the normal to the singular arc at this point is parallel to the n_2 axis. By Proposition 8 this point must lie on either the $n_1 = n_2$ or $n_1 + n_2 = 1$ line. But in either case it would mean that the singular arc crosses a line segment AE or BD more than once, which would contradict 1. shown above.

3. At the point of intersection it must be that $n_1 = 0$ and $n_2 \in (0, 1)$ with

$$0 = F_{\text{arc}}(0, n_2; c)$$

so that

$$\xi(1 - n_2)G'(\tfrac{n_2}{\varepsilon}) = \varepsilon\left(\eta - c + \xi G(\tfrac{n_2}{\varepsilon})\right).$$

The right hand side of the above equation is an increasing function of n_2. The left hand side is a decreasing function of n_2 as differentiation yields

$$\frac{d}{dn_2}\left(\xi(1 - n_2)G'(\tfrac{n_2}{\varepsilon})\right) = -\xi G'(\tfrac{n_2}{\varepsilon}) + \tfrac{\xi}{\varepsilon}(1 - n_2)G''(\tfrac{n_2}{\varepsilon}) < 0,$$

using the properties of G. Hence there may be at most one intersection point.

□

The consequence of the above two Propositions is that if the singular arc intersects the domain Ω, then that intersection is a simple curve joining any two sides of the triangle Ω. Which (if any) sides are joined by this curve depends on the constant c which is not known a priori. Sample singular arcs are shown in Figure 3.4. As a result, for a given value of c, the singular arc will generally divide the domain Ω into three connected (but not necessarily non-empty) regions:

$$\begin{aligned}
\Omega_0^c &= \{(n_1, n_2) : F_{\text{arc}}(n_1, n_2, c) = 0\} \cap \Omega, \\
\Omega_-^c &= \{(n_1, n_2) : F_{\text{arc}}(n_1, n_2, c) < 0\} \cap \Omega, \\
\Omega_+^c &= \{(n_1, n_2) : F_{\text{arc}}(n_1, n_2, c) > 0\} \cap \Omega
\end{aligned}$$

We now have the following result:

Proposition 10. *Let u^* be an optimal control and let (n_1^*, n_2^*) denote the corresponding trajectory. Let c be the value of the Hamiltonian along the trajectory. Then:*

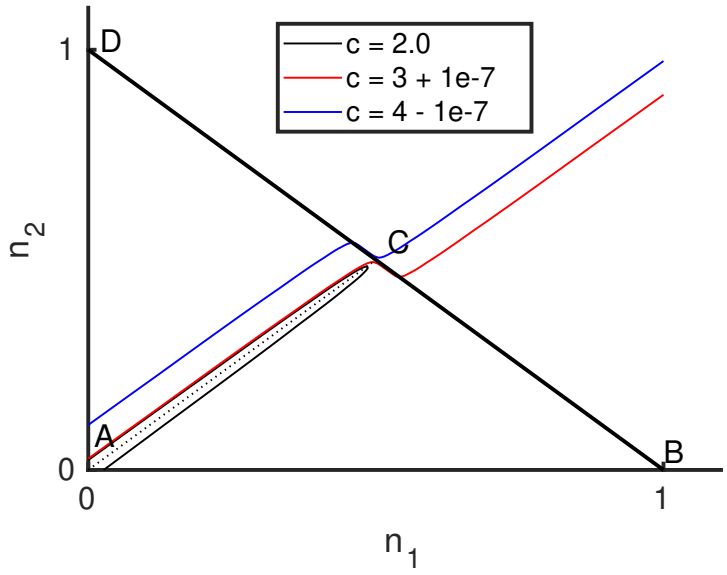

Figure 3.4: Sample singular arcs. The Legendre-Clebsch condition for optimality is only satisfied inside the triangle ABC.

1. *if* (n_1^*, n_2^*) *lies in region* Ω_-^c*, then* u^* *at time* t *may only switch from* $u^* = 0$ *to* $u^* = 1$.

2. *if* (n_1^*, n_2^*) *lies in region* Ω_+^c*, then* u^* *at time* t *may only switch from* $u^* = 1$ *to* $u^* = 0$.

Proof. Let t be a switching time for the optimal control u^* with optimal trajectory $(n_1^*(t), n_2^*(t))$. Since u^* is optimal, then $H(n_1^*(t), n_2^*(t), u^*(t)) = c$ and $\varphi(t) = 0$, i.e. Equations (3.14) and (3.15) are satisfied.

Away from the diagonal $1-n_1-n_2 = 0$ we may compute the co-state variables as the functions of the state variables using Equations (3.14) and (3.15). We then substitute it into the equation for $\dot{\varphi}$ to find that

$$\begin{aligned}\dot{\varphi} &= \frac{n_1^*}{\varepsilon(1-n_1^*-n_2^*)}\left(\varepsilon(\eta - c) + \varepsilon\xi G\left(\tfrac{n_2^*-n_1^*}{\varepsilon}\right) - \xi(1-n_1^*-n_2^*)G'\left(\tfrac{n_2^*-n_1^*}{\varepsilon}\right)\right)\\ &= \begin{cases} > 0 & \text{for } (n_1^*, n_2^*) \in \Omega_-^c,\\ < 0 & \text{for } (n_1^*, n_2^*) \in \Omega_+^c.\end{cases}\end{aligned}$$

Therefore in regions Ω_-^c the value of the switching function changes from negative to positive and hence the value of the control u^* switches from $u^* = 1$ to $u^* = 0$. Analogously, in regions Ω_+^c, the control switches from 0 to 1. □

As a consequence we can formulate the following result:

Proposition 11. *Let* $(\mathbf{n}, u)$ *be an extremal pair and* $\tau \in [0, T]$ *be such that* $u(\tau) = 0$ *and* $\mathbf{n}(\tau)$ *lies in a set* $\Psi = \triangle ABC \cap \Omega_+^c$. *Then* $u(t) = 0$ *for almost all times* $t \in [\tau, T]$.

Proof. Consider an extremal trajectory which at some point τ is in region Ψ with $u(\tau) = 0$. By Proposition 10, the trajectory has to leave region Ψ before it may switch to being 1 or singular. Note that for $u = 0$ we have $\dot{n}_1 > \dot{n}_2$ in region $\triangle ABC$ so the trajectory is confined to lie in triangle ABC (as it cannot cross the AC line segment).

The trajectory may not cross the singular arc either. Indeed, let κ be a tangent to the trajectory. Normal to the singular arc (pointing into the set Ω_+^c) is then ∇F_{arc} and:

$$\begin{aligned}
\kappa^{\mathrm{T}} \nabla F_{\text{arc}} &= \begin{bmatrix} \dot{n}_1 \\ \dot{n}_2 \end{bmatrix} \left[\tfrac{\partial F_{\text{arc}}}{\partial n_1}, \quad \tfrac{\partial F_{\text{arc}}}{\partial n_2} \right] \\
&= \frac{\xi}{\varepsilon}(1 - n_1 - n_2) \Big(2\varepsilon\lambda_2 n_2 G'(\tfrac{n_2 - n_1}{\varepsilon}) \\
&\quad + (1 - n_1 - n_2)(\lambda_1 n_1 - \lambda_2 n_2) G''(\tfrac{n_2 - n_1}{\varepsilon}) \Big) \\
&> 0,
\end{aligned}$$

as $1 - n_1 - n_2 > 0$, $G'(\frac{n_2 - n_1}{\varepsilon}) > 0$, $G''(\frac{n_2 - n_1}{\varepsilon}) > 0$ and $\lambda_1 n_1 - \lambda_2 n_2 > 0$ in ABC. □

The fact that

$$\begin{bmatrix} \dot{n}_1 \\ \dot{n}_2 \end{bmatrix} \left[\tfrac{\partial F_{\text{arc}}}{\partial n_1}, \quad \tfrac{\partial F_{\text{arc}}}{\partial n_2} \right] > 0$$

in the above proposition has yet another consequence. Suppose that the control is singular and switches to 0. Then the inequality above tells us that the trajectory departs from the singular arc and enters set $\Psi = \triangle ABC \cap \Omega_+^c$. As a corollary to Proposition 11 we obtain the following:

Corollary 1. *If a control* u *is extremal and switches from singular to* 0 *at time* τ, *then no further switches are possible and* $u(t) = 0$ *for almost all* $t \in (\tau, T]$.

But from Equation (3.15) we also have that:

Proposition 12. *Any extremal control ends with a full-dose interval.*

Proof. Let u^* be an extremal control and let (n_1^*, n_2^*) and (p_1^*, p_2^*) be respectively corresponding trajectory and co-trajectory. Given the terminal conditions in the

equations for (p_1^*, p_2^*) (see Theorem 2), we see that the value of the switching function at the terminal time T satisfies (see Equation (3.9))

$$\varphi(T) = -p_1^*(T)n_1^*(T) = -\omega n_1^*(T) < 0,$$

as $n_1^*(t) > 0$ for all times t. By continuity of φ, it means that there exists $\tau \in (0, T]$ such that $\varphi(t) < 0$ for $t \in (T-\tau, T]$. But according to the Hamiltonian-minimising property of the extremal control, it must be that $u^*(t) = 1$ for $t \in (T - \tau, T]$. □

Putting together Corollary 1 and Proposition 12 we finally obtain:

Corollary 2. *Switch from a singular control to* 0 *is not optimal.*

3.3.6 Numerical results

In the previous section we established some theoretical properties of the optimal control, namely:

(i) the equations for singular control u_{sing} and singular arc F_{arc}, i.e. Equations (3.12) and (3.13) respectively,

(ii) Proposition 12 and Corollary 2 which put some constraints on the structure of the optimal control.

In this section we find a candidate for the optimal solution to this problem using direct numerical methods. We then verify that the obtained solution really does satisfy the properties of Theorem 2, and, as a consequence, points (i) and (ii) above. Given that the problem at hand is complex enough that verifying sufficient conditions for optimality is not possible in practice, we can only relay on numerical evidence.

Methods

The differential equations were solved using the MATLAB ode45 function. To fully utilise the theoretical analysis conducted in previous section we formulated a gradient-based numerical method for computing the optimal control. This method can be thought of as an extension of a gradient method proposed in [63] to account for singular controls. For a given optimal constrol structure (e.g. 1-0-singular-1) the method finds a local minimum of the objective functional with respect to the switching times. The method is described in details in Appendix A.

The method was run for each of the allowed (i.e. satisfying Proposition 12 and Corollary 2) optimal control structures with up to four switches. The method

Control structure (S=singular)	Min. J	Relative J
1-S-1	3.12	-
1-0-S-1	3.12	-
1-0-1-S-1	3.12	-
0-1-S-1	3.12	-
0-1-0-S-1	3.12	-
1-S-1-0-1	3.12	-
1-0-1-0-1	3.28	5.15%
S-1-0-1	3.40	8.87%
0-S-1-0-1	3.40	8.87%
S-1	3.46	10.84%
0-1-0-1	3.55	13.80%
1-0-1	3.67	17.79%
S	4.38	40.47%
0-1	6.10	95.64%
1	11.70	274.93%
0	63.40	1931.90%

Table 3.2: Minimal values of the objective functional for each control structure as computed by the proposed gradient method. Grayed-out rows contain the best structure (1-S-1) as a degenerate case and hence yield identical performance.

was run ten times with randomised initial switching times so as to mitigate the risk of the gradient method finding a sub-optimal local minimum. More than four switches were not considered for two reasons. Firstly, even with more than two switching times, the method converged to the 1-singular-1 solution which indicates that more complicated optimal control structures do not add additional benefit. Secondly, bearing in mind the applied aspect of this study, solutions which incorporate more than four switching times were deemed to be too impractical to use in a clinical setting.

Table 3.2 shows the minimum value of the objective functional obtained for each control structure. Note that the grayed-out rows are those which include the optimal 1-singular-1 solution candidate as a degenerate special case (e.g. 1-singular-1 is 0-1-singular-1 with the first interval having length 0), hence they yield the same value of the objective functional J.

The (dimensional) parameter values used in all simulations are listed in Table 3.1. As the results in the previous section were all obtained for a general penalty function G, a particular choice has to be made to perform numerical simulations. We set

$$G(z) = \tfrac{1}{2}(1 + \tanh(z)),$$

noting that all properties listed in Section 3.3.2 are satisfied by this choice.

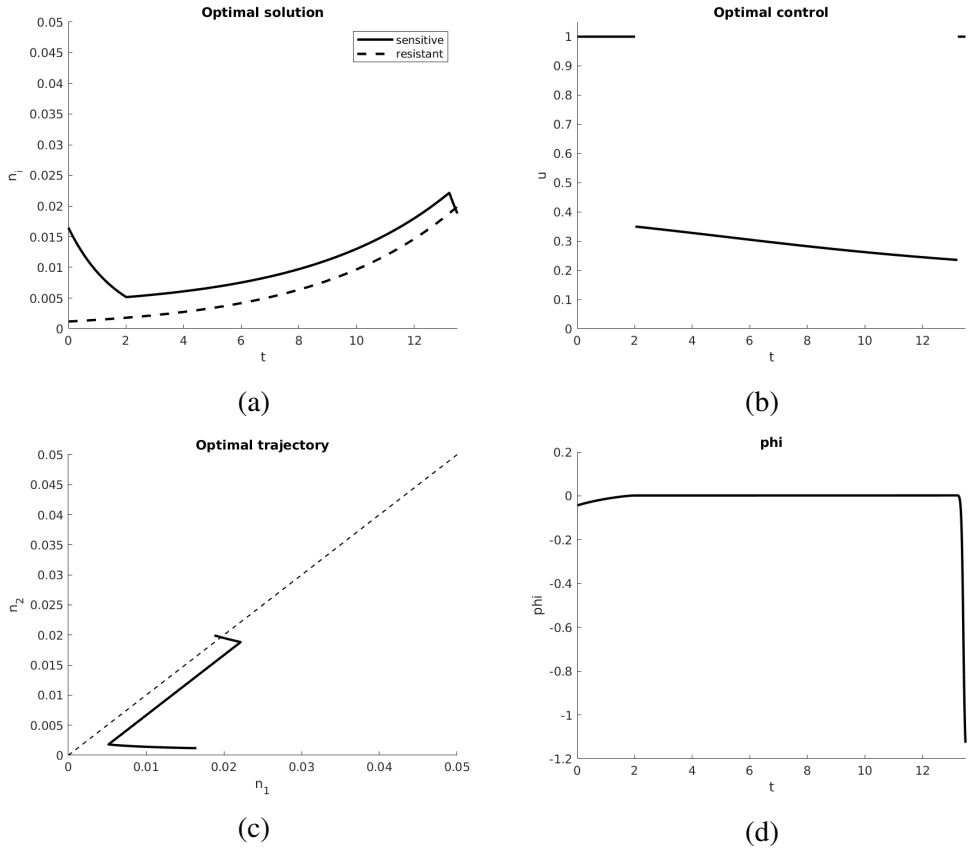

Figure 3.5: A candidate for optimal control (a), together with the corresponding solution (b), trajectory (c) and the switching function (d).

Results

The results of the algorithm are shown in Figure 3.5. In Figure 3.5b we see the candidate for optimal solution which is of a form 1-singular-1. Note that this structure is in line with the results from the previous section. Figures 3.5a and 3.5c show the solution and trajectory corresponding to the optimal control. In particular note that the singular piece of the control is responsible for maintaining the tumour in a drug-sensitive state. Finally, Figure 3.5d shows the switching function. In order to compute the switching function and the Hamiltonian we adapted the following procedure:

(i) numerically minimise the objective functional to obtain a control u^* and the corresponding trajectory $\mathbf{n}^*$,

(ii) use the computed control and trajectory to solve Equation (3.7) backwards in time to obtain the adjoint trajectory $\mathbf{p}^*$,

(iii) substitute u^*, $\mathbf{n}^*$ and $\mathbf{p}^*$ into the switching function φ or the Hamiltonian H.

We note that the switching function φ is aligned with the numerically computed control u^* as expected – its values are negative when $u^* = 1$ and 0 when u^* follows the singular arc. We have also verified that the Hamiltonian is indeed constant up to a numerical error (result not shown).

3.4 Summary

In this Chapter we presented the insights obtained from theoretical analysis of a simplified model. Although the model was purposefully designed to be simple enough to allow for analytic traceability, we will show that a lot of its properties are shared with more complicated models which are to be defined in chapters to follow.

The main theoretical results of this section are the insights into the structure of optimal control summarised in Propositions 6 and 12 and Corollary 2. Together they show that: (1) switches from no-dose/full-dose to singular, or from singular to full-dose do not violate the Pontryagin Minimum Principle, while a switch from singular to no-dose can never be optimal, and (2) that the optimal control must end with a full-dose interval.

Numerical methods were used to find a suitable candidate for the optimal control. Control structures up to and including four switching times (i.e. concatenations or up to five 0/1/singular intervals) were tested. As shown in Table 3.2 the 1-singular-1 optimal control yielded the lowest value of the objective functional. It can be seen that the singular control does not only form part of the solution, but also is crucial in preserving the tumour in a drug-sensitive state. As the singular arc appears due to the introduction of the non-linear resistance penalty in the objective function, this conclusion from the simplified model supports our hypothesis that intermediate chemotherapy dosage mitigates drug resistance. It also shows that the objective function as defined in this chapter is fit for purpose, i.e. forces the control to maintain the tumour in the drug-resistant state.

In the Chapters to follow we will build upon model (3.2) to construct more complicated and biologically adequate models.

Chapter 4

Base model with mutations

In the previous Chapter we considered a baseline model which was simple enough to conduct an extensive theoretical analysis. One limitation of that model was that it did not include the biological process to which the acquired drug resistance is most often attributed: mutations [22, 28, 36]. In this Chapter we will extend the results from the previous one by introducing mutations into the model.

We note that the structure of this Chapter is very similar to that of Chapter 3. Certain proofs follow the same strategy as in Chapter 3, but are more involved algebraically, hence they were moved to Appendix B as to not obstruct the flow of the narrative.

4.1 Formulation

Recall that the model considered in Chapter 3 is a competition model with common carrying capacity. It includes an additional death term associated with drug action in the equation describing the dynamics of the sensitive cell subpopulation, while the drug is assumed to have no influence on the dynamics of the resistant cells. As discussed in Section 2.1.1, there exists a consensus in the experimental – as well as modelling – literature stating that the acquired drug resistance is a result of mutation of cancer cells [15, 22, 28, 36]. When cancer cells are subjected to the strong selective force imposed by the cytotoxic agent, only those which had gained resistance may survive to reproduce. From the point of view of mathematical modelling we would therefore expect cells flowing from one subpopulation to the other.

Many mathematical approaches have been used to achieve that goal. Ledzewicz and Schättler [44] construct a model based on a "one-copy forward gene amplification hypothesis". This hypothesis states that upon cell division, one daughter cell will be an exact copy of the parent cell while the other may undergo a mutation (here gene amplification) and switch from sensitive to resistant (or vice-versa) with some positive probability. In their two-compartment model this resulted in a flow between the compartments proportional to the division rate of the cells. Note that in their work Ledzewicz and Schättler assumed tumour cells proliferated according to Malthus low, so the division rate is proportional to the number (or volume) of cells. Similar approach, although extended to a larger (possibly infinite) number of resistance levels was adapted by Śmieja et al. [62, 63].

As for non-linear models, Monro and Gaffney [48] assume that the two subpopulations follow Gompertzian growth model and that the mutations are Darwinian at a "rate proportional to the growth rate of the tumour". Similar approach (this time using a logistic growth model) is adapted in a work by Świerniak [66]. The latter model, apart from two compartments for tumour cells, includes a variable carrying capacity resulting from evolving vasculature. We explore this area of modelling further in the next chapter.

Tumour cell subpopulations in our model follow logistic growth for which we assume that the tumour cells proliferate at a rate proportional to the volume of cells, while the death rate scales with the square of the volume of cells. The mutation rates are then proportional to the proliferation rates (and thus the cell volumes) so that we arrive at the following system of equations:

$$\begin{aligned} \dot{N}_1 &= \lambda_1 N_1 \left(1 - \frac{N_1 + N_2}{K}\right) - \tau_1 N_1 + \tau_2 N_2 - \beta_1 N_1 u(t), & N_1(0) &= N_1^0, \\ \dot{N}_2 &= \lambda_2 N_2 \left(1 - \frac{N_1 + N_2}{K}\right) + \tau_1 N_1 - \tau_2 N_2, & N_2(0) &= N_2^0, \end{aligned} \tag{4.1}$$

where τ_1 and τ_2 are the (non-negative) mutation rates respectively from the sensitive to resistant phenotype and vice-versa. Note that the flows in and out of each compartment are balanced: as expected, no cells appear or disappear as a result of mutations. The mutation rates τ_1 and τ_2 can be interpreted as follows: τ_i/λ_i for $i = 1, 2$ is the fraction of proliferating cells which undergo a mutation per day. As a result, we must have $\tau_i < \lambda_i$ for $i = 1, 2$. In practice we expect the mutation rates to be much smaller than the proliferation rates, so we assume $\min(\lambda_1, \lambda_2) > \max(\tau_1, \tau_2)$ [48].

In the remaining part of this chapter we conduct an analogous analysis of System (4.1) as we did in the previous chapter for model (3.1): we find and

classify the steady states and search for optimal controls paying special attention to the existence of singular arcs.

4.1.1 Theoretical properties

Before we proceed to model analysis, we first perform a nondimensionalisation. The non-dimensional model reads:

$$\begin{aligned} \frac{dn_1}{dt^*} &= \lambda_1^* n_1 (1 - n_1 - n_2) - \tau_1^* n_1 + \tau_2^* n_2 - n_1 u^*(t^*), & n_1(0) &= n_1^0, \\ \frac{dn_2}{dt^*} &= \lambda_2^* n_2 (1 - n_1 - n_2) + \tau_1^* n_1 - \tau_2^* n_2, & n_2(0) &= n_2^0, \end{aligned} \tag{4.2}$$

where:

$$t^* = \beta_1 t, \quad n_i(t^*) = \frac{N_i(t)}{K}, \quad n_i^0 = \frac{N_i^0}{K},$$
$$\lambda_i^* = \frac{\lambda_i}{\beta_1}, \quad \tau_i^* = \frac{\tau_i}{\beta_1}, \quad u^*(t^*) = u(t),$$

for $i = 1, 2$. We will again drop the asterisks for notational convenience.

We will first analyse System (4.1) for $u(t) \equiv u \in (0, 1]$ constant. We can immediately notice that the vector field on the right hand side of (4.1) is of class $\mathbf{C}^\infty$ in $\mathbb{R}^2$ which guarantees local uniqueness and existence of solutions.

We are only interested in the behaviour of the system for a realistic tumour size. As in the previous chapter we restrict our domain of interest to the region Ω defined as

$$\Omega = \{(n_1, n_2) \subset \mathbb{R}^2 : n_1,\ n_2 \geq 0 \ \text{ and } \ n_1 + n_2 \leq 1\}.$$

Our first observation is that

Theorem 4. *Set Ω is invariant under System (4.2).*

Proof. We will first show that the solutions with non-negative initial conditions remain non-negative. Notice that for $n_1 = 0$ we have $\dot{n}_1 = \tau_2 n_2$. For n_1 to become negative it would therefore require n_2 to be negative so that $\dot{n}_1 < 0$. Similarly, for n_2 to become negative it would have to be that n_1 is negative in the first place. Therefore, provided that we start with non-negative initial conditions, both variables will remain positive. Note also that if $n_1 + n_2 = 1$ the trajectories indeed point into the triangle Ω:

$$(\dot{n}_1, \dot{n}_2)\ (1, 1)^T = -n_1 u \leq 0,$$

thus completing the proof. □

This, together with the remark above, shows global existence of non-negative solutions to System (4.2).

4.1.2 Steady states

We now proceed to the analysis of steady states of System (4.2). Any steady state satisfies the system of algebraic equations

$$\begin{aligned} 0 &= \lambda_1 n_1 (1 - n_1 - n_2) - \tau_1 n_1 + \tau_2 n_2 - n_1 u, \\ 0 &= \lambda_2 n_2 (1 - n_1 - n_2) + \tau_1 n_1 - \tau_2 n_2, \end{aligned}$$

which is obviously satisfied by $(0, 0)$. Assuming $n_i \neq 0$ we can divide the ith equation by n_i, $i = 1, 2$. Next, we multiply the first equation by λ_2 and the second equation by λ_1, and subtract obtained equations getting

$$-\lambda_2\tau_1 + \lambda_2\tau_2\frac{n_2}{n_1} - \lambda_2 u - \lambda_1\tau_1\frac{n_1}{n_2} + \lambda_1\tau_2 = 0$$

at a positive steady state.

Therefore the system has two steady states: $S^{1*} = (0, 0)$ and $S^{2*} = \left(n_1^*, \sigma n_1^*\right)$, where:

$$n_1^* = \frac{(\lambda_2 - \tau_2)\sigma + \tau_1}{\lambda_2\sigma(1 + \sigma)}$$

and σ is the positive solution of

$$\lambda_2\tau_2 z^2 + (\lambda_1\tau_2 - \lambda_1\tau_1 - \lambda_2 u)\, z - \lambda_1\tau_1 = 0,$$

that is:

$$\sigma = \sigma(u) = \frac{-(\lambda_1\tau_2 - \lambda_2\tau_1 - \lambda_2 u) + \sqrt{(\lambda_1\tau_2 - \lambda_2\tau_1 - \lambda_2 u)^2 + 4\lambda_1\lambda_2\tau_1\tau_2}}{2\lambda_2\tau_2} > 0.$$

It is obvious that the positive steady state always exists as the free term of the quadratic relation is negative while the coefficient next to z^2 is positive. Furthermore,

$$n_1^* + \sigma n_1^* = 1 - \frac{\tau_2\sigma - \tau_1}{\lambda_2\sigma}.$$

To check that this steady state lies in Ω we need to verify that $\tau_2\sigma - \tau_1 \geq 0$. This is equivalent to

$$\lambda_1\tau_2 + \lambda_2\tau_1 - \lambda_2 u \leq \sqrt{(\lambda_1\tau_2 - \lambda_2\tau_1 - \lambda_2 u)^2 + 4\lambda_1\lambda_2\tau_1\tau_2}.$$

If u is large enough so that the left hand side is negative, then the steady state lies in Ω. If not, after squaring both sides and rearranging we are left with

$$0 \leq 2\lambda_1\lambda_2\tau_1 u,$$

which is true. Hence this steady state always lies in Ω.

Notice that σ has a biological interpretation: it is the ratio of the number of resistant cells to the number of sensitive cells at the steady state. We may be interested for a maximum dose of chemotherapy $\bar{u}$ which can be administered before the tumour turns resistant. To do that, we calculate:

$$\bar{u} = \max_{u\in[0,1]} \{u : \sigma(u) \leq 1\}.$$

The $\sigma(u) \leq 1$ inequality is equivalent to:

$$\sqrt{(\lambda_1\tau_2 - \lambda_2\tau_1 - \lambda_2 u)^2 + 4\lambda_1\lambda_2\tau_1\tau_2} \leq 2\lambda_2\tau_2 + \lambda_1\tau_2 - \lambda_2\tau_1 - \lambda_2 u.$$

Now u cannot be large enough for the right hand side to be negative, i.e.

$$u \leq \frac{2\lambda_2\tau_2 + \lambda_1\tau_2 - \lambda_2\tau_1}{\lambda_2} := \bar{u}_1.$$

If that is the case, then squaring both sides yields

$$4\lambda_1\lambda_2\tau_1\tau_2 \leq 4\lambda_2^2\tau_2^2 + 4\lambda_2\tau_2(\lambda_1\tau_2 - \lambda_2\tau_1 - \lambda_2 u),$$

so that

$$u \leq \frac{\lambda_1\tau_2 - \lambda_2\tau_1 - \lambda_1\tau_1 + \lambda_2\tau_2}{\lambda_2} = \frac{(\lambda_1 + \lambda_2)(\tau_2 - \tau_1)}{\lambda_2} := \bar{u}_2.$$

Finally:

$$\bar{u} = \max(0, \min(\bar{u}_1, \bar{u}_2)).$$

We note that if $\tau_1 > \tau_2$, i.e. mutation rate towards resistance is larger than mutation rate towards sensitivity, we will always have $n_2 > n_1$ at the equilibrium.

We now proceed to the analysis of the stability of the steady states. The Jacobian matrix of System (4.2) is:

$$\mathbf{J}(n_1, n_2) = \begin{pmatrix} \lambda_1(1 - 2n_1 - n_2) - \tau_1 - u & -\lambda_1 n_1 + \tau_2 \\ -\lambda_2 n_2 + \tau_1 & \lambda_2(1 - n_1 - 2n_2) - \tau_2 \end{pmatrix}.$$

Recall that the conditions for local asymptotic stability are $\operatorname{tr}\mathbf{J} < 0$ and $\det\mathbf{J} > 0$. At S^{1*} these are equivalent to:

$$u > \lambda_1 + \lambda_2 - (\tau_1 + \tau_2),$$
$$u < \lambda_1 - \frac{\lambda_2\tau_1}{\lambda_2 - \tau_2}.$$

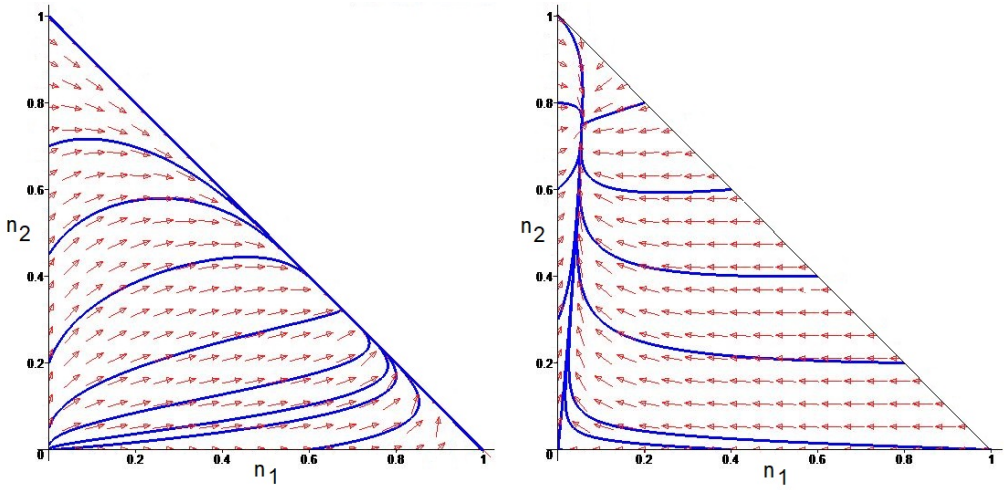

(a) (b)

Figure 4.1: Phase portraits for System (4.2) with (a) $u = 0$ and (b) $u = 0.3$.

In particular it needs to be that

$$\lambda_1 + \lambda_2 - (\tau_1 + \tau_2) < \lambda_1 - \frac{\lambda_2 \tau_1}{\lambda_2 - \tau_2},$$

or (using $\lambda_2 > \tau_2$) equivalently:

$$(\lambda_2 - \tau_2)^2 + \tau_1 \tau_2 < 0,$$

which is a contradiction. Therefore S^{1*} is always unstable.

At S^{2*} the Jacobian becomes:

$$\mathbf{J}(S^{2*}) = \begin{pmatrix} -\lambda_1 n_1^* - \tau_2 \sigma & -\lambda_1 n_1^* + \tau_2 \\ -\lambda_2 \sigma n_1^* + \tau_1 & -\lambda_2 \sigma n_1^* - \tau_1/\sigma \end{pmatrix},$$

Clearly $\operatorname{tr} \mathbf{J} < 0$. Furthermore,

$$\det \mathbf{J} = \frac{\lambda_1 \tau_1 n_1^*}{\sigma} + \lambda_2 \tau_2 \sigma^2 n_1^* + \lambda_1 \tau_1 n_1^* + \lambda_2 \tau_2 \sigma n_1^* > 0,$$

so the steady state S^{2*} is always asymptotically stable.

Similarly as in previous chapter we may apply Bendixson-Dulac [8] theorem as follows:

$$\frac{\partial}{\partial n_1}\left(\frac{\dot{n}_1}{n_1 n_2}\right) + \frac{\partial}{\partial n_2}\left(\frac{\dot{n}_2}{n_1 n_2}\right) = -\frac{\lambda_1}{n_2} - \frac{\lambda_2}{n_1} - \frac{\tau_1}{n_2^2} - \frac{\tau_2}{n_1^2} < 0$$

to exclude periodic solutions in Ω. By the Poincaré-Bendixson theorem we conclude that S^{2*} is in fact globally asymptotically stable.

Parameter	Value	Unit	Role
T	30	day	therapy duration
λ_1	0.192	1/day	proliferation rate of sensitive cells
λ_2	0.096	1/day	proliferation rate of resistant cells
K	17000	mm^3	carrying capacity
β_1	0.45	1/day	chemotherapy sensitivity parameter
τ_1	0.001	1/day	mutation rate towards resistance
τ_2	0.002	1/day	mutation rate towards sensitivity
$N_1(0)$	280	mm^3	initial volume of tumour sensitive cells
$N_2(0)$	20	mm^3	initial volume of tumour resistant cells
η_1	3	–	weight for sensitive tumour cells in the objective functional
η_2	6	–	weight for resistant tumour cells in the objective functional
ω_1	60	–	weight for the terminal volume of sensitive cells in the objective functional
ω_2	120	–	weight for the terminal volume of resistant cells in the objective functional
ξ	1	–	weight for the resistance penalty in the objective functional
ε	0.001	–	smoothing factor for the resistance penalty G

Table 4.1: Nominal values of the parameters used in the simulations. Note that the parameters for the objective functional are given for the nondimensionalised version.

Sample trajectories of System (4.2) are shown in Figure 4.1. Most of the parameter values were carried over from the previous Chapter, with an exception of τ_1 and τ_2 which are taken to be $0.01\frac{1}{day}$ and $0.02\frac{1}{day}$ respectively to highlight the differences in possible behaviours. The full list of parameters is shown in Table 4.1. In Figure 4.1 we show two phase spaces of System (4.2) for $u = 0$ and $u = 0.3$. In both cases a single, positive attracting steady state exists. Notice that in case $u = 0$ the line segment $n_1 + n_2 = 1$ is invariant under System (4.2).

4.2 Optimal control

We now conduct an analysis of the optimal control problem analogous to that performed in the previous chapter. Before proceeding, however, we will generalise the objective functional defined previously. Recall that one of the simplifying assumptions we have adapted hitherto was that the penalty weights associated with both cell types were equal. Typically in this kind of problems authors assign

higher weights to the resistant cells [44, 68]. We now relax the assumption of equal weightings and re-define the objective functional as

$$\begin{aligned} J(u(\cdot)) &= M\left(n_1(T) + n_2(T)\right) + \int_0^T L\left(n_1(t), n_2(t), u(t)\right) dt \\ &= \omega_1 n_1(T) + \omega_2 n_2(T) + \int_0^T \left(\eta_1 n_1(t) + \eta_2 n_2(t) + \xi G\left(\frac{n_2(t) - n_1(t)}{\varepsilon}\right)\right) dt, \end{aligned} \tag{4.3}$$

with $\omega_1 \leq \omega_2$ and $\eta_1 \leq \eta_2$.

The optimal control problem becomes: for a fixed terminal time T find a measurable function u such that the objective J defined by (4.3) is minimised subject to dynamics given by (4.2).

4.2.1 Existence of Optimal Control

Similarly as in Section 3.3.3 we will use the version of the Filippov Existence Theorem to verify that the optimal solution to the optimal control problem defined above exists.

Using the notation from Section 3.3.1, we take $\Gamma = \mathbb{R}^2$ and $A = \Omega$. The right hand-side of Equation (4.2), i.e. the function

$$\mathbf{F}(n_1, n_2, u) = \begin{pmatrix} F_1(n_1, n_2, u) \\ F_2(n_1, n_2) \end{pmatrix} = \begin{pmatrix} \lambda_1 n_1(1 - n_1 - n_2) - \tau_1 n_1 + \tau_2 n_2 - n_1 u(t) \\ \lambda_2 n_2(1 - n_2 - n_1) + \tau_1 n_1 - \tau_2 n_2 \end{pmatrix}$$

is continuously differentiable in $A \times U$, while the functions M and L appearing in the objective functional are continuously differentiable in $A \times U$ and A respectively. Furthermore, noting that $\mathbf{F}$ is linear in the control and L does not depend on the control u explicitly, the sets

$$\begin{aligned} Q(n_1, n_2) &= \{(\bar{y}, \mathbf{y}) : \bar{y} \geq L(n_1, n_2, v), \mathbf{y} = \mathbf{F}(n_1, n_2, v) \text{ for some } v \in [0, 1]\}, \\ &= [L(n_1, n_2, 0), \infty) \times [F_1(n_1, n_2, 1), F_1(n_1, n_2, 0)] \times \{F_2(n_1, n_2)\} \end{aligned}$$

are convex for all $(n_1, n_2) \in \Gamma$. The assumptions of Theorem 1 are therefore satisfied and an optimal control exists.

4.2.2 Singular control

To analyse the optimal control we follow the same procedure as in the previous chapter. Here we summarise the main results, noting that ultimately the best

numerically computed control has the same structure as before. Let us first define the Hamiltonian:

$$\begin{aligned} H(\mathbf{p},\mathbf{n},u) &= p_1\Big(\lambda_1 n_1(1-n_1-n_2)-\tau_1 n_1+\tau_2 n_2-n_1 u\Big) \\ &+ p_2\Big(\lambda_2 n_2(1-n_1-n_2)+\tau_1 n_1-\tau_2 n_2\Big)+\eta_1 n_1+\eta_2 n_2+\xi G(\tfrac{n_2-n_1}{\varepsilon}), \end{aligned} \tag{4.4}$$

where $\mathbf{p}$ is the vector of co-state variables, and the switching function φ:

$$\varphi(t)=\frac{\partial H}{\partial u}=-p_1(t)n_1(t). \tag{4.5}$$

Notably, we can formulate the following Proposition, analogous to Proposition 6:

Proposition 13. *Singular controls u_{sing} are of order 1 and, as functions of the state variables, are given by*

$$\begin{aligned} u_{sing} &= \\ &\varepsilon^2\frac{1}{\xi n_1}\left(\eta_1\left(\lambda_2(1-n_1-2n_2)-\tau_2-\frac{\lambda_2 f_2}{\lambda_2 n_2-\tau_1}\right)+\eta_2(\lambda_2 n_2-\tau_1)\right)\frac{1}{G''(\frac{n_2-n_1}{\varepsilon})} \\ &-\varepsilon\frac{1}{\xi n_1}\left(\lambda_2(1-n_1-3n_2)+\tau_1-\tau_2-\frac{\lambda_2 f_2}{\lambda_2 n_2-\tau_1}\right)\frac{G'(\frac{n_2-n_1}{\varepsilon})}{G''(\frac{n_2-n_1}{\varepsilon})} \\ &-\frac{1}{n_1}\Big((\lambda_1 n_1-\lambda_2 n_2)(1-n_1-n_2)-2\tau_1 n_1+2\tau_2 n_2\Big). \end{aligned} \tag{4.6}$$

Legendre-Clebsch optimality condition is satisfied if and only if $n_1 < n_2$, while the singular arc satisfies the equation

$$\begin{aligned} 0=F_{arc}(n_1,n_2,c) &= (\lambda_2 n_2-\tau_1)\Big(\eta_1 n_1+\eta_2 n_2-c+\xi G(\tfrac{n_2-n_1}{\varepsilon})\Big) \\ &-\Big(\lambda_2 n_2(1-n_1-n_2)+\tau_1 n_1-\tau_2 n_2\Big)\Big(\tfrac{\xi}{\varepsilon}G'(\tfrac{n_2-n_1}{\varepsilon})-\eta_1\Big) \end{aligned} \tag{4.7}$$

for some constant $c\in\mathbb{R}$.

Proof. Analogous to proof of Proposition 6, see Appendix B. □

We omit the proof of the above Proposition as it follows exactly the same procedure as the proof of Proposition 6 with only the arithmetic computations being slightly more involved.

The equations for the singular arc and singular control are more complicated than in previous chapter. As a result, the geometry of the singular arc is also

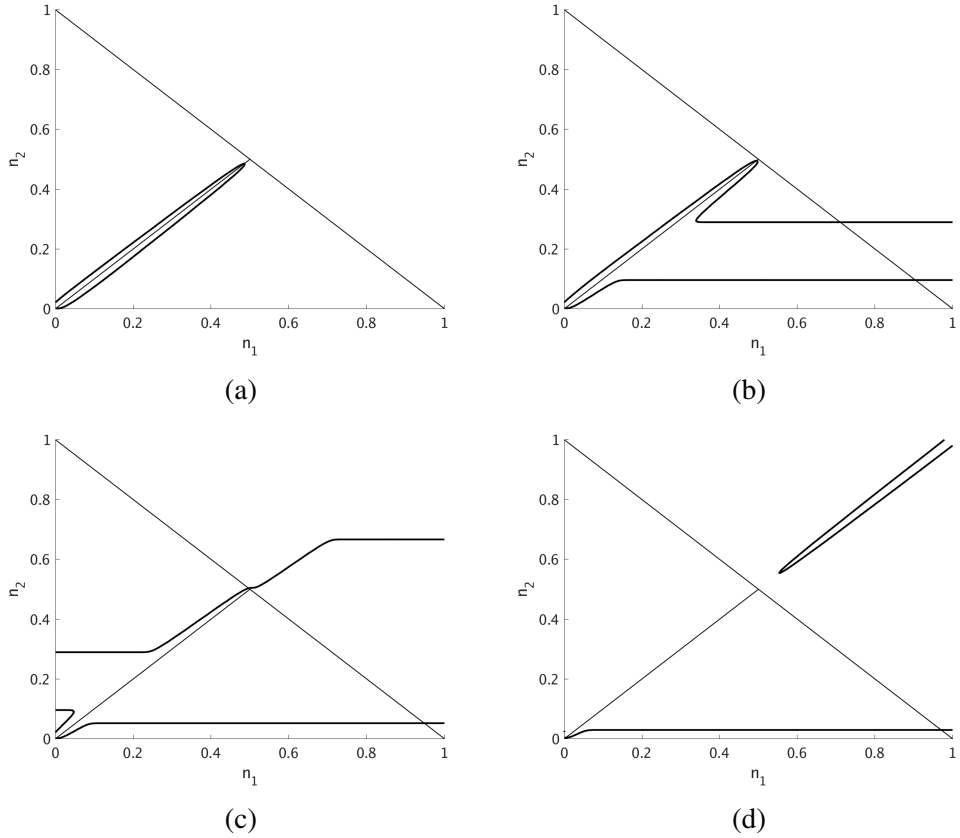

Figure 4.2: Singular arcs for different values c of the constant Hamiltonian: (a) $c = 3$, (b) $c = 4$, (c) $c = 5$ and (d) $c = 10$.

more complicated, hence we appeal to numerical methods. Sample singular arcs are shown in Figure 4.2.

Consider the following subsets of Ω:

$$\Omega_1^c = \{(n_1, n_2) \in \Omega : F_{arc}(n_1, n_2; c) > 0 \text{ and } \lambda_2 n_2 (1 - n_1 - n_2) + \tau_1 n_1 - \tau_2 n_2 > 0\},$$
$$\Omega_2^c = \{(n_1, n_2) \in \Omega : F_{arc}(n_1, n_2; c) < 0 \text{ and } \lambda_2 n_2 (1 - n_1 - n_2) + \tau_1 n_1 - \tau_2 n_2 > 0\},$$
$$\Omega_3^c = \{(n_1, n_2) \in \Omega : F_{arc}(n_1, n_2; c) > 0 \text{ and } \lambda_2 n_2 (1 - n_1 - n_2) + \tau_1 n_1 - \tau_2 n_2 < 0\},$$
$$\Omega_4^c = \{(n_1, n_2) \in \Omega : F_{arc}(n_1, n_2; c) < 0 \text{ and } \lambda_2 n_2 (1 - n_1 - n_2) + \tau_1 n_1 - \tau_2 n_2 < 0\}.$$

We can then formulate the following proposition:

Proposition 14. *Let u^* be optimal, (n_1^*, n_2^*) a corresponding trajectory and let $\tau \in (0, T)$ be a bang-bang switch. The optimal control may switch from 1 to 0 only if $(n_1^*(\tau), n_2^*(\tau)) \in \Omega_1^c \cup \Omega_4^c$ and from 0 to 1 only if $(n_1^*(\tau), n_2^*(\tau)) \in \Omega_2^c \cup \Omega_3^c$.*

Proof. For u^* being optimal, we have $H(n_1^*(t), n_2^*(t), u^*(t)) = c$ and $\varphi(t) = 0$. Computing the co-state variables as the functions of the state variables and substituting it into the equation for $\dot{\varphi}$, we find

$$\dot{\varphi}(\tau) = \frac{n_1^* F_{arc}(n_1^*, n_2^*; c)}{\lambda_2 n_2^*(1 - n_1^* - n_2^*) + \tau_1 n_1^* - \tau_2 n_2^*} = \begin{cases} > 0 & \text{for} \quad (n_1^*, n_2^*) \in \Omega_1^c \cup \Omega_4^c, \\ < 0 & \text{for} \quad (n_1^*, n_2^*) \in \Omega_2^c \cup \Omega_3^c, \end{cases}$$

for (n_1^*, n_2^*) away from the curve $\lambda_2 n_2^*(1 - n_1^* - n_2^*) + \tau_1 n_1^* - \tau_2 n_2^* = 0$, where n_1^* and n_2^* are evaluated at $t = \tau$. If now $\dot{\varphi}(\tau) > 0$, the switching function changes sign from negative to positive, so the control switches from 1 to 0 and vice-versa. □

Note however, that if $n_1 + n_2 < 1 - \frac{\tau_2}{\lambda_2}$, then

$$\lambda_2 n_2(1 - n_1 - n_2) + \tau_1 n_1 - \tau_2 n_2 > 0.$$

If the ratio $\frac{\tau_2}{\lambda_2}$ is small, then the sets $\Omega_{3,4}^c$ are very close to the $n_1 + n_2 = 1$ line. As this is often the case in practice (mutation rate is much smaller than proliferation rate), we may restrict our attention to sets $\Omega_{1,2}^c$. This is because any control which would result in a trajectory in sets $\Omega_{3,4}^c$ is unlikely to be optimal as it allows the tumour to grow very near to its carrying capacity. We cannot easily exclude such controls a priori, but we expect the optimally controlled solutions to be confined to sets $\Omega_{1,2}^c$.

Furthermore we can again show that the optimal control ends with a full dose interval:

Proposition 15. *Any extremal control u^* ends with a full-dose interval.*

Proof. Analogous to the proof of Proposition 12 and hence omitted. □

4.2.3 Numerical results

In the previous section we have shown that the optimal control for the problem defined in this chapter shows very similar properties to the optimal control for the problem defined in Chapter 3. It is therefore reasonable to expect that the actual optimal control will be similar. A candidate for such control was again computed numerically with methods set out in Section 3.3.6.

Table 4.2 shows the minimum values of the objective functional in each control class. It can again be seen that the 1-singular-1 yields the lowest value of the objective functional. Note that in this case the controls starting with a singular interval were not admissible, as u_{sing} lied outside the allowed range at the initial point.

Control structure (S=singular)	Min. J	Relative J
1-S-1	5.03	-
1-0-S-1	5.03	-
1-0-1-S-1	5.03	-
0-1-S-1	5.03	-
0-1-0-S-1	5.03	-
1-S-1-0-1	5.03	-
1-0-1-0-1	5.33	6.09%
1-0-1	5.86	16.60%
0-1-0-1	5.86	16.60%
0-1	10.64	111.70%
1	13.44	167.20%
0	65.43	1180.94%

Table 4.2: Minimal values of the objective functional for each control structure as computed by the proposed gradient method. Grayed-out rows contain the best structure (1-S-1) as a degenerate case and hence yield identical performance.

The solution which employs the best numerically computed strategy is shown in Figure 4.3. This similarity gives us confidence in the numerical results as, given the theoretical analysis conducted in the previous section, we did not expect the mutations to alter the solutions to a significant degree.

In particular, we again see in Figure 4.3 that the singular part of the control is crucial in maintaining the tumour in a sensitive state.

4.3 Conclusions

In this chapter we extended the model proposed in Chapter 3 by introducing a flow between subpopulations to represent mutations. The mutations altered the long-term behaviour of the system to some degree: we have now only two steady states (rather than three). For biologically realistic parameter values only one (positive) is stable. This is in contrast to the previous model in which there were no strictly positive steady states. Nevertheless, as seen in Figure 4.1a, the steady state is very close to $(n_1, n_2) = (0, 1)$ which was the stable steady state in the previous model.

As for the optimal control problem, the best solution obtained numerically is very similar to that from the previous chapter. As seen in Table 4.2 the lowest value of the objective functional J is again obtained for the 1-singular-1 control. In fact a lot of properties of the singular arc obtained in Chapter 3 transfer to

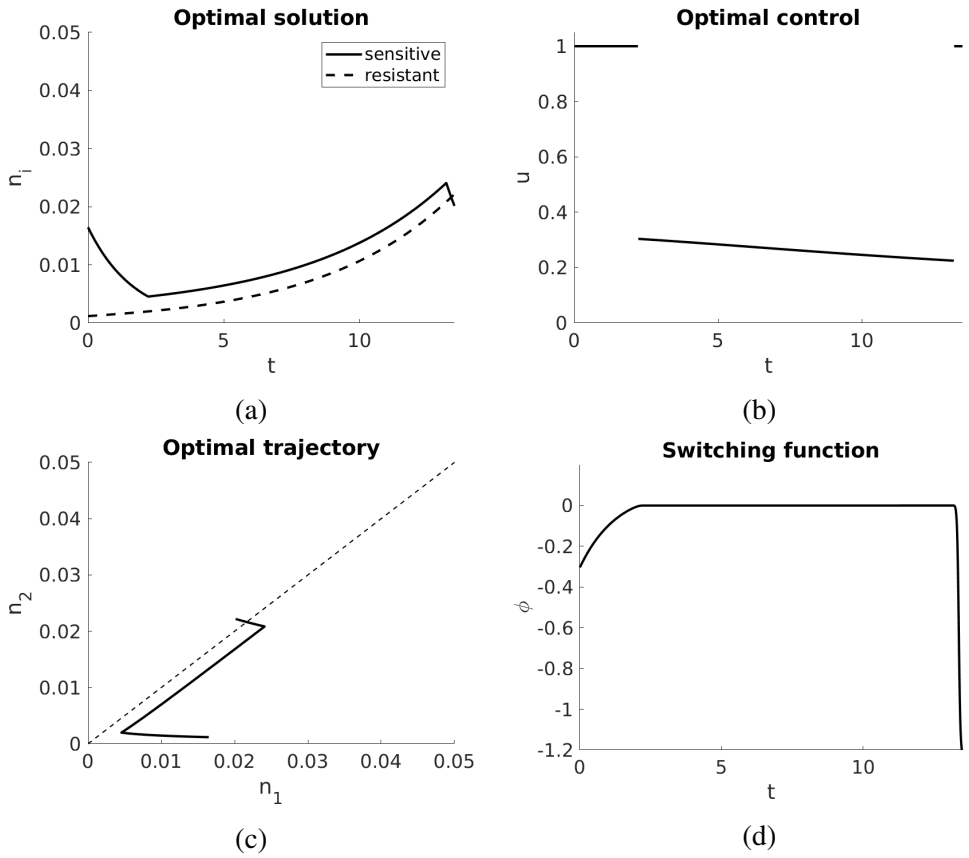

Figure 4.3: Optimal solution (a), together with the corresponding control (b), trajectory (c) and the switching function (d).

the problem discussed in this chapter. In conclusion, the structure of the best numerically computed control remains the same, with only the switching times differing to some extent. The singular portion of the optimal control is a result of the resistance penalty implemented through the function G in the objective. Its role is to preserve the tumour in the chemotherapy sensitive state.

Chapter 5

Extended Model

In the previous chapters we described a simplified model of drug-resistant tumour growth and its response to chemotherapy. The simplified model ignored some of the biological processes which are associated with tumours, in particular it did not take into account explicit competition between tumour cells, as well as angiogenesis. In this chapter we propose a model which extends the model described by System (4.1) and includes these two processes. As the theoretical analysis of the model becomes more difficult, the optimal control part of this section relies mostly on numerical simulations. The theoretical results obtained in the previous chapter nevertheless offer some additional confidence in the numerical results, as the numerically optimised control appears to have the same structure as the one which solved the problem for the simplified model using a different numerical method which relied on analytical results.

5.1 Model formulation

Recall that in the previous section we considered the model of competing subpopulations of tumour cells with the flow between these subpopulations and additional death term associated with the treatment. One limitation of this model is the absence of competition coefficients. Widely accepted hypothesis states that drug resistance is owed to the process of Darwinian natural selection. Rapid mutation rates coupled with a strong selective force imposed by the cytotoxic agent result in an overgrowth of the resistant subpopulation. In the absence of the drug, however, typically it is the sensitive cells which dominate, thus suggesting that they are better fit for existence in a drug-free environment [22, 28]. This is in line

with clinical results in which tumours initially respond well to the administered drug but then become resistant as the therapy progresses [38].

Recall from Section 2.2 that the process of competition between two populations is quite well studied [49] and involves the so-called competition coefficients (here denoted α_{12} and α_{21}) which we introduce as follows:

$$\begin{aligned} \dot{N}_1 &= \lambda_1 N_1 \left(1 - \frac{N_1 + \alpha_{12} N_2}{K}\right) - \tau_1 N_1 + \tau_2 N_2 - \beta_1 N_1 u(t), & N_1(0) &= N_1^0, \\ \dot{N}_2 &= \lambda_2 N_2 \left(1 - \frac{N_1 + \alpha_{21} N_2}{K}\right) + \tau_1 N_1 - \tau_2 N_2, & N_2(0) &= N_2^0. \end{aligned} \tag{5.1}$$

The positive competition coefficients measure the competitive effect of one population on the other and are, in general, not equal. It is a well-known result from mathematical ecology that in the above model, in the absence of therapy ($u(t) \equiv 0$) and mutations ($\tau_1 = \tau_2 = 0$), that two populations may coexist only if both of the completion coefficients are sufficiently small, less than some threshold depending on the model parameters. For the model in the form proposed above this threshold is equal to 1. If either of the competition coefficients is greater than the threshold, then the only non-negative stable stationary states have either $N_1 = 0$ or $N_2 = 0$. Note that introduction of therapy and mutations into the model will alter this result – this will be discussed further in Section 5.2.1.

The other aspect of tumour growth which has so far been ignored is angiogenesis. As discussed in Section 2.1, angiogenesis is the process of recruitment of new blood vessels from existing ones. The new blood vessels allow tumour cells access to oxygen and nutrients, thus allowing it to grow beyond the diffusion limit of $1 - 2mm^3$ [56]. From the point of view of mathematical modelling, this process corresponds to an increase in carrying capacity. A mathematical model of this phenomenon was originally proposed by Hahnfeldt et al. [30] and studied further in many other works [9, 18, 53, 54]. We adapt their approach and modify the model above to take into account time evolution of carrying capacity as follows:

$$\begin{aligned} \dot{N}_1 &= \lambda_1 N_1 \left(1 - \frac{N_1 + \alpha_{12} N_2}{K}\right) - \tau_1 N_1 + \tau_2 N_2 - \beta_1 N_1 u(t), \\ \dot{N}_2 &= \lambda_2 N_2 \left(1 - \frac{N_2 + \alpha_{21} N_1}{K}\right) + \tau_1 N_1 - \tau_2 N_2, \\ \dot{K} &= -\mu K + b(N_1 + N_2) - d(N_1 + N_2)^{2/3} K - \beta K u(t), \end{aligned} \tag{5.2}$$

with initial condition (N_1^0, N_2^0, K^0). Equation for K is related to the size of the vasculature at the tumour site. Parameter μ denotes the natural death rate of endothelial cells, while parameters b and d control the rate at which the tumour

cells secrete pro- and anti-angiogenic signals. It is assumed that both the resistant and sensitive cells secrete those signals at the same rates. The exponent $2/3$ is the area/volume ratio which appears ultimately as a consequence of the half-life of angiogenic inhibitors greatly exceeding that of angiogenic stimulators. See [30] for the detailed derivation of the third equation above.

Throughout this chapter we analyse some of the theoretical properties of System (5.2). We will then move on into the analysis of a more general (with respect to the previous chapters) optimal control problem. The objective is to find, for a fixed therapeutic horizon T, a measurable function $u : [0, T] \to [0, 1]$ which minimises the objective functional J given by:

$$\begin{aligned} J(u(\cdot)) &= M(N_1(T), n_2(T)) + \int_0^T L(N_1(t), N_2(t), u(t))dt \\ &= \omega_1 N_1(T) + \omega_2 N_2(T) \\ &+ \int_0^T \left(\eta_1 N_1(t) + \eta_2 N_2(t) + \tfrac{\xi}{2}\left(1 + \tanh\left(\tfrac{N_2(t)-N_1(t)}{\varepsilon}\right)\right)\right) dt. \end{aligned} \tag{5.3}$$

Note that we now allow the sensitive and resistant cells to have different weightings.

Finally, towards the end of this chapter, we perform numerical simulations to assess the sensitivity of the optimal control to the mutation rates and competition coefficients.

5.2 Theoretical properties

In this section we analyse basic theoretical properties of System (5.2). To gain some preliminary insights into the behaviour of the system we first analyse its behaviour for a constant, indefinite therapy, i.e. $u(t) \equiv u = \text{const}$. Let $\Omega = (\mathbb{R}^+)^2 \times \mathbb{R}^{++}$ (where $\mathbb{R}^{++} = (0, \infty)$) and note that the right-hand side vector field associated with System (5.2) is of class $\mathbf{C}^\infty$ in Ω. Therefore, the Picard-Lindelöf Theorem gives local uniqueness and existence of solutions with given initial conditions.

Proposition. *The set Ω is positively invariant under System (5.2).*

Proof. Firstly note that the straight line $N_1 = N_2 = 0$ is invariant under System (5.2). Next, if $N_1 = 0$ then $\dot{N}_1 = \tau_2 N_2$. Hence for N_1 to become negative we require that $\tau_2 N_2 \leq 0$, i.e. $N_2 \leq 0$. Analogously, N_2 may become negative if and only if N_1 becomes negative first. Therefore, provided that we start with

initial conditions such that $N_1 \geq 0$ and $N_2 \geq 0$, both N_1 and N_2 will remain non-negative.

Due to the form of the first and second equations of System (5.2) it is necessary to assume $K(0) > 0$. Assume that $K(t) = 0$ at some time moment. Then $\dot{K}(t) = b(N_1(t) + N_2(t)) > 0$, so K cannot become negative and Ω is invariant under System (5.2). □

Proposition. *For initial contition* $(N_1(0), N_2(0), K(0))$ *the solution to System* (5.2) *exists for all* $t \geq 0$.

Proof. By the non-negativity of the solution and parameters, we can estimate

$$\begin{aligned} \dot{N}_1 &\leq \lambda_1 N_1 + \tau_2 N_2, \\ \dot{N}_2 &\leq \lambda_2 N_2 + \tau_1 N_1, \\ \dot{K} &\leq b(N_1 + N_2). \end{aligned}$$

It follows that

$$\frac{d}{dt}(N_1 + N_2 + K) \leq c(N_1 + N_2 + K),$$

where $c = \max\{\lambda_1 + \tau_1 + b, \lambda_2 + \tau_2 + b\}$. Hence

$$N_1 + N_2 + K \leq O\left(\mathrm{e}^{ct}\right) \text{ for } t \geq 0$$

and the solution exists for all $t \geq 0$. □

5.2.1 Steady states

We now move into the analysis of steady states in order to understand possible long-term model behaviours. To find the steady states we equate the right-hand side of System (5.2) to 0:

$$\begin{aligned} 0 &= \lambda_1 N_1 \left(1 - \frac{N_1 + \alpha_{12} N_2}{K}\right) - \tau_1 N_1 + \tau_2 N_2 - \beta_1 N_1 u, \\ 0 &= \lambda_2 N_2 \left(1 - \frac{N_2 + \alpha_{21} N_1}{K}\right) + \tau_1 N_1 - \tau_2 N_2, \\ 0 &= -\mu K + b(N_1 + N_2) - d(N_1 + N_2)^{2/3} K - \beta K u. \end{aligned}$$

Existence

We may first note that at a steady state it must be that both N_1 and N_2 are greater than 0 which is in line with our choice of the domain Ω. We proceed by elimi-

nating K from the first two equations by computing:

$$K = \frac{\lambda_1 (N_1 + \alpha_{12} N_2)}{\lambda_1 - \tau_1 + \tau_2 \frac{N_2}{N_1} - \beta_1 u},$$

$$K = \frac{\lambda_2 (N_2 + \alpha_{21} N_1)}{\lambda_2 - \tau_2 + \tau_1 \frac{N_1}{N_2}}$$

to get:

$$\lambda_1 (N_1 + \alpha_{12} N_2)\left(\lambda_2 - \tau_2 + \tau_1 \tfrac{N_1}{N_2}\right) = \lambda_2 (N_2 + \alpha_{21} N_1)\left(\lambda_1 - \tau_1 + \tau_2 \tfrac{N_2}{N_1} - \beta_1 u\right). \tag{5.4}$$

Denoting $\frac{N_2}{N_1} = \delta$, the above equation is equivalent to

$$\mathcal{F}(\delta) \equiv a_3 \delta^3 + a_2 \delta^2 + a_1 \delta + a_0 = 0, \tag{5.5}$$

where

$$\begin{aligned} a_3 &= \lambda_2 \tau_2 > 0, \\ a_2 &= \lambda_2(\lambda_1 - \tau_1 - \beta_1 u) + \lambda_2 \alpha_{21} \tau_2 - \lambda_1 \alpha_{12}(\lambda_2 - \tau_2), \\ a_1 &= \lambda_2 \alpha_{21}(\lambda_1 - \tau_1 - \beta_1 u) - \lambda_1 \alpha_{12} \tau_1 - \lambda_1(\lambda_2 - \tau_2), \\ a_0 &= -\lambda_1 \tau_1 < 0. \end{aligned} \tag{5.6}$$

We now use the Descartes' rule of signs to determine the number of positive solutions to Equation (5.5). Depending on the signs of a_1 and a_2 we may have either one or three roots. If a_1 and a_2 are of the same sign or $a_1 < 0 < a_2$ there is only one sign change and there is only one positive root. If $a_2 < 0 < a_1$ there can be one or three positive roots. To relate back to the plain competition model, we now consider two cases: (i) $\alpha_{12}\alpha_{21} \leq 1$ and (ii) $\alpha_{12}\alpha_{21} > 1$.

Case (i): Suppose $a_1 > 0$. Then

$$\lambda_2(\lambda_1 - \tau_1 - \beta_1 u) \geq \frac{\lambda_1 \alpha_{12}(\lambda_2 - \tau_2)}{\alpha_{12}\alpha_{21}} + \frac{\lambda_1 \alpha_{12} \tau_1}{\alpha_{21}} > \lambda_1 \alpha_{12}(\lambda_2 - \tau_2) - \lambda_2 \alpha_{21} \tau_2,$$

hence $a_2 > 0$. In this case the polynomial $\mathcal{F}$ has only one positive root.

If $a_1 < 0$, by the Descartes' rule of signs, only one sign change occurs in $\mathcal{F}$ and there is only one positive root.

Case (ii): The only way there can be three roots is when $a_2 < 0 < a_1$. This is equivalent to the following constraint on the chemotherapy dose:

$$\lambda_1 - \tau_1 - \frac{\lambda_1 \alpha_{12}(\lambda_2 - \tau_2)}{\lambda_2} + \alpha_{21}\tau_2 < \beta_1 u < \lambda_1 - \tau_1 - \frac{\lambda_1(\lambda_2 - \tau_2)}{\lambda_2 \alpha_{21}} - \frac{\lambda_1 \alpha_{12} \tau_1}{\lambda_2 \alpha_{21}}. \tag{5.7}$$

In this case there may be one or three roots. In order for there to be three roots, polynomial $\mathcal{F}$ needs to have to extrema, say at $\delta_\pm$, such that $\delta_\pm > 0$. Differentiating $\mathcal{F}$ and equating it to 0 yields:

$$\delta_\pm = \frac{-a_2 \pm \sqrt{a_2^2 - 3a_1a_3}}{3a_3}$$

For $\delta_\pm$ to be both real and positive it has to be that

$$a_2^2 - 3a_1a_3 > 0.$$

In the generic case, polynomial $\mathcal{F}$ has therefore three positive roots only if the two inequalities above are satisfied and has one positive root if otherwise.

Let now $\delta = N_2/N_1$ be a positive solution of Equation (5.5). Then from the second equation of System (5.6) we get:

$$N_1 = \frac{\delta(\lambda - \tau_2) + \tau_1}{\lambda\delta(\delta + \alpha_{21})}K,$$

from where it follows that

$$N_2 = \frac{\delta(\lambda - \tau_2) + \tau_1}{\lambda(\delta + \alpha_{21})}K.$$

Substituting the above into the third equation of System (5.6) and setting

$$\kappa = \frac{\delta(\lambda - \tau_2) + \tau_1}{\lambda\delta(\delta + \alpha_{21})},$$

we get:

$$N_1^* = \kappa K^*, \qquad N_2^* = \delta\kappa K^*, \qquad K^* = \frac{(b\kappa(1+\delta) - \mu - \beta u)^{\frac{3}{2}}}{\kappa(1+\delta)d^{\frac{3}{2}}},$$

which exists positively provided $b\kappa(1+\delta) - \mu - \beta u > 0$. If this inequality is not satisfied, the chemotherapy kills endothelial cells fast enough so that the tumour cannot grow at all. As this is not biologically realistic, in what follows we will assume that:

$$\beta u < b\kappa(1+\delta) - \mu, \tag{5.8}$$

i.e. at least one positive steady state exists.

Stability

Now that we know that the system has one or three steady states we proceed to analysing their stability.

The Jacobian matrix of System (5.2) at a general point $S = (N_1, N_2, K) \in \Omega$ reads

$$\mathbf{J}(S) =$$

$$\begin{pmatrix} \lambda_1\left(1 - \frac{2N_1+\alpha_{12}N_2}{K}\right) - \tau_1 - \beta_1 u & \tau_2 - \frac{\lambda_1\alpha_{12}N_1}{K} & \frac{\lambda_1 N_1(N_1+\alpha_{12}N_2)}{K^2} \\ \tau_1 - \frac{\lambda_2\alpha_{21}N_2}{K} & \lambda_2\left(1 - \frac{2N_2+\alpha_{21}N_1}{K}\right) - \tau_2 & \frac{\lambda_2\bar{N}_2(\bar{N}_2+\alpha_{21}\bar{N}_1)}{\bar{K}^2} \\ b - \frac{2}{3}dK(N_1+N_2)^{-\frac{1}{3}} & b - \frac{2}{3}dK(N_1+N_2)^{-\frac{1}{3}} & -\mu - d(N_1+N_2)^{\frac{2}{3}} - \beta u \end{pmatrix}.$$

At the steady state, however, we may simplify the Jacobian. From the first equation in (5.6) we get

$$\lambda_1\left(1 - \kappa(1 + \alpha_{12}\delta)\right) - \tau_1 + \tau_2\delta - \beta_1 u = 0,$$

or, equivalently,

$$\lambda_1\left(1 - \kappa(2 + \alpha_{12}\delta)\right) - \tau_1 - \beta_1 u = -\lambda_1\kappa - \tau_2\delta.$$

Similarly from the second equation:

$$\lambda_2\left(1 - \kappa\delta\left(2 + \tfrac{\alpha_{21}}{\delta}\right)\right) - \tau_2 = -\lambda_2\delta\kappa - \frac{\tau_1}{\delta}.$$

From the third equation we then get:

$$-\mu - d(N_1^* + N_2^*)^{\frac{2}{3}} - \beta u = -b\kappa(1 + \delta).$$

Using the relations above we obtain the Jacobian at a steady state:

$$\mathbf{J}(S^*) = \begin{pmatrix} -\lambda_1\kappa - \tau_2\delta & -\lambda_1\alpha_{12}\kappa + \tau_2 & \lambda_1\kappa^2(1 + \delta\alpha_{12}) \\ -\lambda_2\alpha_{21}\delta\kappa + \tau_1 & -\lambda_2\delta\kappa - \frac{\tau_1}{\delta} & \lambda_2\kappa^2\delta(\delta + \alpha_{21}) \\ b - \frac{2}{3}\frac{b\kappa(1+\delta)-\mu-\beta u}{\kappa(1+\delta)} & b - \frac{2}{3}\frac{b\kappa(1+\delta)-\mu-\beta u}{\kappa(1+\delta)} & -b\kappa(1 + \delta) \end{pmatrix}.$$

The characteristic polynomial then reads:

$$\mathcal{P}(\lambda) = \lambda^3 + c_2\lambda^2 + c_1\lambda + c_0,$$

where

$$
\begin{aligned}
c_2 &= \lambda_1\kappa + \tau_2\delta + \lambda_2\delta\kappa + \frac{\tau_1}{\delta} + b\kappa(1+\delta) > 0,\\
c_1 &= \lambda_1\lambda_2\delta\kappa^2(1-\alpha_{12}\alpha_{21}) + \frac{\lambda_1\kappa\tau_1}{\delta}(1+\alpha_{12}\delta) + \lambda_2\delta\kappa\tau_2(\delta+\alpha_{21})\\
&\quad + \frac{2}{3}\frac{\kappa(b\kappa(1+\delta)-\mu-\beta u)}{(1+\delta)}(\lambda_1(1+\delta\alpha_{12}) + \lambda_2\delta(\delta+\alpha_{21}))\\
&\quad + b\kappa^2\delta(\lambda_1(1-\alpha_{12}) + \lambda_2(1-\alpha_{21})) + b\kappa(1+\delta)\left(\tau_2\delta + \frac{\tau_1}{\delta}\right),\\
c_0 &= \frac{2}{3}\kappa(b\kappa(1+\delta)-\mu-\beta u)\Big(\lambda_1\lambda_2\delta\kappa(1-\alpha_{12}\alpha_{21}) + \frac{\lambda_1\tau_1}{\delta}(1+\alpha_{12}\delta)\\
&\quad + \lambda_2\delta\tau_2(\delta+\alpha_{21})\Big).
\end{aligned}
$$

Recall that the Routh-Hurwitz criterion gives the following conditions for local stability: $c_2, c_1, c_0 > 0$ and $c_1c_2 > c_0$. We note that the resulting inequalities are in general hard to interpret biologically. Out of the four inequalities required, however, one is immediately satisfied as $c_2 > 0$. The condition $c_0 > 0$ is equivalent to

$$
\lambda_1\lambda_2\delta\kappa(1-\alpha_{12}\alpha_{21}) + \frac{\lambda_1\tau_1}{\delta}(1+\alpha_{12}\delta) + \lambda_2\delta\tau_2(\delta+\alpha_{21}) > 0. \tag{5.9}
$$

Condition $c_1 > 0$ does not have a clear biologic interpretation. However, we may formulate a slightly simpler sufficient condition for $c_1 > 0$, namely:

$$
\delta\kappa\,(\lambda_1(1-\alpha_{12}) + \lambda_2(1-\alpha_{21})) + (1+\delta)\left(\tau_2\delta + \frac{\tau_1}{\delta}\right) > 0. \tag{5.10}
$$

If now (5.9) and (5.10) above are satisfied, we have:

$$
\begin{aligned}
c_1c_2 &> b\kappa(1+\delta)\left(\lambda_1\lambda_2\delta\kappa^2(1-\alpha_{12}\alpha_{21}) + \frac{\lambda_1\kappa\tau_1}{\delta}(1+\alpha_{12}\delta) + \lambda_2\delta\kappa\tau_2(\delta+\alpha_{21})\right)\\
&> c_0,
\end{aligned}
$$

as $b\kappa(1+\delta) > \frac{2}{3}(b\kappa(1+\delta)-\mu-\beta u)$.

We note that, for example, if α_{12} and α_{21} are both smaller than 1, then the inequalities above are satisfied and there exists a single, locally stable steady state (bearing in mind condition (5.8)). If only a single steady state exists, we generally expect it to be locally stable. In general, though, the conditions for stability are hard to interpret and we refer to numerical simulations to gather further insights into model behaviour.

5.3 Numerical results

It appears that a full classification of the steady states does not immediately lead to any actionable insights from the biological perspective. In this section we explore the model properties numerically and show that it allows us to draw some conclusions about the behaviour of this biological system. In this section the majority of the parameters remain fixed (the values are summarised in Table 5.1). We will treat the chemotherapy dose u as a bifurcation parameter. We also consider different scenarios regarding the competition coefficients α_{12}, α_{21} and mutation rates τ_1 and τ_2. This is mainly to investigate which of these parameters ultimately determine model behaviour.

5.3.1 Steady states

Sample trajectories and phase portraits projected onto the (N_1, N_2) plane of System (5.2) are shown in Figure 5.1. In this plot, the chemotherapy dose is taken to be $u = 0.35$. Depending on the values of competition coefficients two cases are possible. In the first case (subplots (a) and (b)) we have $\alpha_{12} = 0.9$ and $\alpha_{21} = 1.3$ and there is a single locally stable steady state. Numerical results suggest its global stability. In the second case (subplots (c) and (d)) we take $\alpha = 0.9$ and $\alpha_{21} = 1.7$. We see that the system exhibits bistability: there are two locally stable steady states. Numerical simulations clearly show two basins of attraction separated by the black solid line as seen in subplot (d). This result is relevant from a biological perspective as we can think of the two steady states as being sensitive when $N_1 > N_2$ and resistant if otherwise. From therapeutic point of view maintaining the tumour in a sensitive phenotype is desirable.

As noted above, as well as emphasised in the previous section, the values of competition coefficients are a major factor determining system's qualitative behaviour. This observation prompted a bifurcation analysis with respect to these coefficients, a problem we studied previously in [4]. The resulting analysis is shown in Figure 5.2.

Another natural bifurcation parameter, which we can in fact control directly, is the chemotherapy dose. Figure 5.3 shows a bifurcation diagram in which the total tumour size at the steady state is plotted against the chemotherapy dose u. In Figure 5.3a the competition coefficients are chosen so that only one steady state may exist. The important conclusion to be made with regard to this Figure is that the minimum tumour size at a steady state is achieved for an intermediate dose. In Figure 5.3b, on the other hand, there exist an interval for u in which there are three steady states and the system exhibits bistability. The minimum

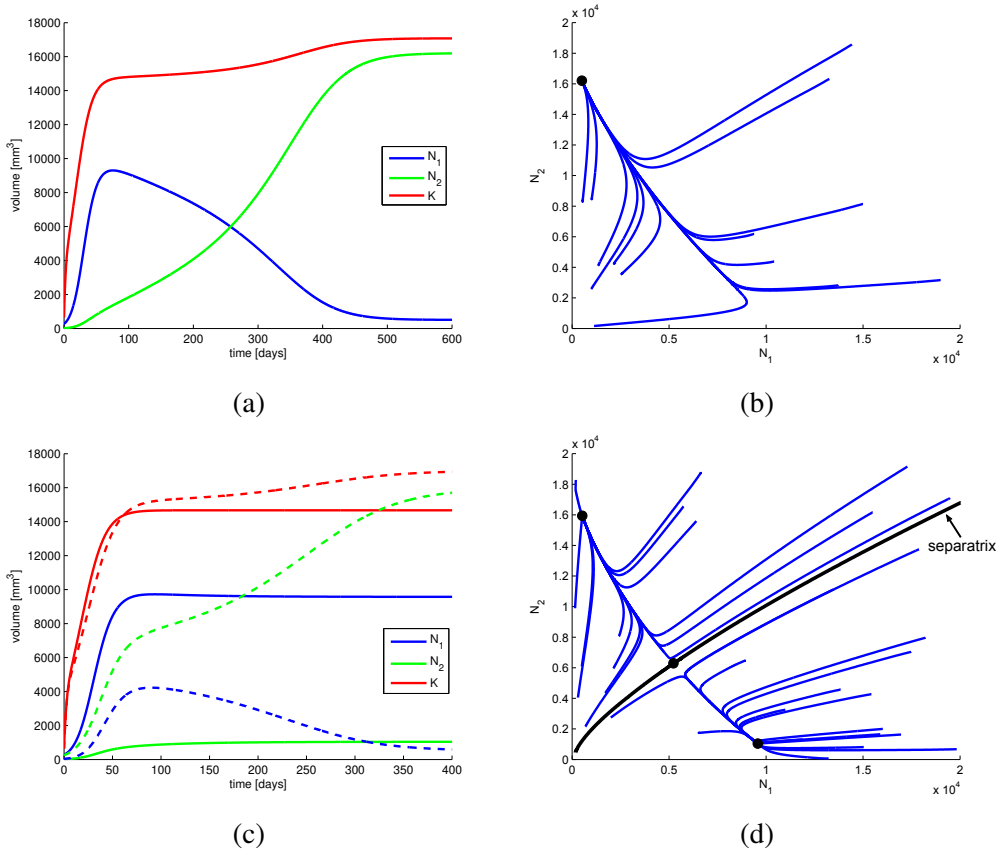

Figure 5.1: Numerical solutions and phase portraits for System (5.2), when (a), (b) $\alpha_{12} = 0.9$, $\alpha_{21} = 1.3$ and (c), (d) $\alpha_{12} = 0.9$, $\alpha_{21} = 1.7$. In (a) the initial condition is chosen as $[280, 20, 650]$, in (c) as $[280, 20, 650]$ (solid lines) and $[40, 260, 650]$ (dashed lines). Black solid line in (d) represents the separatrix. The chemotherapy dose is $u = 0.35$.

tumour volume is again achieved for an intermediate dose. However increasing the dose beyond the threshold at which the "sensitive" (blue) steady state disappears results in the discontinuous switch to the "resistant" (red) steady state. What is more, simply reverting the dose change is not enough to return to the "sensitive" steady state as the system remains in the "resistant" steady state's basin of attraction.

This phenomenon, known in general as hysteresis, is of major importance from the point of view ot chemotherapy planning. Once the critical dose is exceeded, the tumour locks in in the resistant phenotype which may be of disastrous consequences to the patient. Note that the upper bound for the chemotherapy dose $\bar{u}$ can be determined analytically: it is the right-hand side of inequality (5.7)

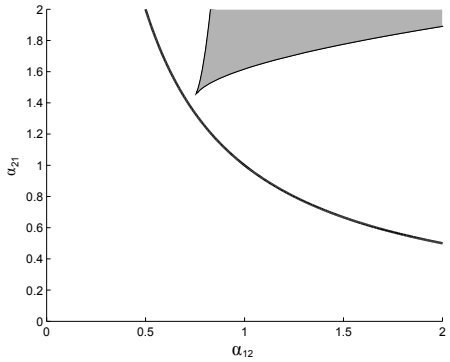

Figure 5.2: Bifurcations with respect to competition coefficients. Shadowed region shows the range of competition coefficients for which three positive steady states exist simultaneously (for $u = 0.35$). The black solid line depicts the curve $\alpha_{12}\alpha_{21} = 1$. Note that for any pair $(\alpha_{12}, \alpha_{21})$ lying below and on this line the coexistence of more than one positive steady state is not possible regardless of other model parameters (including chemotherapy dose).

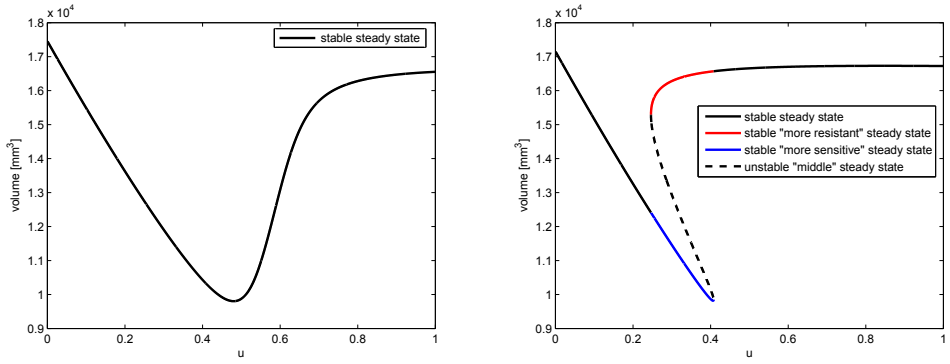

(a) (b)

Figure 5.3: Bifurcation diagrams for System (5.2). Total volume of the two cell types are plotted against a chemotherapy dose u at the steady states. Solid lines depict stability, while dashed ones instability. The parameter values are: (a) $\alpha_{12} = 0.5$ and $\alpha_{21} = 1.7$, (b) $\alpha_{12} = 0.9$ and $\alpha_{21} = 1.7$.

divided by β_1:

$$\bar{u} = \frac{1}{\beta}\left(\lambda_1 - \tau_1 - \frac{\lambda_1(\lambda_2 - \tau_2)}{\lambda_2\alpha_{21}} - \frac{\lambda_1\alpha_{12}\tau_1}{\lambda_2\alpha_{21}}\right),$$

provided, of course, that $\bar{u} \in (0, 1]$ and $\bar{u}$ is greater than the left-hand side of inequality (5.7).

5.3.2 Therapy optimisation

In this section we investigate how we can use model (5.2) to optimise therapy scheduling. We focus on optimising the schedule for long-term and for short-term time horizon. We define the long-term problem as maximisation, using constant, indefinite therapy, of patient survival defined as a time needed for the tumour to reach an arbitrary critical (fatal) volume N_{crit}. As a short-term problem we consider solving an optimal control problem analogous to that solved in previous two chapters in a time window of $T = 30$ days.

Given the uncertainty around the values of competition parameters and mutation rates, towards the end of this section we perform numerical simulations to estimate robustness of the solution to the optimal control problem. Although it is widely agreed that the emergence of ADR is due to mutations and cell competition [22, 28], the exact numerical values of the relevant parameters (i.e. α_{12}, α_{21}, τ_1 and τ_2) associated with these two processes are hard, if not impossible, to estimate. We therefore consider the following parameter range (while keeping all other parameters fixed):

$$\Lambda = \{(\alpha_{12}, \alpha_{21}, \tau_1, \tau_2) : \alpha_{12}, \alpha_{21} \in [0.5, 2] \text{ and } \tau_1, \tau_2 \in [0.001, 0.05]\}.$$

The competition parameters are assumed to be between 0.5 and 2 as any larger imbalance would result in one cell type quickly overcoming the other. The mutation rates need to be significantly lower than the proliferation rates $\lambda_{1,2}$, hence 0.05 is chosen as an upper bound. At the same time they need to be large enough to not become completely negligible (hence $\tau_{1,2} \geq 0.001$). All other parameters are set as shown in Table 5.1.

Survival time maximisation

In this subsection we focus on finding an optimal (constant) therapy dose $u \in [0, 1]$ which maximises the survival time, i.e. time needed for the tumour to reach a critical volume N_{crit}. The critical tumour volume is chosen to be $N_{\text{crit}} = 7500\ mm^3$, about 40% of the equilibrium volume for uncontrolled growth. This choice of 40% is to some degree arbitrary, but nevertheless allows us to illustrate important qualitative properties of System (5.2). Note that authors of studies adapting similar approach use various fractions of maximum volume. For example Geng et al. [25] use a ratio of ca. 8%, while Monro and Gaffney [48] use a ratio of 25%. We found that 7500 mm^3 resulted in realistic survival times in our model.

To further illustrate the benefits of intermediate dosage we extend the theoretical analysis done in the previous section and perform numerical simulations.

Table 5.1: Nominal parameter values. Parameters marked with * are varied between simulations (see text).

Name	Value		Unit	Role
λ_1	1.92	$\times 10^{-1}$	1/day	Proliferation rate of sensitive cells
λ_2	0.96	$\times 10^{-1}$	1/day	Proliferation rate of resistant cells
$^*\tau_1$	2.00	$\times 10^{-3}$	1/day	Mutation rate towards the resistant phenotype
$^*\tau_2$	1.00	$\times 10^{-3}$	1/day	Mutation rate towards the sensitive phenotype
$^*\alpha_{12}$	1.00		-	Competition coefficient
$^*\alpha_{21}$	1.00		-	Competition coefficient
μ	0.00		1/day	Natural death rate of endothelial cells
b	5.85		1/day	Vascular growth rate stimulated by cancer cells
d	8.73	$\times 10^{-3}$	$\text{day}^{-1}\text{vol}^{-2/3}$	Vascular inhibition rate by cancer cells
β_1	0.15		$\text{day}^{-1}\text{conc}^{-2/3}$	Sensitivity rate of sensitive cells to the chemotherapy agent
β	0.05		$\text{day}^{-1}\text{conc}^{-2/3}$	Sensitivity rate of the vasculature to the chemotherapy agent
ω_1	5.00			Weight for a final number of sensitive cells in the objective functional
ω_2	2.50	$\times 10^{1}$		Weight for a final number of resistant cells in the objective functional
η_1	1.00			Weight for a running number of sensitive cells in the objective functional
η_1	5.00			Weight for a running number of resistant cells in the objective functional
ξ	1.00	$\times 10^{3}$		Weight for a resistance penalty in the objective functional
ε	1.00	$\times 10^{1}$		The “margin" parameter in the resistance penalty function

We measure how much time is needed for the tumour to reach a critical volume N_{crit} for a given chemotherapy dose u. The results of this analysis are shown in Figure 5.4.

The results above have been achieved only for selected values of competition coefficients and mutation rates. In paragraphs to follow we will test their robustness by performing similar analysis across the parameter space Λ. In Figure 5.4 we show the maximum survival time and the associated dose for a given set of parameters α_{12}, α_{21} (left plot), and τ_1, τ_2 (right plot).

What can be universally seen is that there is a substantial region in each plot in which the intermediate dose is optimal. In Figure 5.4a the optimal dose is

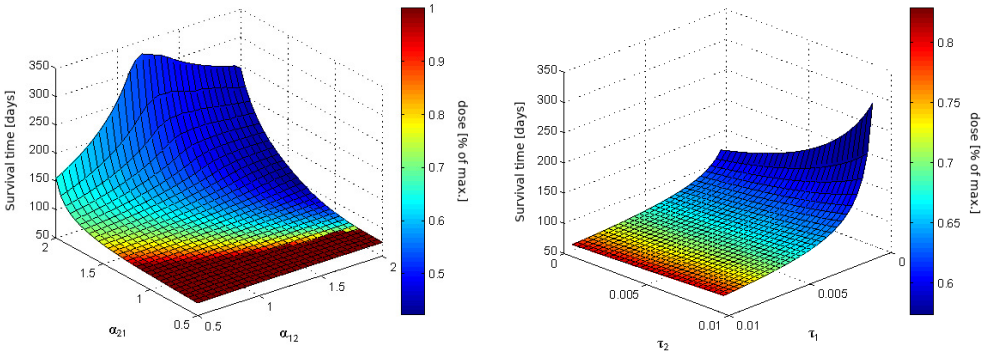

(a) (b)

Figure 5.4: Dependence of maximum survival time for System (5.2) on (a) the competition coefficients $\alpha_{12}, \alpha_{21} \in [0.5, 2]$ (here: $\tau_1 = 0.02$, $\tau_2 = 0.01$) and (b) on the mutation rates $\tau_1, \tau_2 \in [0.001, 0.01]$ (here: $\alpha_{12} = 0.9$, $\alpha_{21} = 1.7$). Colour represents the chemotherapy dose which yields the maximum survival time. The initial condition is chosen as $[280, 20, 650]$.

seen to decrease as the competition coefficients increase, with both the optimal dose and survival time being more sensitive to the value of α_{21} (i.e. the degree in which the sensitive cells suppress the resistant cells), than to α_{12}. Similarly, the survival time increases and the optimal dose decreases as τ_1 (mutation rate towards resistance) becomes smaller, while the result is less sensitive to the value of τ_2.

Optimal control problem

In this section we revisit the optimal control problem analogous to those considered in previous chapters. We look for a chemotherapy dose $u : [0, T] \to [0, 1]$ such that the objective functional J given by (5.3) is minimised subject to dynamics (5.2).

We first address the problem of existence of optimal control to this problem. The right-hand side of System (5.2) is unbounded as K approaches 0 which requires a slightly more care than the analogous proofs in previous chapters. In order not to obstruct the flow of the narrative, the proof is provided in Appendix B.

We are interested not only in a solution for selected parameter values, but rather in the robustness of the solution across all values of the competition coefficients α_{12} and α_{21} and mutation rates τ_1 and τ_2 in Λ.

To model the optimal control problem we used a Python-based open-source optimisation modelling language Pyomo (www.pyomo.org) [34, 35] with its differential algebraic equation extension Pyomo.DAE [50]. The non-linear optimi-

sation algorithm used was IPOPT (www.coin-or.org/ipopt) [74] which is an implementation of primal-dual interior point method.

By solving the optimal control problem numerically for a given quadruple $\psi \in \Lambda$ of parameters, say $\psi = (\alpha_{12}, \alpha_{21}, \tau_1, \tau_2)$, we may define a mapping

$$u_{opt} : \Lambda \times [0, T] \to [0, 1],$$

where $u_{opt}(\psi, t)$ is the value of the optimal solution to the optimal control problem for a set of parameters ψ at time t.

We now draw 400 quadruples of parameters from Λ and solved the optimal control problem numerically using the parameters drawn, obtaining a candidate for optimal control in each case. Note that, contrary to the previous chapters, no assumption is made regarding the structure of the optimal control. All parameters are assumed independent and are such that the values α_{12}, α_{21}, $\log_{10}\tau_1$, $\log_{10}\tau_2$ are uniformly distributed on the appropriate ranges. Note that we chose log-uniform distribution for τ_1 and τ_2 due to the parameter range spanning three orders of magnitude. For a given time $t \in [0, T]$ the value $u_{opt}(\psi, t)$ becomes a random variable defined on Λ and we can analyse it as such.

Given that System (5.2) is also sensitive to the choice of chemotherapy sensitivity parameters β_1 and β we repeated the above procedure for three different pairs of those parameters, namely:

$$(\beta_1, \beta) \in \{(0.45, 0.00), (0.45, 0.15), (0.15, 0.05)\}.$$

Figure 5.5 shows a distribution of u_{opt} for each of the three pairs of chemotherapy sensitivity parameters above. The left column shows the median dose together with the 15th, 25th, 75th and 85th percentile. The right column is a histogram of mean doses. In case (a) $\beta_1 = 0.45$, $\beta = 0.00$, and (b) $\beta_1 = 0.45$, $\beta = 0.15$ we see that the solution was of a form 1-singular-1 with the average singular dose being between 15% and 40% of the maximum dose. The switch to the singular dose consistently happens after around 5 days, which is perhaps due to the initial conditions being the same for all patients. If β_1 is decreased (as it is in case (c) with $\beta_1 = 0.15$ and $\beta_1 = 0.05$), then the numerically optimal dose favours a simple application of a full dose throughout the treatment window, although solutions of the form 1-singular-1 still exist.

A question which emerges from the above analysis is as follows: is there a relatively easy criterion which would allow us to determine whether to apply a "full dose" protocol (i.e. $u(t) \equiv 1$), or an "intermediate dose" 1-singular-1 protocol. To answer that question we took the numerically optimised controls and labelled them as "full dose" (average dose > 0.99) or "intermediate dose" (average dose < 0.99). We note that although the threshold was chosen arbitrarily,

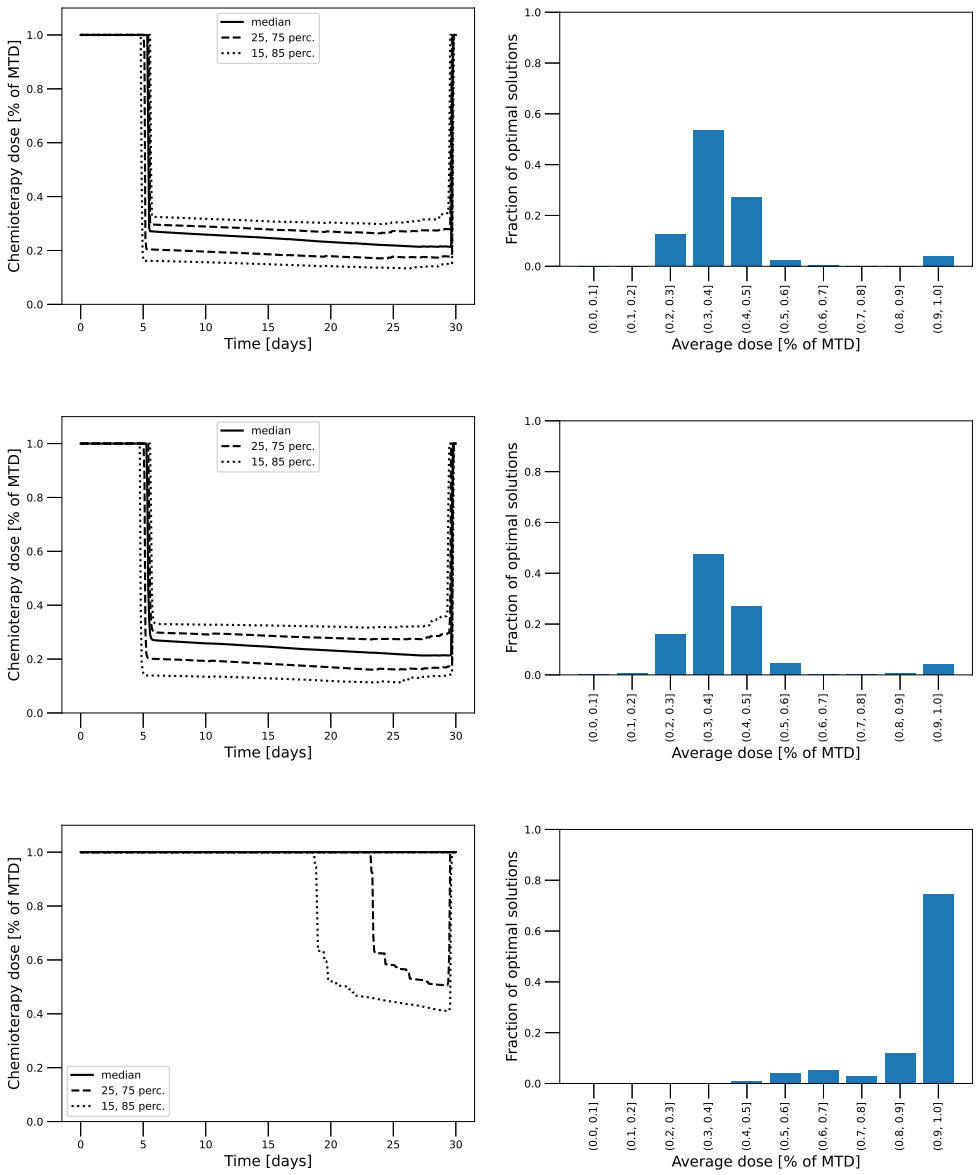

Figure 5.5: Selected percentiles of $u_{opt}(\psi, t)$ (left), and distribution of mean dose (right) among the virtual patients. The competition (α_{12}, α_{21}) and mutation (τ_1, τ_2) parameters were randomised between patients, while the remaining parameters were held constant. Results are shown for different pairs of chemotherapy sensitivity parameters: (a) $\beta_1 = 0.45$, $\beta = 0$, (b) $\beta_1 = 0.45$, $\beta = 0.15$, (c) $\beta_1 = 0.15$, $\beta = 0.05$.

there seem to be a large gap between the "intermediate dose" and "full dose" protocols as seen in the histograms in Figure 5.5. We then projected the labelled

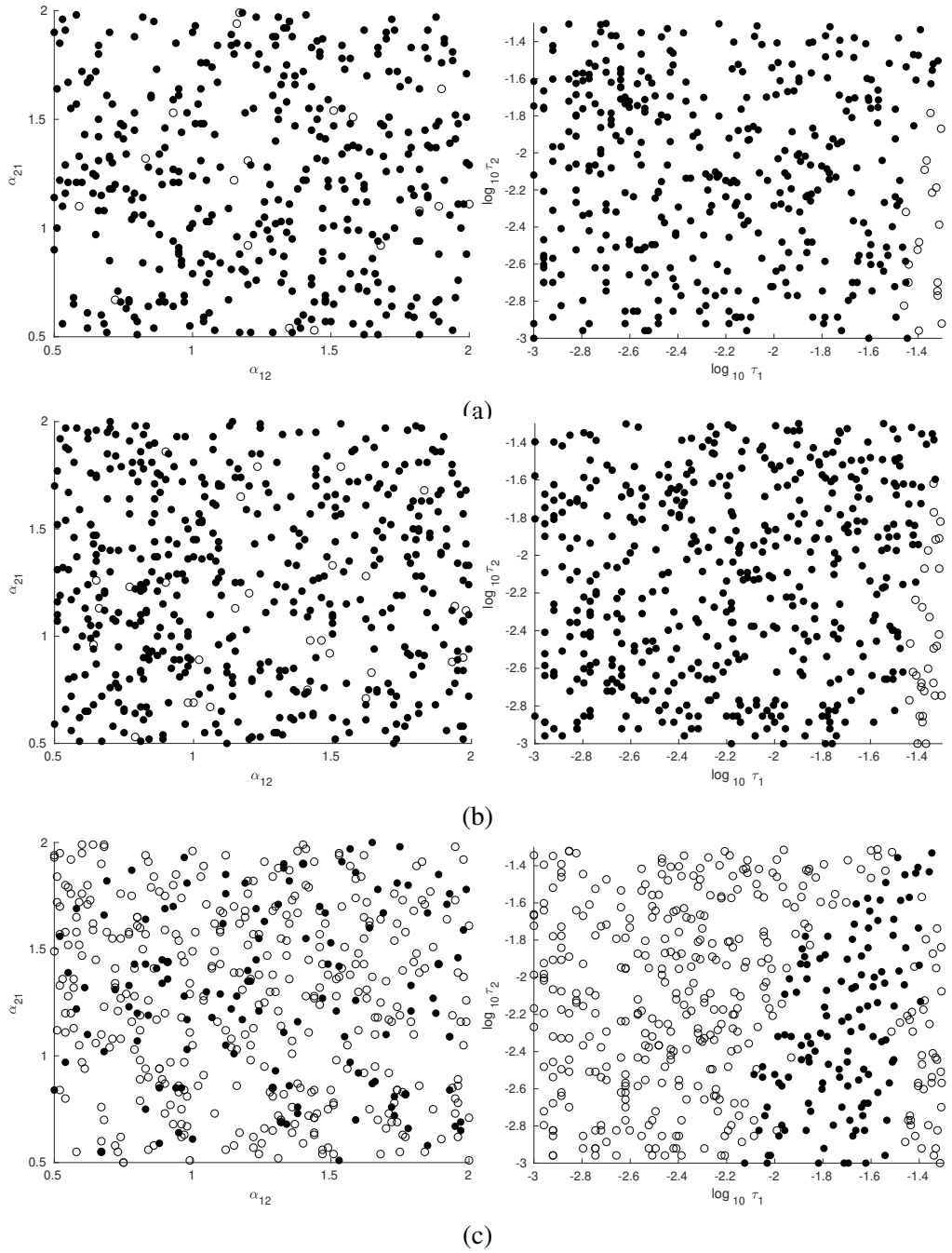

Figure 5.6: Classification of mean drug dose in numerically optimised treatments depending on randomised competition coefficients and mutation rates. Full-dose and intermediate dose protocols are labelled by empty and filled circles respectively. Results are shown for different pairs of chemotherapy sensitivity parameters: (a) $\beta_1 = 0.45, \beta = 0$, (b) $\beta_1 = 0.45, \beta = 0.15$, (c) $\beta_1 = 0.15, \beta = 0.05$.

results onto the $(\alpha_{12}, \alpha_{21})$ and (τ_1, τ_2) planes as shown in Figure 5.6. It can be observed that the competition coefficients have little effect on the decision whether to use full dose or intermediate dose protocol, while relatively clear clusters can be seen in the (τ_1, τ_2) space. In particular, regardless of other parameter values, large values of τ_1 result in full dose protocols being optimal.

5.4 Summary

The analysis performed in this chapter shows that introduction of variable carrying capacity resulted in conclusions similar to those obtained for the simplified model with $K(t) \equiv K$ (constant).

We note in particular that the introduction of competition coefficients resulted in a more complex bifurcation picture with the system exhibiting hysteresis. We showed that by exceeding a threshold dose (which can be computed analytically), under certain parameter assumptions the tumour shows a switching behaviour when it changes into a resistant phenotype in a discontinuous manner. This had not been observed in previous chapters and is of major consequence for therapy planning. It is particularly dangerous in cases when a full hysteresis loop is present and when reversing an increase in dose may not be followed by a transition back to sensitive phenotype.

The most important features of the model remain in place: optimal survival times are achieved for intermediate doses. In the range of the parameters considered the vast majority of the numerical solutions to the optimal control problem remain of the form 1-singular-1. This suggests that the results from Chapter 3 concerning the structure of optimal control remain valid.

Introduction of a variable carrying capacity $K(t)$ into the model serves yet another purpose: it is now possible to model the effects of chemotherapy on the vasculature. This is important from a biological perspective, as chemotherapy is not selective and affects endothelial cells as well as cancer cells [38]. Even more importantly, this also opens an entirely new avenue for investigation of combined (e.g. chemotherapy and anti-angiogenic) therapies. This adds another layer of complexity to the mathematical models, as the subtle interplay between those two therapies is very counter-intuitive [37], as preliminarily investigated by us in [3].

We pay particular attention to the values of competition coefficients and mutation rates. Since we do not have access to any database of patients to perform parameter fitting, we largely relay on values present in the literature. It is therefore crucial for us to test how the candidate for optimal solution behaves when

the parameter values change. This is to avoid a pitfall of taking a very "special" set of parameter values which just happens to yield a solution involving a singular interval. By testing the conclusions over a fairly exhaustive subset of the parameter space we remain confident that the structure of the numerical solution is a property not of the parameter values, but rather that of the structure of the system itself.

We also observe certain patterns with respect to the dependence of the solution on the mutation rates (but no similar patterns were found for competition coefficients). In particular, as seen in Figure 5.6, when the mutation rate towards resistance is large, then the optimal solution appears to be to apply a full dose protocol. This is in line with our intuition: if the cells mutate quickly towards resistance, we cannot possibly stop the tumour from growing using chemotherapy anyway, so the least we can do is to kill as many cells as we possibly can. If the mutation towards resistance is lower, maintaining a certain level of the sensitive subpopulation is beneficial as it prevents the resistant subpopulation from growing.

We were unable to formally show that the 1-singular-1 protocol is really theoretically optimal. Nevertheless the numerical results suggest that in a wide range of scenarios it achieves better performance than the bang-bang protocols with a comparable number of switches. In particular, it maintains the tumour in a chemo-sensitive state, thus supporting the hypothesis

In conclusion, we show that even in the extended model with varying carrying capacity, the raise in chemoresistant subpopulation may be stopped (or at least delayed) by using intermediate dosage. That conclusion remains largely valid, regardless of the parameters which quantify the relationships (i.e. competition and mutations) between the two types of cells.

Chapter 6

Conclusions

In this dissertation we developed a mathematical model of drug-resistant tumour growth under angiogenic signalling. This was done in order to test whether by using appropriate drug dosage one can mitigate the risk of the tumour becoming resistant. The primary tool for this task was a theory of dynamical systems of mathematical ecology, in particular ordinary differential equations. In addition, we applied the optimal control theory framework to address the issue of drug resistance.

We have found that by introducing an additional term in objective functional we can shift the therapeutic focus from maximising cell kill to minimising drug resistance. This was done to align the objectives set out in the mathematical framework with the research hypothesis, as well as the new trends in therapeutic paradigms, i.e. the metronomic therapy. The additional term, the "penalty for resistance", was verified to serve its intended purpose, i.e. maintained the tumour in the drug sensitive state.

By analysing the optimal control problem we showed that the penalty for resistance resulted in the intermediate drug doses yielding better value of the performance index than full-dose (or bang-bang) dosage strategies. We were able to compute an analytic formula for the intermediate (or singular) doses. Such a formula can serve as a starting point for mathematically driven experiment design. We also used the fact that such formula can be derived explicitly to extend an existing numerical method of solving optimal control problems which was previously applicable solely to problems with bang-bang solutions.

While we were unable to formally show that intermediate doses are truly optimal, the numerical method has shown that dosage strategies incorporating an intermediate (singular) dose interval outperform the bang-bang controls. This

assertion was tested for controls with up to five control switches. We note that although it is possible that even better strategy exists among the controls with a greater number of switches, they were excluded from our analysis on the grounds that they would be impractical to apply in clinical setting. Furthermore, the numerically computed strategies achieve our goal of maintaining the tumour in a drug-sensitive state.

Numerical optimality of intermediate drug doses is a property which has been largely consistent among the three mathematical models considered, thus suggesting robustness of the result. Furthermore, we analysed how sensitive the numerically optimised control is to the parameters which quantify the relations between the sensitive and resistant cells, i.e. the competition coefficients and mutation rates. We found that the mutation rates play a decisive role in determining which of the full-dose or intermediate dose protocols is better.

The optimal control numerical results are consistent with the simplified analysis performed under an assumption of constant, indefinite chemotherapy. Optimal survival times for virtual patients were achieved for intermediate drug doses. What is more, we found that systems describing drug-resistant tumour growth exhibit hysteresis with respect to the chemotherapy dose which is major importance from the clinical perspective. What is more, the mathematical analysis suggests that the hysteresis is a result of a difference in competitive effects exerted by one cell type on the other, rather than other mechanisms (e.g. mutations).

Note that the models described in this thesis essentially have a "building block" structure in the sense that it is relatively easy to add new elements, e.g. another types of therapies. This would result in models of combined therapies – an example of such model, combining chemiotherapy and radiation, has been studied by us in the context of optimal control in [6, 7].

We close these remarks by concluding that mathematical modelling supports the hypothesis that the risk of drug resistance can be mitigated by appropriate chemotherapy dosing, as is evident both from qualitative analysis of the differential equations, as well as the results from optimal control theory. The next steps would be to verify these theoretical results in an experimental setting and to fine-tune the model using experimental data.

Bibliography

[1] N. André, L. Padovani, and E. Pasquier. Metronomic scheduling of anticancer treatment: the next generation of multitarget therapy? *Fut. Oncology*, 7(3):385–394, 2011. [citation on page 3]

[2] R. Araujo and R. McElwain. A history of the study of solid tumour growth: the contribution of mathematical modelling. *Bulletin of Mathematical Biology*, 66:1039–1091, 2004. [citation on page 1 and 2]

[3] P. Bajger and M. Bodzioch. Mathematical model of endothelial cell proliferation and maturation. *Mathematica Applicanda*, 46:3–12, 2018. [citation on page 76]

[4] P. Bajger, M. Bodzioch, and U. Foryś. Role of cell competition in acquired chemotherapy resistance. *Proceedings of the 16th Conference on Computational and Mathematical Methods in Science and Engineering*, 1:132–141, 2016. [citation on page 67]

[5] P. Bajger, M. Bodzioch, and U. Foryś. Singularity of controls in a simple model of acquired chemotherapy resistance. *Discrete and Continuous Dynamical Systems Series B*, 24(5):2039–2052, 2019. [citation on page 15 and 91]

[6] P. Bajger, K. Fujarewicz, and A. Świerniak. Optimal control in a model of chemotherapy-induced radiosensilisation. *Submitted to Mathematica Applicanda*. [citation on page 80]

[7] P. Bajger, K. Fujarewicz, and A. Świerniak. Effects of pharmacokinetics and DNA repair on the structure of optimal controls in a simple model of radiochemotherapy. *2018 23rd International Conference on Methods & Models in Automation & Robotics (MMAR)*, 2018. [citation on page 15 and 80]

[8] I. Bendixson. Sur les courbes définies par des équations différentielles. *Acta Mathematica*, 24:1–88, 1901. [citation on page 20, 22, and 50]

[9] M. Bodnar and U. Foryś. Three types of simple DDE's describing tumor growth. *Journal of Biological Systems*, 15:1–19, 2007. [citation on page 60]

[10] A. Boumendjel, J. Boutonnat, and J. Robert. *ABC Transporters and Multidrug Resistance*. Wiley, 2009. [citation on page 10]

[11] F. Bray, J. Ferlay, I. Soerjomataram, R. Siegel, L. Torre, and A. Jemal. Global cancer statistics 2018: GLOBOCAN estimates of incidence and mortality worldwide for 36 cancers in 185 countries. *CA: A Cancer Journal for Clinicians*, 68:394–424, 2018. [citation on page 1]

[12] A. Bressan and B. Picolli. *Introduction to the Mathematical Theory of Control*. AIMS, 2007. [citation on page 23 and 24]

[13] R. Cagan and P. Meyer. Rethinking cancer: current challenges and opportunities in cancer research. *Disease Models & Mechanisms*, 10:349–352, 2017. [citation on page 1]

[14] L. Cesari. *Optimization – Theory and Applications*. Springer, 1983. [citation on page 23 and 24]

[15] R. H. Chisholm, T. Lorenzi, and J. Clairambault. Cell population heterogeneity and evolution towards drug resistance in cancer: Biological and mathematical assessment, theoretical treatment optimisation. *Biochimica et Biophysica Acta (BBA) - General Subjects*, 1860(11, Part B):2627 – 2645, 2016. Systems Genetics - Deciphering the Complex Disease with a Systems Approach. [citation on page 2 and 45]

[16] M. Clynes. *Multiple Drug Reistance in Cancer 2: Molecular, Cellular and Clinical Aspects*. Kluwer Academic, Boston, 2000. [citation on page 10]

[17] V. DeVita and E. Chu. A history of cancer chemotherapy. *Cancer Research*, 68:8643–8653, 2008. [citation on page 9]

[18] A. d'Onofrio, A. Gandolfi, and A. Rocca. The dynamics of tumour-vasculature interaction suggests low-dose, time-dense anti-agniogenic schedulings. *Cell Proliferation*, 42:317–329, 2009. [citation on page 60]

[19] S. Farber. Some observations on the effect of folic acid antagonists on acute leukemia and other forms of incurable cancer. *Blood*, 4:160–167, 1949. [citation on page 9]

[20] J. Ferlay, M. Colombet, I. Soerjomataram, and et al. Global and regional estimates of the incidence and mortality for 38 cancers: GLOBOCAN 2018, 2018. [citation on page 1]

[21] M. Folkman, D. Long, and F. Becker. Growth and metastasis of tumor in organ culture. *Cancer*, 16:453–467, 1963. [citation on page 2 and 8]

[22] J. Foo and F. Michor. Evolution of acquired resistance to anti-cancertherapy. *Journal of Theoretical Biology*, 355:10–20, 2014. [citation on page 2, 8, 9, 10, 45, 59, and 70]

[23] J. Furth and M. Khan. The transmission of leukemia to mice with a single cell. *American Journal of Cancer*, 31:276–282, 1937. [citation on page 9]

[24] R. Gatenby and P. Maini. Mathematical oncology: Cancer summed up. *Nature*, 421:321–321, 2003. [citation on page 1]

[25] C. Geng, H. Paganetti, and C. Grassberger. Prediction of treatment response for combined chemo- and radiation therapy for non-small cell lung cancer patients using a bio-mathematical model. *Sci Rep*, 7, 12 2017. [citation on page 70]

[26] B. Gompertz. On the nature of the function expressive of the law of human mortality, and on a new mode of determining the value of life contingencies. *Philosophical Transactions of the Royal Society*, 115:513–585, 1825. [citation on page 12]

[27] L. Goodman, M. Wintrobe, W. Damshek, and M. Goodman. Nitrogen mustard therapy. *Journal of American Medical Association*, 132:126–132, 1946. [citation on page 9]

[28] M. Gottesman. Mechanisms of cancer drug resistance. *Annual Review of Medicine*, 53:615–627, 2002. [citation on page 2, 8, 10, 45, 59, and 70]

[29] P. Hahnfeldt, J. Folkman, and L. Hlatky. Minimizing long-term tumor burden: The logic for metronomic chemotherapeutic dosing and its antiangiogenic basis. *Journal of Theoretical Biology*, 220(4):545 – 554, 2003. [citation on page 2]

[30] P. Hahnfeldt, D. Panigrahy, J. Folkman, and L. Hlatky. Tumor development under angiogenic signaling: A dynamical theory of tumor growth, treatment response, and postvascular dormancy. *Cancer Research*, 59:4770–4775, 1999. [citation on page 60 and 61]

[31] D. Hanahan, G. Bergers, and E. Bergsland. Less is more, regularly: metronomic dosing of cytotoxic drugs can target tumor angiogenesis in mice. *J. Clin. Invest.*, 105(8):1045–1047, 2000. [citation on page 3 and 26]

[32] D. Hanahan and R. Weinberg. The hallmarks of cancer. *Cell*, 100:57–70, 2000. [citation on page 7]

[33] D. Hanahan and R. Weinberg. Hallmarks of cancer: The new generation. *Cell*, 144:646–674, 2011. [citation on page 7, 8, and 97]

[34] W. E. Hart, C. D. Laird, J.-P. Watson, D. L. Woodruff, G. A. Hackebeil, B. L. Nicholson, and J. D. Siirola. *Pyomo–optimization modeling in python*, volume 67. Springer Science & Business Media, second edition, 2017. [citation on page 15 and 72]

[35] W. E. Hart, J.-P. Watson, and D. L. Woodruff. Pyomo: modeling and solving mathematical programs in python. *Mathematical Programming Computation*, 3(3):219–260, 2011. [citation on page 15 and 72]

[36] G. Housman, S. Byler, S. Heerboth, K. Lapinska, M. Longacre, N. Snyder, and S. Sarkar. Drug resistance in cancer: An overview. *Cancers*, 6(3):1769–1792, sep 2014. [citation on page 10 and 45]

[37] R. Jain. Normalization of tumor vasculature: An emerging concept in antiangiogenic therapy. *Science*, 307:58–62, 2005. [citation on page 2, 8, and 76]

[38] I. Kareva, D. Waxman, and G. Klement. Metronomic chemotherapy: An attractive alternative to maximum tolerated dose therapy that can activate anti-tumor immunity and minimize therapeutic resistance. *Cancer Letters*, 358:100–106, 2015. [citation on page 9, 10, 11, 60, and 76]

[39] A. Laird. Dynamics of tumor growth. *British Journal of Cancer*, 18:490–502, 1964. [citation on page 12]

[40] A. Laird. Dynamics of tumor growth: comparison of growth rates and extrapolation of growth curve to one cell. *British Journal of Cancer*, 19:278–291, 1965. [citation on page 12]

[41] A. Lasota, M. Mackey, and M. Ważewska-Czyżewska. Minimizing therapeutically induced anemia. *Journal of Mathematical Biology*, 13:149–158, 1981. [citation on page 2]

[42] U. Ledewicz and H. Schättler. *Optimal Control for Mathematical Models of Cancer Therapies*. Springer, 2015. [citation on page 14, 15, 26, 30, 31, and 32]

[43] U. Ledzewicz and H. Schättler. Optimal bang-bang controls for a two-compartment model in cancer chemotherapy. *Journal of Optimization Theory and Applications*, 114(3):609–637, Sep 2002. [citation on page 11 and 15]

[44] U. Ledzewicz and H. Schättler. Drug resistance in cancer chemotherapy as an optimal control problem. *Discr. Cont. Dyn. Syst., Ser. B*, 6:129–150, 2006. [citation on page 2, 17, 18, 26, 31, 46, and 52]

[45] E. Lindelöf. Sur l'application de la mèthode des approximations successives aux èquations diffèrentielles ordinaires du premier ordre. *Comptes rendus hebdomadaires des séances de l'Académie des sciences*, 116:454–457, 1894. [citation on page 19]

[46] T. Malthus. *An Essay on the Principle ofPopulation*. 1798. [citation on page 11]

[47] F. Michor and K. Beal. Improving cancer treatmentvia mathematical modeling: Surmounting the challenges is worth the effort. *Cell*, 163:1059–1063, 2015. [citation on page 2]

[48] H. Monro and E. Gaffney. Modelling chemotherapy resistance in palliation and failed cure. *Journal of Theoretical Biology*, 257:292–302, 2009. [citation on page 2, 9, 17, 18, 46, and 70]

[49] J. Murray. *Mathematical Biology I. An introduction.* Springer, 2002. [citation on page 1, 2, 14, 18, and 60]

[50] B. Nicholson, J. D. Siirola, J.-P. Watson, V. M. Zavala, and L. T. Biegler. pyomo.dae: a modeling and automatic discretization framework for optimization with differential and algebraic equations. *Mathematical Programming Computation*, 10(2):187–223, 2018. [citation on page 15 and 72]

[51] E. Pasquier, M. Kavallaris, and N. André. Metronomic chemotherapy: new rationale for new directions. *Nat. Rev. Clin. Onc.*, 7:455–465, 2010. [citation on page 26]

[52] L. Pecorino. *Molecular Biology of Cancer. Mechanisms, targets and therapeutics*. Oxford University Press, 2012. [citation on page 7]

[53] J. Poleszczuk, M. Bodnar, and U. Foryś. New approach to modeling of antiangiogenic treatment on the basis of Hahnfeldt et al. model. *Proceedings of the XVII National Conference of Applications of Mathematics in Biology and Medicine*, pages 591–603, 2011. [citation on page 60]

[54] J. Poleszczuk and I. Skrzypczak. Tumor angiogenesis model with variable vessels' effectiveness. *Applicationes Mathematicae*, 38:33–49, 2011. [citation on page 60]

[55] L. Pontryagin, V. Boltyanskii, R. Gamkrelidze, and E. Mishchenko. *The Mathematical Theory of Optimal Processes*. MacMillan, New York, 1964. [citation on page 29]

[56] D. Ribatti. Judah folkman, a pioneer in the study of angiogenesis. *Angiogenesis*, 11:3–10, 2008. [citation on page 2 and 60]

[57] P. Savage, J. Stebbing, M. Bower, and T. Crook. Why does cytotoxic chemotherapy cure only some cancers? *Nat Clin Pract Oncol*, 6(1):43–52, 2009. [citation on page 9 and 26]

[58] O. Scharovsky, L. Mainetti, and V. Rozados. Metronomic therapy: changing the paradigm that more is better. *Curr Oncol*, 16(2):7–15, 2009. [citation on page 10 and 26]

[59] R. Simon and L. Norton. The Norton-Simon hypothesis: designing more effective and less toxic chemotherapeutic regimens. *Nature Clinical Practice Oncology*, 3:406–407, 2006. [citation on page 9]

[60] P. Skehan. On the normality of growth dynamics of neoplasms *in vivo*: a data base analysis. *Growth*, 50:496–515, 1986. [citation on page 12]

[61] H. Skipper, F. Schabel, and W. Wilcox. Experimental evaluation of potential anticancer agents. XII. on the criteria and kinetics associated with "curability" of experimental leukemia. *Cancer Chemotherapy Records*, 35:1–111, 1964. [citation on page 9]

[62] J. Śmieja and A. Świerniak. Different models of chemotherapy taking into account drug resistance stemming from gene amplification. *International Journal of Applied Mathematics and Computer Science*, 13(3):297–305, 2003. [citation on page 2 and 46]

[63] J. Śmieja, A. Świerniak, and Z. Duda. Gradient method for finding optimal scheduling in infinite dimensional models of chemotherapy. *Journal of Theoretical Medicine*, 3:25–36, 2000. [citation on page 15, 40, 46, and 91]

[64] J. Spratt, J. Meyer, and J. Spratt. Rates of growth of human neoplasms: part II. *Journal of Surgical Oncology*, 61:68–83, 1996. [citation on page 12]

[65] G. Swan. Role of optimal control in cancer chemotherapy. *Math. Biosci.*, 101:237–284, 1990. [citation on page 14 and 18]

[66] A. Świerniak. Direct and indirect control of cancer populations. *Bulletin of Polish Academy of Sciences*, 56:367–378, 2008. [citation on page 46]

[67] A. Świerniak, M. Kimmel, J. Śmieja, K. Puszyński, and K. Psiuk-Maksymowicz. *System Engineering Approach to Planning Anticancer Therapies*. Springer, 2016. [citation on page 14]

[68] A. Świerniak, A. Polański, J. Śmieja, and M. Kimmel. Modelling growth of drug resistant cancer populations as the system with positive feedback. *Math Comput Model*, 37(11):1245 – 1252, 2003. Modeling and Simulation of Tumor Development, Treatment, and Control. [citation on page 2 and 52]

[69] A. Świerniak and J. Śmieja. Cancer chemotherapy optimization under evolving drug resistance. *Nonlin. Anal.*, 47:375–386, 2000. [citation on page 11 and 15]

[70] Y. Tamazali and J. Kemp-Symonds. Principles of oncological therapy. *Clinical Equine Oncology*, pages 118–197, 2015. [citation on page 9]

[71] A. Tsoularis and J. Wallace. Analysis of logistic growth moddels. *Mathematical Biosciences*, 179(1):21–55, 2002. [citation on page 12]

[72] J. Vargas, E. Stanzl, N. Teng, and P. A.Wender. Cell-penetrating, guanidinium-rich molecular transporters forovercoming efflux-mediated multidrug resistance. *Molecular Pharmaceutics*, 11:2553–2565, 2014. [citation on page 10 and 97]

[73] P.-F. Verhulst. Researches mathématiques sur la loi d'accroissement de la population. *Nouv. mém. de l'Academie Royale de Sci. et Belles-Lettres de Bruxelles*, 18:1–41, 1845. [citation on page 11 and 18]

[74] A. Wächter and L. Biegler. On the implementation of an interior-point filter line-search algorithm for large-scale nonlinear programming. *Mathematical Programming*, 106:25–57, 2006. [citation on page 73]

Appendices

Appendix A

Numerical Method

For the purpose of solving the optimal control problem formulated in Chapters 3 and 4 we extended (see [5]) the gradient method proposed by Śmieja et al. [63]. In their paper, Śmieja et al. introduced an iterative method for computing optimal switching times for bang-bang control problems. By computing a gradient with respect to the switching times they turned the problem into a finite dimensional optimisation task (provided the number of switches is fixed).

Their method, however, relied on the fact that a local perturbation to a switching time in a bang-bang control alters the control only locally. In case of singular controls, altering a switching time which occurs prior to a switch to a singular control will make the trajectory follow a different singular arc and, as a result, have a non-local effect on the control.

Our method relies on the fact that in two-dimensional problems in Chapters 3 and 4 we can compute the singular control and arcs as feedback functions of the state variables. This may not be possible in general, but we note that for two-dimensional problems this should be doable as the adjoint variables can be eliminated from the resulting algebraic equations.

The method can be described as follows. Suppose that the structure of a control is fixed. By structure of the control we understand a finite sequence with elements from the set 0, 1, s which correspond respectively to an application of no dose, full dose and a (pre-computed) singular dose. By fixing the structure of the control, the optimisation problem now becomes a problem of finding optimal switching times, as the values of the singular control have been computed as a feedback function of state variables and are known. With a slight abuse of notation we can redefine the objective functional as a function of the switching

times:

$$J = J(t_1, t_2, ..., t_{n-1}), \qquad \text{with } 0 = t_0 < t_1 < t_2 < ... < t_n = T,$$

where T is a fixed terminal time. The gradient with respect to the switching times can then be approximated (e.g. by finite differences). The optimisation procedure can then be defined as follows: starting with switching times $\mathbf{t}^{(0)} = (t_1^{(0)}, ..., t_{n-1}^{(0)})$, $k = 0$ and a suitable learning rate α, we update the switching times iteratively:

1. Compute the gradient $\nabla J(\mathbf{t}^{(k)})$ (e.g. using finite differences).
2. Set $\mathbf{t}^{(k+1)} := \mathbf{t}^{(k)} - \alpha \nabla J(\mathbf{t}^{(k)})$ and $k := k + 1$.
3. Repeat Steps 1 and 2 until a prescribed tolerance has been reached.

This method is suitable for finding local minima. To ensure robustness we ran the method with different initial structures and switching times to ensure that a true minimum is found. As part of the procedure we also verify numerically that the resulting control and corresponding trajectory and co-trajectory satisfy the requirements of the Pontryagin minimum principle.

Note that this method yields best-in-class controls, i.e. optimal switching times for a given control structure, rather than converging to the theoretically optimal solution of the optimal control problem.

Appendix B

Mathematical Proofs

B.1 Proof of Proposition 13

This Appendix contains the proof of Proposition 13 from Chapter 4. We first set up the notational prerequisites. Let us define

$$\mathbf{n} = (n_1, n_2)^T, \qquad \mathbf{p} = (p_1, p_2)^T$$

and

$$\mathbf{f}(\mathbf{n}) = \begin{pmatrix} f_1(n_1, n_2) \\ f_2(n_1, n_2) \end{pmatrix} = \begin{pmatrix} \lambda_1 n_1(1 - n_1 - n_2) - \tau_1 n_1 + \tau_2 n_2 \\ \lambda_2 n_2(1 - n_2 - n_1) + \tau_1 n_1 - \tau_2 n_2 \end{pmatrix}, \qquad \mathbf{g}(\mathbf{n}) = \begin{pmatrix} -n_1 \\ 0 \end{pmatrix}$$

and

$$L(\mathbf{n}, u) = \eta_1 n_1 + \eta_2 n_2 + \xi G(\tfrac{n_2 - n_1}{\varepsilon}).$$

We furthermore repeat the definition of Hamiltonian (4.4) and switching function for reference:

$$\begin{aligned} &H(\mathbf{p}, \mathbf{n}, u) = \mathbf{p}^T (\mathbf{f}(\mathbf{n}) + \mathbf{g}(\mathbf{n})u) + L(\mathbf{n}, u) \\ &= p_1\Big(\lambda_1 n_1 (1 - n_1 - n_2) - \tau_1 n_1 + \tau_2 n_2 - n_1 u\Big) \\ &\quad + p_2\Big(\lambda_2 n_2 (1 - n_1 - n_2) + \tau_1 n_1 - \tau_2 n_2\Big) + \eta_1 n_1 + \eta_2 n_2 + \xi G(\tfrac{n_2 - n_1}{\varepsilon}) \end{aligned}$$

and

$$\varphi(t) = \frac{\partial H}{\partial u} = -p_1(t) n_1(t).$$

We also note that the following relationships hold:

$$[\mathbf{f}, \mathbf{g}] = \begin{pmatrix} -\lambda_1 n_1^2 - \tau_2 n_2 \\ -\lambda_2 n_1 n_2 + \tau_1 n_1 \end{pmatrix}, \qquad [\mathbf{g}, [\mathbf{f}, \mathbf{g}]] = -[\mathbf{f}, \mathbf{g}]. \tag{B.1}$$

Equipped with this notation we can now give prove Proposition 13.

Proof. If a control is singular on an interval $I \subset [0,T]$, then $\varphi \equiv \dot{\varphi} \equiv \ddot{\varphi} \equiv ... \equiv 0$ identically on I. Furthermore, by the Pontryagin Minimum Principle, it must be that $H \equiv c = \text{const}$. In particular, the following three relations must hold for almost all t in I:

$$c = H, \qquad 0 = \varphi = \dot{\varphi} = \ddot{\varphi} \tag{B.2}$$

for some constant $c \in \mathbb{R}$. Equations (4.6) and (4.7) may be obtained by directly solving the above system for p_1, p_2 and u in terms of n_1 and n_2.

If the control is singular over an interval $I \subset [0,T]$ we immediately get, using Equation (4.5), that

$$0 = \varphi = -p_1 n_1 \implies p_1 = 0.$$

Using this and (B.1) we get from $\dot{\varphi} = 0$ that

$$p_2 \left(\lambda_2 n_2 - \tau_1\right) = \eta_1 - \tfrac{\xi}{\epsilon} G'(\tfrac{n_2 - n_1}{\varepsilon}),$$

that is:

$$p_2 = \frac{\eta_1 - \frac{\xi}{\epsilon} G'(\frac{n_2 - n_1}{\varepsilon})}{\lambda_2 n_2 - \tau_1},$$

at least away from $n_2 = \tau_1/\lambda_2$.

Substituting the above into Equation (4.4) for H and equating the resulting expression to 0 yields (4.7), the required equation for the singular arc.

Similarly a substitution of p_1, p_2 into $\ddot{\varphi} = 0$ results in (4.6), the equation for the singular control as a feedback function of the state variables.

The Legendre-Clebsch condition may be obtained quite elegantly: from Equations (3.10) and (B.1) it follows that

$$\begin{aligned}
\frac{\partial}{\partial u}\left(\frac{\partial^2 \varphi}{\partial t^2}\right) &= \left(\mathbf{p}^{\mathrm{T}}[\mathbf{g},[\mathbf{f},\mathbf{g}]] - \frac{\partial L}{\partial \mathbf{n}}^{\mathrm{T}} \frac{\partial \mathbf{g}}{\partial \mathbf{n}}\mathbf{g} - \mathbf{g}^{\mathrm{T}} \frac{\partial^2 L}{\partial \mathbf{n}^2}\mathbf{g}\right) \\
&= \left(- \mathbf{p}^{\mathrm{T}}[\mathbf{f},\mathbf{g}] + \frac{\partial L}{\partial \mathbf{n}}^{\mathrm{T}} \mathbf{g} - \mathbf{g}^{\mathrm{T}} \frac{\partial^2 L}{\partial \mathbf{n}^2}\mathbf{g}\right), \qquad \text{using } \dot{\varphi} = 0, \\
&= -\mathbf{g}^{\mathrm{T}} \frac{\partial^2 L}{\partial \mathbf{n}^2}\mathbf{g} = -\frac{n_1^2}{\epsilon^2} \xi G''(\tfrac{n_2 - n_1}{\varepsilon}).
\end{aligned}$$

Using the properties of G, we see that the Legendre-Clebsch condition $(-1)^1 \frac{\partial}{\partial u}\frac{\partial^2}{\partial t^2}\varphi > 0$ is satisfied if and only if $n_1 > n_2$. □

B.2 Proof of Existence of Optimal Control Solution to Problem in Chapter 5

In this chapter we address the problem of existence of solution of minimising the objective functional (5.3) subject do dynamics (5.2). We will use the notation

established in Section 3.3.1. The challenge in this proof is to find appropriate sets Γ and A. We will make use of the following Lemma:

Lemma 2. *For any initial data (N_1^0, N_2^0, K^0) there exist positive constants N_T and K_T, K^T such that any admissible trajectory (N_1, N_2, K) of System (5.2) starting at (N_1^0, N_2^0, K^0) satisfies*

$$(N_1(t), N_2(t), K(t)) \in \left\{(N_1, N_2, K) : 0 \leq N_1 + N_2 \leq N_T \text{ and } K_T \leq K \leq K^T\right\}$$

for all $t \in [0, T]$.

Proof. Notice that we have already shown that all trajectories starting with $N_1^0, N_2^0 \geq 0$ and $K^0 > 0$ remain non-negative. We also have:

$$\dot{N}_1(t) + \dot{N}_2(t) \leq \lambda_1 N_1(t) + \lambda_2 N_2(t)$$

for all $t \in [0, T]$, so clearly

$$N_1(t) + N_2(t) \leq \left(N_1^0 + N_2^0\right) e^{\bar{\lambda} T} := N_T$$

for all $t \in [0, T]$, where $\bar{\lambda} = \max(\lambda_1, \lambda_2)$.

Furthermore we have:

$$\begin{aligned}\dot{K}(t) &= -\mu K(t) + b(N_1(t) + N_2(t)) - d(N_1(t) + N_2(t))^{2/3} K(t) - \beta K(t) u(t) \\ &\leq b(N_1(t) + N_2(t)) \\ &\leq b N_T\end{aligned}$$

for all $t \in [0, T]$, so

$$K(t) \leq bTN_T + K^0 := K^T$$

for $t \in [0, T]$.

Likewise,

$$\begin{aligned}\dot{K}(t) &\geq -\left(\mu + d(N_1(t) + N_2(t))^{2/3} + \beta u(t)\right) K(t) \\ &\geq -\left(\mu + d N_T^{2/3} + \beta\right) K(t),\end{aligned}$$

so that

$$K(t) \geq K^0 e^{-\left(\mu + d N_T^{2/3} + \beta\right) T} := K_T$$

for $t \in [0, T]$. □

This shows that all trajectories are confined to a compact set

$$A = \left\{(N_1, N_2, K) : 0 \leq N_1 + N_2 \leq N_T \text{ and } K_T \leq K \leq K^T\right\}$$

with N_T, K_T, K^T defined as above. Using the notation from Section 3.3.1, we can take $\Gamma = \mathbb{R}^2 \times (0, +\infty)$ and A as above, noting $A \subset \Gamma$. The right-hand side of System (5.2), i.e. the function

$$\begin{aligned}\mathbf{F}(N_1, N_2, K, u) &= \begin{pmatrix} F_1(N_1, N_2, K, u) \\ F_2(N_1, N_2, K), \\ F_3(N_1, N_2, K, u) \end{pmatrix} \\ &= \begin{pmatrix} \lambda_1 N_1 \left(1 - \frac{N_1 + \alpha_{12} N_2}{K}\right) - \tau_1 N_1 + \tau_2 N_2 - \beta_1 N_1 u(t), \\ \lambda_2 N_2 \left(1 - \frac{N_2 + \alpha_{21} N_1}{K}\right) + \tau_1 N_1 - \tau_2 N_2, \\ -\mu K + b(N_1 + N_2) - d(N_1 + N_2)^{2/3} K - \beta K u(t), \end{pmatrix}\end{aligned}$$

is continuously differentiable in $A \times U$ (as $K \geq K_T > 0$ in A). Similarly, the functions L is continuously differentiable in $A \times U$ and M is continuous in A. Similarly as before, for each $(N_1, N_2, K) \in \Gamma$ we have:

$$\begin{aligned}Q(N_1, N_2, K) &= \{(\bar{y}, \mathbf{y}) : \bar{y} \geq L(N_1, N_2, v), \mathbf{y} = \mathbf{F}(N_1, N_2, K, v) \text{ for some } v \in [0, 1]\}, \\ &= [L(N_1, N_2, 0), \infty) \times [F_1(N_1, N_2, K, 1), F_1(N_1, N_2, K, 0)] \times \{F_2(N_1, N_2, K)\} \\ &\quad \times [F_3(N_1, N_2, K, 1), F_3(N_1, N_2, K, 0)]\end{aligned}$$

due to $\mathbf{F}$ being linear in u and L being independent of u, so that Q is convex.

The assumptions of Theorem 1 are therefore satisfied and an optimal solution exists.

List of Figures

List of Tables